ANTI-CANCER AND ANTI-MALARIAL 4-AMINOQUINOLINE DERIVATIVES: SYNTHESIS AND SOLID-STATE INVESTIGATIONS

By: Candice Soares de Melo

B.Sc. (Hons)

Thesis presented for the degree of

MASTER OF SCIENCE

in the Department of Chemistry

Faculty of Science

UNIVERSITY OF CAPE TOWN

Supervisors: Professor Kelly Chibale

Professor Mino R. Caira

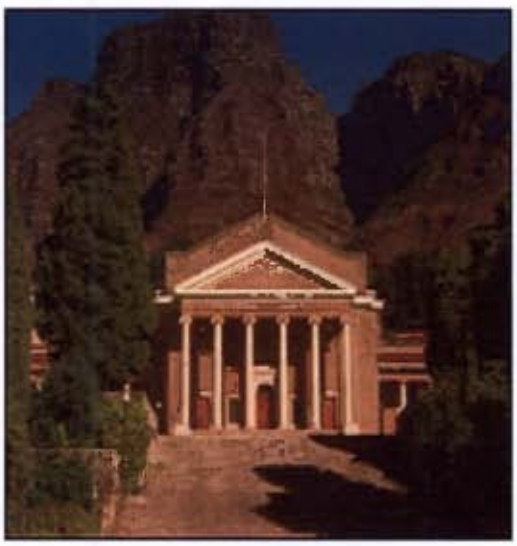

December 2006

ACKNOWLEDGEMENTS

My special thanks to:

my supervisors, Professor Kelly Chibale and Professor Mino Caira, for their excellent guidance, support and encouragement throughout the course of this work.

my colleagues in the University of Cape Town Medicinal Chemistry laboratories and the Supramolecular Chemistry group for their ideas and support during my project.

Noel Hendricks and Pete Roberts for the NMR experiments, Tommy van der Merwe (University of the Witswatersrand) for mass spectroscopy, Pierro Benincasa for microanalysis, Dr. Hong Su for the crystal structure analysis.

collaborators who assisted in biological testing of synthesized compounds; Dr. Susan Yeh, (Division of Pharmacology, University of Cape Town), Prof. Philip J. Rosenthal and Jiri Gut (School of Medicine, University of California San Francisco, USA), Prof. Connie Medlen and Margo Nel (Division of Pharmacology, University of Pretoria), Prof. P. Rasoanaivo (Institut Malgache de recherches appliquees in Madagascar).

my sincere gratitude to the NRF for financial support

my family and friends, especially my mother Cheryl, for their constant love, support and encouragement.

ABSTRACT

The work presented in this thesis is two-fold: (i) development of single agents that provide inhibition of both the growth of malaria parasites and of tumour cells *in vitro*, and (ii) inclusion of these potential novel inhibitors in cyclodextrin host molecules in an attempt to render these dual drugs water-soluble.

(i) Of all the current clinically established antimalarials, the 4-aminoquinolines have proven to be the most significant and efficacious for the treatment and prophylaxis of malaria. However, their efficacy has decreased by the spread of drug resistant strains of the causative agent *Plasmodium falciparum*. Future research into 4-aminoquinoline derivatives as antimalarial agents is still warranted and justified on the basis of several considerations. The quinoline moiety has also been shown to be a substructure in multi-drug resistance reversal agents against certain cancer cell lines and antitumour agents which have demonstrated the ability to act as differentiation-inducing agents.

The strategy employed for this project was to hybridize chalcone moieties and their Mannich base derivatives with the 4-aminoquinoline moiety. This dual drug concept uses the basic structure of the chalcone scaffold, which has a wide range of known antimalarial and anticancer activities, and is hybridised with the 4-aminoquinoline moiety, in order to exert maximal biological activity and overcome or prevent drug resistance. Structural variation on the aromatic rings of the chalcone scaffold allowed preliminary structure-activity relationship studies to be undertaken.

Synthesized compounds were evaluated against chloroquine-sensitive and chloroquine-resistant *Plasmodium falciparum* strains. Despite the lower antiplasmodial activities associated with these compounds compared to chloroquine, the target compounds on average possess favourable resistance indices. Cytotoxicity assays were performed on HeLa cells to establish the sensitivity of the cancer cell lines to the synthesized compounds. A general trend observed against both *Plasmodium falciparum* strains and HeLa cells is that target hybrid **2**, in which the 4-aminoquinoline moiety is attached to ring **B**, is more active than target hybrid **1**, in which the 4-aminoquinoline moiety is attached to ring **A.** The results of the

preliminary structure-activity relationship studies demonstrate the importance of *meta*-relationship between the 4-aminoquinoline moiety and the ketone linker and a methoxy-substituent on the chalcone aromatic ring, for both antiplasmodial and anticancer activity.

Conversion of the chalcones into the corresponding Mannich bases led to an increase in potency against both D10 and W2 strains and HeLa cells *in vitro*. Mannich base derivatives showed greater antiplasmodial activities in the resistant W2 strain (IC_{50} ranging from 0.004 to 0.08 μM) than the reference drug chloroquine (IC_{50} = 0.099 μM). The ability of the phenolic Mannich base derivatives to inhibit β-haematin formation and the cysteine protease falcipain 2 was also determined, in efforts aimed at understanding the mechanism of action. There is a fairly good correlation between antimalarial activity against D10 and inhibition of β-haematin formation. There was no correlation between the ability of the compounds to inhibit falcipain 2 and antiplasmodial activity against W2 *in vitro*. The pyrrolidine-derived Mannich base **CDM37** is a promising antimalarial agent as it shows superior activity in both the chloroquine-sensitive (IC_{50} = 0.111 μM) and chloroquine-resistant (IC_{50} = 0.0039 μM) *P. falciparum* strains as well as inhibition of falcipain 2 (IC_{50} = 11.51 μM) and β-haematin formation (0.219 equiv).

(ii) Cyclodextrins have the ability to form inclusion complexes with various guest molecules and are of interest in this project due to their ability to act as solubilisers, stabilisers and carriers of poorly soluble drug molecules. Two β-cyclodextrin complexes and three γ-cyclodextrin complexes were formed with selected target compounds by the method of kneading. Although five inclusion complexes were obtained as established by powder X-ray diffraction, subsequent recrystallization of the kneaded material did not yield single crystals required for full X-ray structure determination, which is an essential requirement for pharmaceutical use of cyclodextrin inclusion complexes. Consequently the hypothesis of improving the water-solubility and hence the bioavailability of target compounds through cyclodextrin inclusion could not be fully explored.

ABBREVIATIONS

CD	Cyclodextrin
CP	Cysteine protease
Cys	Cysteine
DCM	Dichloromethane
DDT	Dichlorodiphenyltrichloroethane
DHFR	Dihydrofolate reductase
DIMEB	Heptakis(2,6-di-O-methyl)-β-cyclodextrin
DMSO	Dimethylsulphoxide
DNA	Deoxyribonucleic acid
DSC	Differential Scanning Calorimetry
dUMP	2'-Deoxyuridylic acid
dTMP	Deoxythymidine-5-phosphate
ED_{50}	Effective dose of a drug necessary to produce a therapeutic effect in 50% of the test sample
equiv	Equivalent
Fe	Iron
FV	Food vacuole
GSH	Glutathione
h	Hours
H_2O-Fe(III)PPIX	Aquaferriprotoporphyrin IX
HAP	Histo-aspartic protease
HDAC	Histone deacetylase

His	Histidine
HRMS	High resolution mass spectroscopy
HRP-2	Histidine-rich protein II
HSM	Hot Stage Microscopy
IC_{50}	Inhibitory concentration to inhibit 50% of enzyme activity or parasite growth
IR	Infrared
K	Kelvin
Leu	Leucine
MDR	Multi-drug resistance
MDRR	Multi-drug resistance reversal
mol	Mole
MS	Mass spectroscopy
NADPH	Nicotinamide adenine dinucleotide phosphate-oxidase
NMP	N-Methyl-2-Pyrrolidone
NMR	Nuclear magnetic resonance
NPP	New permeability pathways
P	*Plasmodium*
Pgp	P-glycoprotein
Pgh1	P-glycoprotein homologue 1
PXRD	Powder X-ray diffraction
RBC	Red blood cell
RBM	Roll Back Malaria
Phe	Phenylalanine

PfA-M1	*Plasmodium falciparum* aminopeptidase of the M1 group of metalloproteases
PfCRT	*P. falciparum* chloroquine resistance transporter
rt	Room temperature
SP	Sulfadoxine-pyrimethamine
TGA	Thermogravimetric Analysis
TRIMEB	Heptakis(2,3,6-tri-O-methyl)- β-cyclodextrin
TLC	Thin layer chromatography
TrxR	Thioredoxin reductase
UV	Ultra-violet
WHO	World Health Organization

The following abbreviations are used in the EXPERIMENTAL chapter:

cm^{-1}	wavelength
s	singlet
d	doublet
dd	doublet of doublets
EI	Electron impact
FT	Fourier transform
Hz	Hertz
J	Coupling constant
t	triplet
q	quartet
m	multiplet
mp	melting point

m/z	mass to charge ratio
δ	chemical shift
ppm	parts per million
R_f	retention factor

TABLE OF CONTENTS

CHAPTER 3: SYNTHESIS AND CHARACTERIZATION OF TARGET COMPOUNDS **52**

CHAPTER 1

INTRODUCTION

1.1 History of Malaria

Malaria, a disease caused by the parasitic protozoa of the genus *Plasmodium*, is one of the most serious and widespread threats to human health.[1] The malaria parasite and the human race have had a long host-parasite connection; references to malaria are found in myths, legends and historical accounts of ancient Egypt, China, India and Greece.[2] For many centuries, the cause of malaria was attributed to a poisonous vapor emanating from stagnant water, a theory that gave the disease its name from the Italian word "mal' aria" meaning "bad air". Civilizations as early as the Etruscans (1st millennium BC) drained marshes and swamps in an effort to combat the disease.[3] The first important step towards identifying the true cause of the disease was taken by Meckel in 1847, who associated a pigment he saw in the blood, spleen and liver of cadavers with malaria infection.[5] However, it was not until 1880 that the French surgeon Charles Alphonse Laveran made the crucial finding that not only the pigment but also a parasite itself was present in the blood of malaria patients. After the protozoal cause of malaria was elicited by Laveran, the next step forward was made in 1899 by Ronald Ross, a British physician, who demonstrated that the female *Anopheles* mosquito was the vector for malaria.[2] In 2002 the genome of *Plasmodium falciparum* and other malaria parasites was determined by an international team of scientists with the hope to design more effective antimalarial drugs, insecticides and vaccines.[4] In many ways, the history of malaria reflects the development of science and medicine over the centuries, from myth and superstition to a thorough scientific basis.

1.2 Global Distribution of Malaria

Although malaria was once prevalent in North America and other temperate regions, the disease today occurs mainly in tropical and subtropical countries, in particular Sub-Saharan Africa and South-East Asia.[3,5] According to the World Health Organization, malaria occurs in over 100 countries with an estimated 300-500 million

cases diagnosed annually, leading to 1.1-2.7 million deaths.[6] About 90% of these deaths occur in Sub-Saharan Africa, where malaria also presents major obstacles in social and economic development. The seriousness of malaria has been increasing in recent years, with epidemics occurring in new areas as a result of deteriorating social and economic conditions, changing land utilization, insecticide-resistant mosquitoes and drug-resistant parasites.[6] Figure 1.1 depicts the current global distribution of malaria.

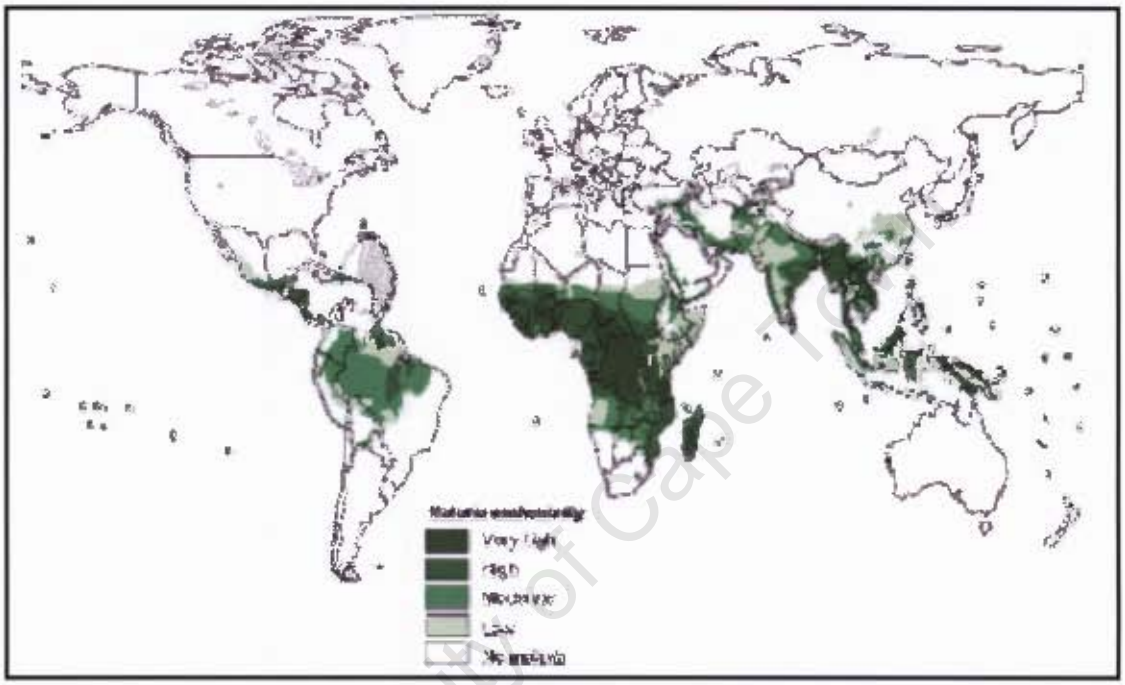

Figure 1.1: Geographic distribution of malaria[7]

1.3 Biology of the Malaria Parasite

Malaria in humans is caused by four species of *Plasmodium* parasites, namely *P. falciparum*, *P. vivax*, *P. ovale* and *P. malariae*, each of which produces a characteristic clinical illness. *Plasmodium falciparum* is the most common species in tropical areas and the most dangerous of the four species, accounting for half of all clinical cases and 90% of fatalities from the disease. *Plasmodium vivax* is the most widespread species, existing in tropical and some temperate zones. The other two plasmodia species are less common and have a variable distribution worldwide.[8] Fortunately, the biology of *P. falciparum* is the best understood of the four species as methods for *in vitro* culture have been available for three decades.[9]

Knowledge of the biology of the malaria parasite is fundamental in understanding the methods of prevention, treatment and research endeavors.

1.3.1 Life Cycle of the Malaria Parasite

The life cycle of the malaria parasite is complex and involves a sexual stage that occurs in the mid-gut of the mosquito, and an asexual stage, which takes place in the human host; first in the liver and then in red blood cells (Figure 1.2).

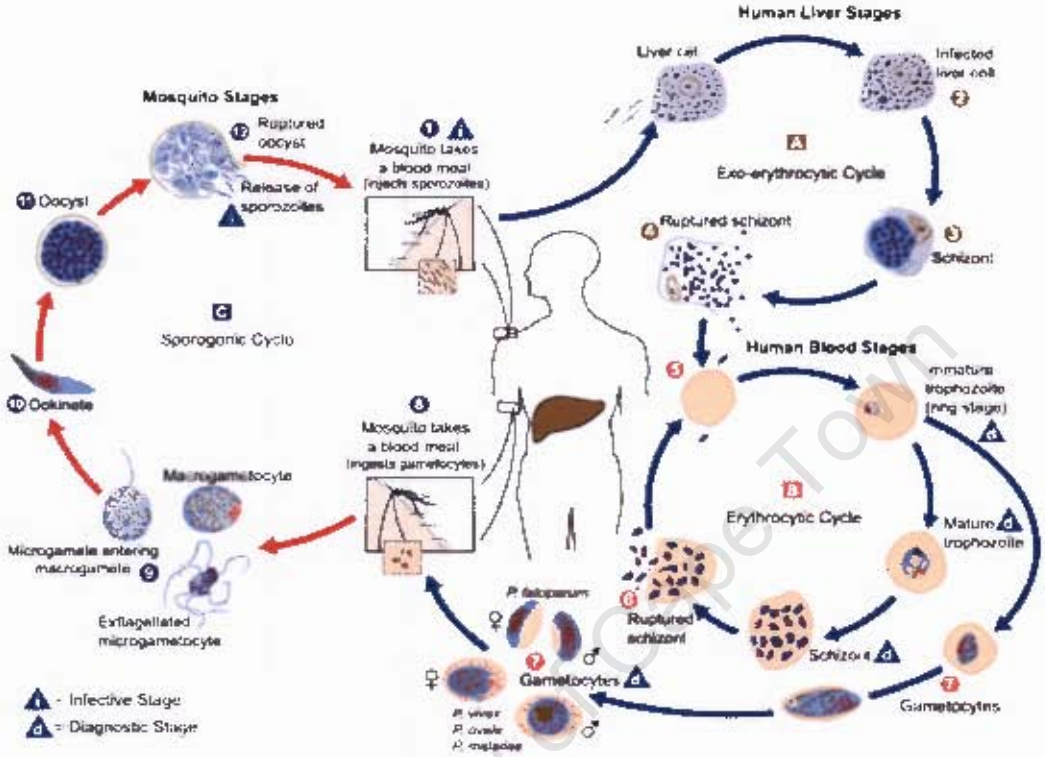

Figure 1.2: Life cycle of the malaria parasite[13]

A human infection begins with the bite of an infected female *Anopheles* mosquito while taking a blood meal in order to nourish her eggs. To ensure an even flowing meal, the mosquito injects anticoagulant saliva that contains the infectious sporozoites into the human bloodstream. The thread-like sporozoites rapidly take refuge from the human's immune system defenses by invading hepatocytes in the liver, where they undergo asexual amplification and develop into an exoerythrocytic (hepatic) schizont during the next 5-15 days. The hepatic schizont, containing up to 30 000 merozoites, bursts upon maturation releasing the merozoites into the bloodstream where they invade the red blood cells (erythrocytes). In the erythrocyte, asexual amplification once again occurs leading to the formation of erythrocytic schizonts, through ring and trophozoite stages. The erythrocyte containing the mature schizont ruptures, releasing a new generation of merozoites, which could invade other red blood cells; it is during this phase that malaria-associated morbidity and mortality occurs. The parasite will

proliferate in this manner until the death of the host or until they are controlled or terminated by the host's immune system or by drugs.

During this repeated cycle, some merozoites differentiate into microgametocytes (male) and macrogametocytes (female), which can be transmitted to the *Anopheles* mosquito during a blood meal. In the mid-gut of the mosquito, mature gametocytes escape from the erythrocyte to form gametes; fertilization then occurs producing zygotes, which develop into ookinetes. The ookinete penetrates the epithelial cells and develops into an oocyst. Between 7-15 days, depending on the species and ambient temperature, a single oocyst divides and ruptures to form more than 10 000 sporozoites, which migrate into the salivary glands. When the infected mosquito feeds again, the Plasmodium life cycle is completed. The time duration on the *P. falciparum* is summarized in Table 1.

Table 1: Length of the Different Stages of Life Cycle of *Plasmodium falciparum*[8]

1	Ookinetes formation	24 to 48 hours
2	Oocysts maturation	9 days
	Time for invasion of salivary glands (1 + 2)	**10 days**
3	Time of circulation of sporozoites in the blood stream	Max. 1 hour
4	Hepatic schizogony	6 days
5	Erythrocytic schizogony	48 hours
6	Gametocytogony	10 days
	Complete cycle (1 to 6)	**27 days**

1.3.2 Biochemistry of the Food Vacuole

1.3.2.1 Background

The intraerythrocytic location of the malaria parasite, providing a safe environment from the host's immune system, leads to a greater difficulty in obtaining the required nutrients from the external environment.[8] The parasite thus modifies the host cell in several ways and intertwines its metabolism with that of the host. Upon invasion of a human erythrocyte, the parasite grows and matures surrounded by cytosol consisting predominately of haemoglobin. Due to the rapid growth and multiplication rate of the parasite, it requires a ready source of amino acids but has a limited ability to synthesize them *de novo*.[11] The parasitic trophozoite circumvents this problem by ingesting and degrading large quantities of host cell haemoglobin and uses these

haemoglobin-derived amino acids in its own proteins.[12] Although 60-80% of the haemoglobin originally present in the red blood cell is degraded,[13,14] there is evidence that only a small quantity of amino acids is used.[15] To explain this, it has been suggested that the parasite digests haemoglobin, not only as a source of nutrients, but also to maintain osmotic stability[16] and to make space for itself within the red blood cell.[17] A key organelle through which the parasite carries out haemoglobin degradation and other important biochemical processes is a specialized acidic (pH 5-5.5) food vacuole (Figure 1.3). The haemoglobin-rich red blood cell cytosol is ingested by the process of endocytosis via an invagination in the parasitophorous vacuolar membrane known as a cytosome and then transported to the food vacuole (FV) by transport vesicles.[18]

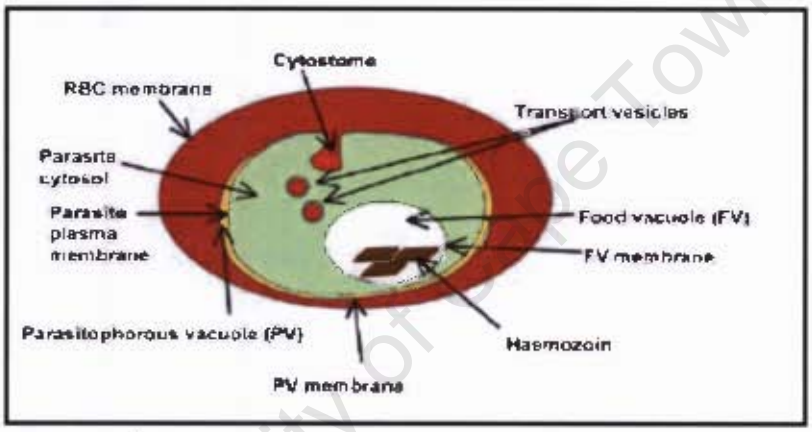

Figure 1.3: A schematic representation of the parasitised red blood cell and of endocytocysis[18]

Disruption of haemoglobin catabolism causes parasite death *in vitro* and *in vivo*. The vital and specialized process of haemoglobin degradation within the food vacuole provides promising targets for the development of novel antimalarial chemotherapeutic agents.

1.3.2.2 Haemoglobin Degradation Pathway

Haemoglobin degradation to peptide fragments is facilitated by multiple proteases within the food vacuole. The distinct but overlapping roles of these proteolytic enzymes suggest that haemoglobin catabolism occurs via a semi ordered pathway.[19,20] Three distinct classes of proteases have been isolated and purified from the food vacuole, characterized and identified.

There are four aspartic proteases (plasmepsins I, II and IV and histo-aspartic protease, or HAP),[20,21] two cysteine proteases (falcipain 2 and 3)[22] and a zinc metalloprotease (falcilysin).[19] The sequence of events leading to the liberation of free amino acids is believed to occur as shown in Figure 1.4 and summarized below.

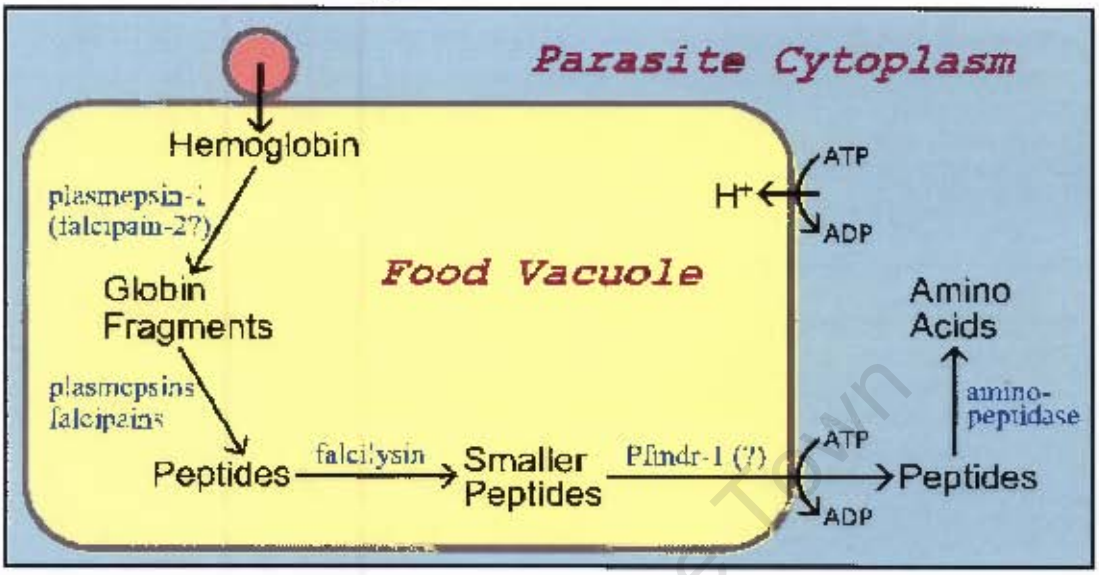

Figure 1.4: Haemoglobin degradation within food vacuole[23]

(a) Plasmepsin I, II and IV commence the degradation process by cleaving native haemoglobin at the same site, location α33Phe-34Leu in the α chain,[20] cleaving the hinge region that maintains quaternary structure. The denatured haemoglobin then undergoes secondary cleavages, with plasmepsin I preferring phenylalanine at the P1 position and plasmepsin II preferring other hydrophobic positions, especially leucine, at the P1' position.[20] Plasmepsin IV and HAP further digest the haemoglobin to form denatured globin fragments.[21]

(b) Once the aspartic proteases have initiated proteolysis to form denatured haemoglobin, falcipain 2 and 3 then hydrolyze these globin fragments into peptide fragments 10-15 amino acids in length. The cysteine proteases are incapable of degrading native haemoglobin at physiological vacuolar pH. There is evidence, however, that cysteine proteases may act upon native haemoglobin under mild reducing conditions,[24] due to the observation of swollen food vacuoles filled with undegraded globin when parasites are treated with cysteine protease inhibitors.[25] There is also evidence that falcipain 2 is involved in cleaving specific components of the host erythrocyte membrane skeletal proteins, thus resulting in host cell rupture and release of merozoites.[26]

(c) Falcilysin, a zinc metalloprotease, functions downstream in the haemoglobin degradation process. Falcilysin cannot cleave haemoglobin or globin, but is capable of proteolyses of the peptides into short oligomers (6-8 amino acids) at sites polar in character, with charged residues at the P1 and/or P4' positions.

(d) The short oligomers are then transported out of the food vacuole into the parasite cytoplasm where they are hydrolyzed by aminopeptidases into amino acids necessary for cell growth. One such aminopeptidase is *Plasmodium falciparum* aminopeptidase of the M1 group of metalloproteases (PfA-M1), which preferentially hydrolyses N-terminal amino acids Leu and Ala.

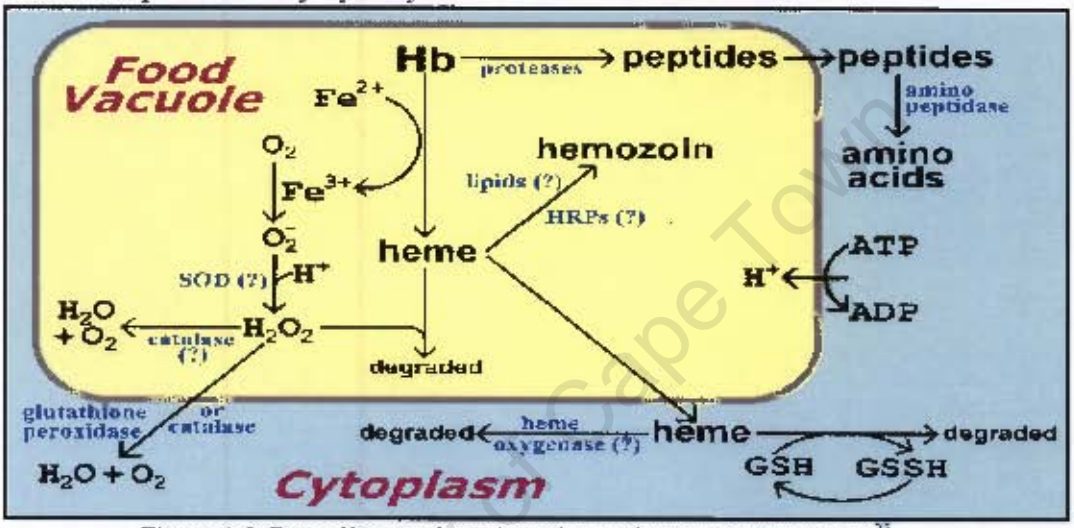

Figure 1.5: Fate of haem released as a by-product in Hb degradation[23]

During this process of haemoglobin degradation, haem in its ferrous form (ferroprotoporphyrin IX or Fe(II)PPIX) is released as a by-product (Figure 1.5) and autoxidised by O_2 to α-haematin (aquaferriprotoporphyrin IX or H_2O-Fe(III)PPIX), which is the ferric form.[18] This leads to the production of hydrogen peroxide through the one electron oxidation of Fe(II). In addition to oxidative assault, α-haematin is toxic to the parasite and requires a detoxification mechanism. It is well established that haematin is converted to haemozoin, a highly insoluble microcrystalline substance.[27] There is no complete agreement as to how haemozoin is formed in the malarial parasite and proposals include catalysis by lipids and/or catalysis by histidine rich protein 2 (HRP-2).[18] Most (approx. 95%) of the iron resulting from the degradation is converted to haemozoin and the remainder is possibly degraded to free iron. It has been suggested that haematin may be degraded into non-haem iron by hydrogen peroxide within the food vacuole,[13] or in the parasite cytosol by glutathione degradation.[14]

1.4 Prevention and Control of Malaria

Effective malaria prevention can be carried out by a number of strategies:[3]

i. Eliminating existing infections that act as a source of transmission. This method of prevention requires aggressive treatment of malaria-infected people, as well as continuous surveillance to diagnose and treat infection promptly. Although this approach has been successful in North America and Europe, it is unfortunately not realistic in developing countries of Africa and Southeast Asia, who lack the infrastructure and resources necessary.[7]

ii. The use of prophylactic drugs has also been effective for travelers and people living in endemic areas. There are several considerations when prescribing chemoprophylactic drugs and depends on the particular location, which has implications on type of species and parasite transmission intensity, as well as individual circumstances. Some available drugs include proguanil, mefloquine, doxycycline and Malarone® (atovaquone/proquanil).

iii. Eliminating exposure to mosquitoes can be achieved by several methods. Some of these methods include permanently destroying bodies of stagnant water by systematic drainage; treating such environments with insecticides to kill mosquito larvae and adult mosquitoes; or using repellent creams containing diethyltoluamide, protective clothing or insecticide-treated nets to prevent contact with mosquitoes.

The discovery of the insecticidal properties of dichlorodiphenyltrichloroethane (DDT) in the 1940s enabled large-scale, wide-area approaches to malaria control for the first time.[28] The World Health Organization (WHO) endorsed this approach and in 1955 submitted a proposal for the eradication of malaria worldwide. The global eradication program involved mass spraying of DDT, antimalarial drug treatment and surveillance. The eradication program was very successful in some countries, and virtually eliminated illness and death due to malaria in countries such as the United States, Sri-Lanka and India.

In other countries, the program sustain or reduce malaria significantly, with sub-Saharan Africa being completely disregarded in "global" eradication efforts.[28] The hope of global eradication was finally abandoned in 1969 due to a number of factors such as lack of financial support, health care workers and community participation, political upheavals and mass population movement, as well as insecticide-resistant mosquitoes and drug-resistant parasites. The WHO thus decided to shift its focus to malaria control. Control programs are based on the following objectives:[29]

i. Early diagnosis and rapid treatment of malaria cases
ii. Sustainable preventive measures adapted to local situation
iii. An immediate and vigorous response to epidemics
iv. Awareness of infection risk

In 1998 the Roll Back Malaria (RBM) movement was launched to coordinate international malaria control. The central goal of RBM is to reduce the global malaria risk, morbidity and mortality by half by 2010. This mandate hopes to accomplish this by meeting targets on insecticide treated nets distribution, intermittent presumptive therapy in pregnant women, prompt and effective treatment and epidemic preparedness.[28] Malarial control requires a multifaceted approach, with the availability of effective and affordable drugs being of great importance.

1.5 Antimalarial Chemotherapy

1.5.1 Introduction

Ideally, a chemotherapeutic agent used in the treatment of *P. falciparum* malaria should be active against drug-resistant strains, provide cure within a reasonable time, be safe with minimum side effects, be suitable for children and pregnant women, orally active and perhaps most importantly, be affordable.[30,31] Unfortunately, the current drugs available and those in development, more often than not require a compromise among desired features. Most clinically established drugs were not rationally designed based on identified targets but through the unexpected identification of antimalarial activity of natural products (quinine and artemisinin), compounds derived from natural products (chloroquine and artesunate), or compounds active against other infectious pathogens (antifolates and tetracyclines).[30]

The recent improvement in the understanding of the biochemistry of the malaria parasite, determination of the genome sequence of *P. falciparum* and advances in malaria genetics has allowed for the determination of many potential drug targets. Understanding on the mode of action of clinically established drugs has been improved due to these advances made.

1.5.2 Classification of Antimalarial Drugs

The current clinically established chemotherapeutic agents can be classified by i.) the stage of the malaria life cycle which they are targeting or ii.) by their mechanism of action.[32-34]

1.5.2.1 Classification according to the Stage of the Life Cycle

Depending on the stage in the malarial life cycle where they act upon, antimalarial drugs can be classified as blood schizonticides, tissue schizonticides, gametocides and sporontocides (Table 2).[33]

Table 2: Classification according to their stage of the life cycle[33]

Tissue schizonticides	Primaquine, pyrimethamine, sulfonamides
Hypnozoiticides	Primaquine, tafenoquine
Blood schizonticides	*Type 1, quick onset*: Chloroquine, mefloquine, quinine,halofantrine, artemisinin *Type 2, slow onset*: Pyrimethamine, sulfonamides, sulfones, other antibiotics, atovaquone
Gametocides	Primaquine (*Plasmodium falciparum*) Quinine (*P. vivax, P. malariae, P. ovale*)
Sporontocides	Primaquine, chloroquine

Blood schizonticides are drugs that suppress the production of plasmodia in the erythrocytes during the asexual intraerythrocytic stage of the malaria life cycle. Tissue schizonticides are active in the liver stage of the parasite life cycle and prevent the development of hepatic schizonts. Due to the fact they act upon the developmental stages of the malaria life cycle, tissue schizonticides are more commonly used for prophylactic purposes than curative. Another group of antimalarial agents acting in the liver stages of the malaria life cycle are the hypnozoiticides, which show activity by destroying the liver schizonticides of *P.vivax* and *P. ovale*. Gametocides eradicate the intraerythrocytic sexual form of the parasite thereby preventing human to mosquito transmission. Lastly sporontocides hinder the development of oocysts and

sporozoites in the mosquito. Although most of the current chemotherapeutic agents act upon the intraerythrocytic stages of the malaria life cycle, there are numerous drugs that target several stages of *Plasmodium* life cycle.

1.5.2.2 Classification according to Mode of Action

Antimalarial drugs can also be classified according to their mode of action in which they exert antimalarial activity. There are four major modes of action for the current clinically established antimalarial drugs:[33] drugs which interfere with the haem detoxification pathway, drugs which inhibit nucleic acid synthesis, drugs which interfere with protein synthesis and those that act by oxidative stress.

1.5.2.2.1 Drugs acting on Haem Detoxification

This category of chemotherapeutic agents includes the most common antimalarial drugs; that being the 4-aminoquinolines such as chloroquine **1.1** and amodiaquine **1.2** and the quinine-type aryl amino alcohols such as quinine **1.3**, quinidine **1.4**, mefloquine **1.5** and halofantrine **1.6** (Figure 1.6).

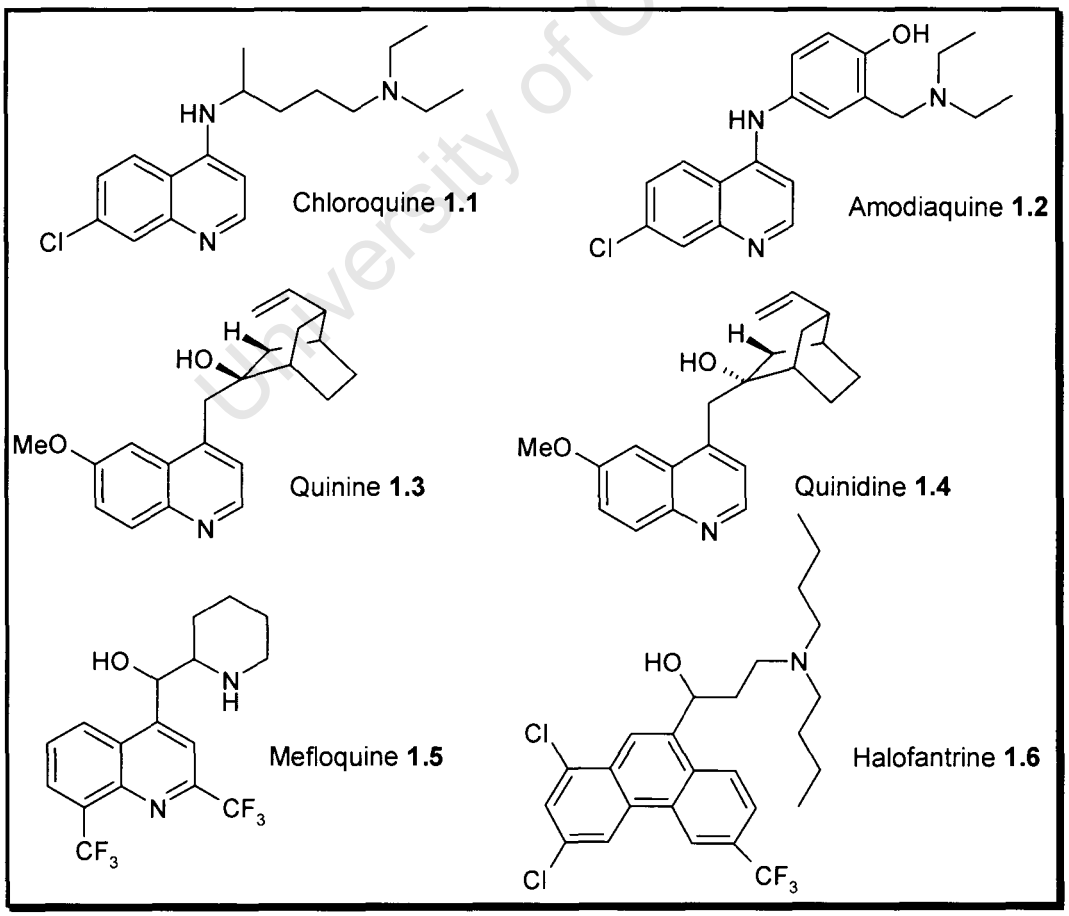

Figure 1.6: Chemical structures of antimalarials acting on heme detoxification

Despite many years of use and study, the exact mechanism of action of quinoline drugs is not completely understood. Nevertheless, it has been known since the 1960's that chloroquine and other quinoline-type antimalarials form complexes with haematin.[35] It is thus generally accepted that this category of antimalarial drugs interfere with the detoxification of free haem, preventing its incorporation into haemozoin. However, it is likely that inhibition of parasite growth is due to a number of synergistic effects.

Chloroquine was developed as an antimalarial during World War II and is one of the most successful drugs ever made. This was based on its affordability, safety, oral administration and high efficacy (prior to resistance). Unfortunately resistance to chloroquine is now widespread. Amodiaquine, a congener of chloroquine, was introduced over 40 years ago and is used as a second line drug in many African countries. It has greater efficacy against chloroquine-resistant *P. falciparum* infections but is not recommended due to its association with hepatitis and agranulocytosis. Quinine is one of the active components contained in the bark of the cinchona tree, which was one of the first agents used for the treatment of malaria, with its use dating back over 350 years. Currently, quinine is mainly used as a parenteral drug for severe *falciparum* malaria in part due to symptomatic toxicity and a complex administration and monitoring.[36] Another active component extracted from the cinchona tree is quinidine, the diastereoisomer of quinine at the secondary alcohol group, which is more potent and toxic than quinine and used as an antiarythmic. In an effort to overcome chloroquine resistant *P. falciparum* strains, mefloquine and halofantrine were developed. Mefloquine, a quinoline methanol derivative, was an effective antimalarial and due to its long half-life (15-33 days) is a good prophylactic. Decline in its use is a result of the development of resistance and undesirable side effects. Halofantrine is a phenanthrene methanol derivative and is used for uncomplicated cases of multi-resistant *falciparum* malaria. Due to a low therapeutic index, treatment efficacy and safety are complex and thus its use is limited.[36]

1.5.2.2.2 Inhibitors of Nucleic Acid Synthesis

This category of antimalarials includes the folate antagonists, sulfonamides and naphthoquinones and is active against the primary exoerythrocytic and asexual blood stages of the malaria parasite.[32,33] Folate antagonists, such as pyrimethamine **1.7** and proquanil **1.8** (Figure 1.7), exert antimalarial activity by exploiting the structural differences between the parasite and host enzyme dihydrofolate reductase (DHFR). Dihydrofolate reductase catalyses the regeneration of tetrahydrofolate, a highly versatile carrier of one-carbon units. These drugs inhibit parasite DHFR, thereby causing a depletion of tetrahydrofolate and an inhibition of DNA synthesis.[33]

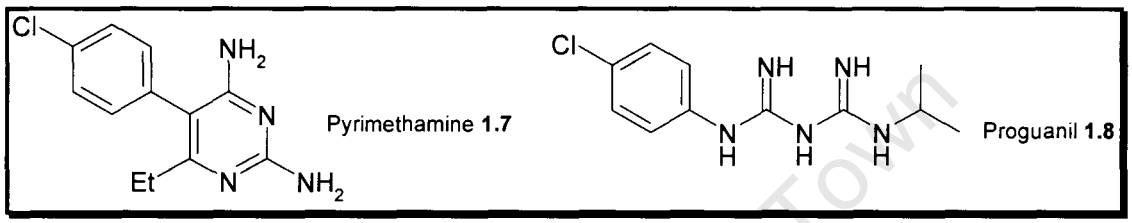

Figure 1.7: Chemical structures of folate antagonists

Pyrimethamine is used only in combination with a sulfonamide (e.g. Sulfadoxine, in Fansidar) and this pyrimethamine-sulfadoxine (SP) treatment has replaced chloroquine in many countries as a first line treatment of *falciparum* malaria. Unfortunately, resistance usually develops within a few years; aided by the slow elimination of SP from the body.[37] The pro-drug proguanil is metabolized by cytochrome P450 to the active metabolite cycloguanil, which then inhibits DHFR. Due to rapid resistance of both *P. falciparum* and *P.vivax*, this drug is now only used in combination with chloroquine or atovaquone. The cause of resistance to these DHFR inhibitors is believed to be a result of single mutations on the encoding gene of the enzyme.

The antimalarial activity of sulfonamides such as sulfadoxine **1.9** and sulfones such as dapsone **1.10** (Figure 1.8) is due to their ability to inhibit dihydropteroate synthase, another enzyme involved in folate metabolism, by mimicking *p*-aminobenzoic acid. Dihydropteroate synthase catalyses the formation of dihydropteroate from hydroxymethyldihydropterin, which ultimately results in reduced pyrimidine synthesis and thus reduced DNA, serine and methionine formation. Although pyrimethamine-sulfadoxine combination drug is still in use in regions of Africa,

resistance to sulfonamides due to single mutations on the corresponding gene is widespread.[33]

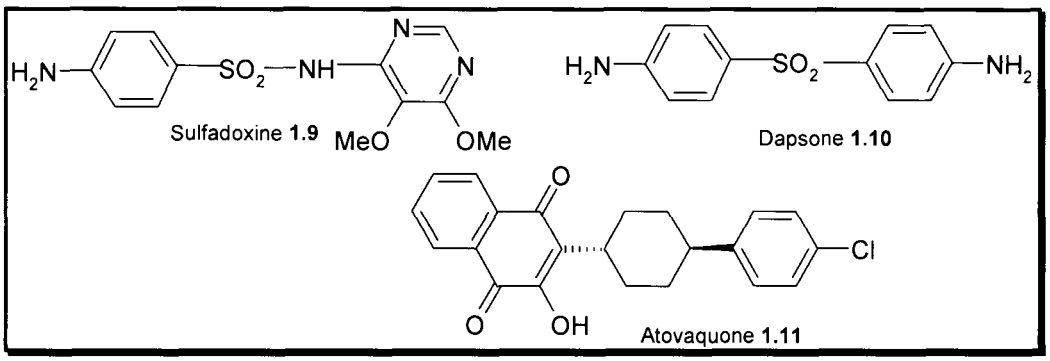

Figure 1.8: Chemical structures of sulfadoxine, dapsone and atovaquone

The last class of nucleic acid inhibitors is the naphthoquinones, with the most efficacious example being atovaquone **1.11** (Figure 1.8). Atovaquone is thought to inhibit mitochondrial respiration in the parasite and is used in combination with proguanil to give rise to Malarone®. Although the mode of action and synergy of this combination is not completely understood, its activity has been attributed to inference with mitochondrial membrane potential.[33]

1.5.2.1.1 Inhibitors of Protein Synthesis

Antibiotics such as tetracycline **1.12** and doxycycline **1.13** (Figure 1.9) are often used in conjunction with other drugs to combat resistant *P. falciparum* malaria or alone as a prophylactic agent. They inhibit parasite protein synthesis by acting on the ribosomes of the mitochondria and/or apicoplast.

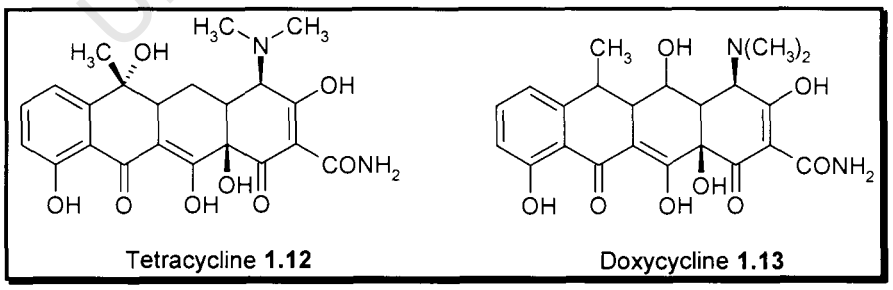

Figure 1.9: Chemical structures of antibiotic antimalarials

1.5.2.2.4 Drugs Generating Oxidative Stress

This group of antimalarials consists of artemisinin **1.14** and its semi-synthetic derivatives (most commonly used artemether **1.15** and sodium artesunate **1.16**, Figure 1.10), which are used for treatment of both uncomplicated and severe *falciparum* malaria. The artemisinins are very effective antimalarials due to their high potency, low prevalence of drug resistance and relative safety.[36] Artemisinin and its derivatives are preferentially used in combination with mefloquine in order to reduce recrudescences and to slow the development of resistance.

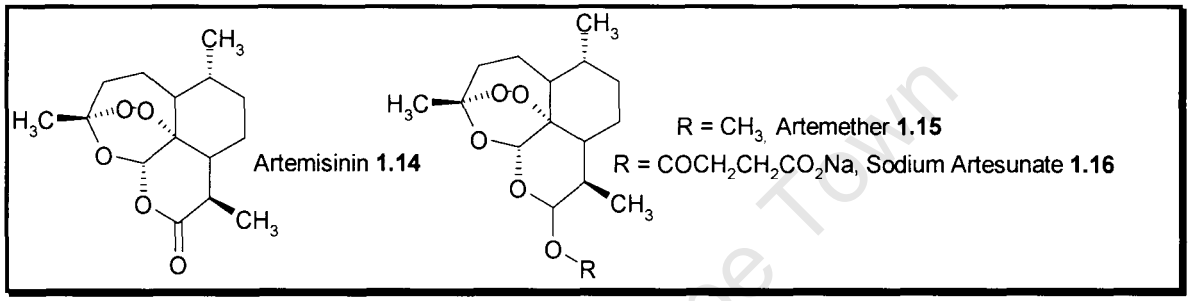

Figure 1.10: Chemical structures of artemisinin and derivatives

Although the mode of action is not completely understood, it is generally accepted that activity is due to the generation of free radicals by an haem-iron mediated mechanism, eventually resulting in total disorganization of the parasite.[33] One suggested mechanism involves cleavage of the peroxide bond in the presence of Fe^{II} haem, followed by electron transfer generating free radicals in the parasitised red blood cells, followed by alkylation of the parasite proteins.[38] The reactive free radicals generated may also cause oxidative stress. However, there is some skepticism regarding this mode of action as it has not been confirmed *in vivo*. Other hypothetical proposals to account for artemisinin antimalarial activity includes inhibition of nuclear factor NF-kB and inhibition of inducible nitric oxide synthase, an enzyme that catalyses the production of nitric oxide.[39] Nitric oxide is a free-radical gas that easily diffuses through cell membranes and has influences on many physiological processes. These findings suggest the possibility of different, unknown targets for this family of drugs.

1.5.3 Cysteine Proteases as Targets in Antimalarial Chemotherapy

Malarial cysteine proteases play crucial roles in parasite infection and development and thus have been considered as preferential targets for therapeutic interventions. Parasitic cysteine proteases contain two principal amino acid residues that are actively involved in the hydrolysis of peptide bonds, namely Cys 25 and His 159.

The cysteine proteases utilize the cysteine thiol group for nucleophilic attack on the amide carbonyl, thus hydrolyzing amide bonds in peptides and proteins. Cysteine protease inhibitors, which have electrophilic moieties, exploit this mechanism by reacting with the active-site cysteine residue. Incubation of cultured malaria parasites with cysteine protease inhibitors developed swollen food vacuoles that contained large quantities of undegraded globin, implicating a role for the falcipains[40] (section 1.3.2.2). Recent studies have demonstrated that cysteine protease inhibitors not only blocked globin hydrolysis but also inhibited earlier stages in haemoglobin degradation pathway,[41] alluding to the fact that cysteine proteases are also required for initial steps in the haemoglobin degradation. It has also been shown *in vivo* that a fluoromethyl ketone is capable of curing a murine infection of malaria[42] and similarly a vinyl sulfone cysteine protease inhibitor were also shown to be potent against murine models of malaria.[43] The degree of inhibition correlated with their inhibition of haemoglobin degradation and parasite development, further supporting the hypothesis that falcipain is the cysteine protease required for haemoglobin degradation. There is also evidence that falcipain 2 is involved in cell rupture and release of merozoites.[26] All of the above implies that cysteine proteases are potential targets for antimalarial chemotherapy.

1.6 Fundamental Understanding of Cancer

Cancer is a general term to describe many disease states, each of which is characterized by cancer cells that undergo a rapid, abnormal and uncontrolled cell division.[44] In normal tissues, the rate of new cell growth and death are kept in balance, ensuring that each tissue maintains a size and architecture appropriate to the body's needs. In cancer cells this balance is disrupted, with the malignant transformation of a cell resulting through the accumulation of mutations in specific classes of genes within the cell (Figure 1.11).

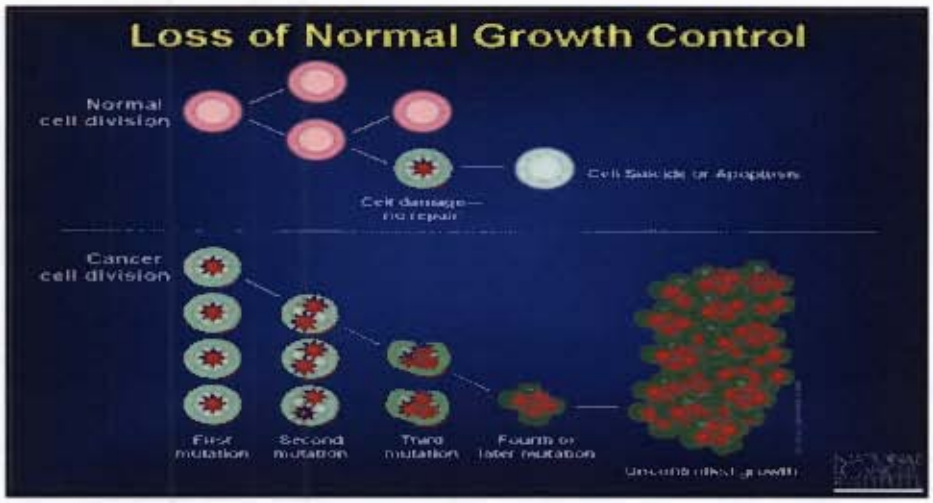

Figure 1.11: Comparison of normal cell division and uncontrolled growth in cancer cells[44]

Two classes of genes, proto-oncogenes and tumor suppressor genes, which stimulate and inhibit cell division respectively, account for much of the uncontrolled proliferation associated with cancer.[45] Mutated forms of proto-oncogenes called carcinogenic oncogenes can cause the stimulatory proteins to become overactive, resulting in excessive multiplication. Mutations in tumor suppressor genes, on the other hand, cause inactivation of suppressor proteins and thus depriving the cells of needed restraints on proliferation. The body does however have backup systems that guard against uncontrolled division. One such system is the cell's ability to undergo apoptosis, where the cell commits suicide if some essential components are damaged or deregulated. Developing cancer cells devise several methods of evading apoptosis, such as inactivating the p53 protein, which helps to trigger cell suicide, or by making excessive amounts of the protein Bcl-2, which wards off apoptosis.[45] Associated with uncontrolled cell growth and division is the invasion of the tumor into surrounding normal tissue. Metastasis is the most feared aspect of cancer and what in fact makes cancer so lethal. Malignant cells have the ability to spread to distant sites in the body, by evading inhibitory messages issued from neighbour tissues, and thus disrupting tissues and organs essential for proper functioning of the body (Figure 1.12).

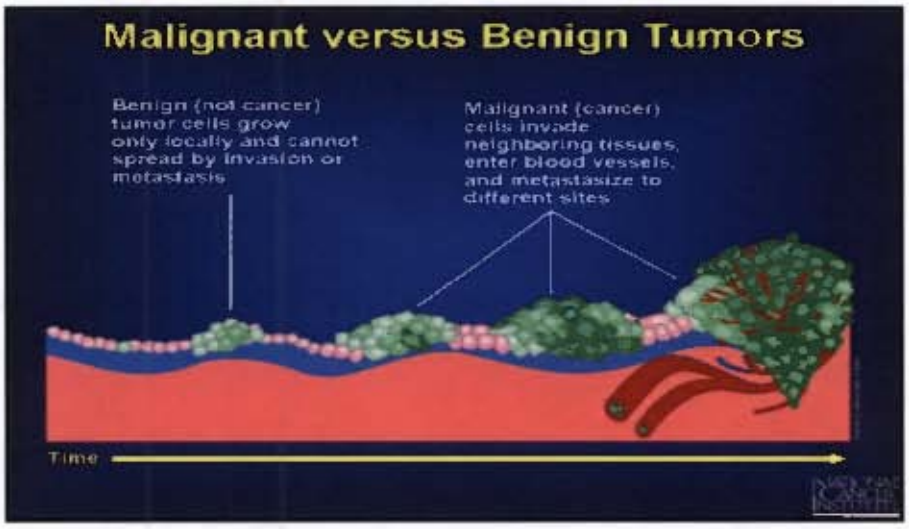

Figure 1.12: Comparison of malignant and benign tumors[44]

To metastasize successfully, cancer cells have to detach themselves from their original location, invade a blood or lymphatic vessel, travel through the circulation to a distant site and establish a new tumor. At every point, cancer cells must evade the controls that keep normal cells in place.

1.7 Current Treatment for Cancer

Most current treatments aim to combat uncontrolled growth, tissue invasion and metastasis and include surgery, radiation and chemotherapy.

1.7.1 Surgery

Surgery was the earliest established therapy for cancer and where feasible is the most widely used approach. Surgical removal of a tumor has benefits such as being quick, efficient and provides a method to confirm that a tumor has been completely excised. Unfortunately, this form of treatment has several limitations:[45]

i. Complete elimination of microscopic extensions of cancer cells is not guaranteed
ii. Large amounts of healthy tissue may have to be removed damaging functioning or appearance
iii. Cancerous cells in vital organs or structures cannot be surgically removed
iv. Cancer that has metastasized throughout the body cannot be treated

1.7.2 Radiation Therapy

Radiation therapy involves the irradiation of powerful x-rays or gamma rays in the region of the tumor. Radiation treatment causes sufficient genetic damage to kill cells directly or to induce apoptosis. In many instances, radiation therapy is preferable to surgery as healthy tissue is preserved, as normal tissue can recover more readily than cancerous cells. It is also has other advantages of destroying microscopic extensions of cancerous tissue and treatment is received without hospitalization. Cancer of the uterine cervix and larynx, early stages of both prostate cancer and Hodgkin's disease are treated well with radiation therapy.[45] As with surgery, this therapy may fail to eradicate all cancerous cells and also cannot treat widespread metastasis, as irradiating the whole body will damage vital delicate tissue.

1.7.3 Chemotherapy

One common denominator for all types of cancers, due to rapid cell division, is the constant demand for DNA and its precursors. Therefore, most chemotherapeutic agents typically exert activity by interfering with the cells ability to replicate DNA, with fast-growing cancer cells being more drastically affected than normal cells.

Some common families of chemotherapeutic agents include the antimetabolites, topoisomerase inhibitors, alkylating agents and plant alkaloids.[45] Antimetabolites exert activity by mimicking molecules necessary in biochemical reactions. An example is the transition-state inhibitor 5-fluorouracil **1.17**, which is converted to the fluorinated analogue of 2'-deoxyuridylic acid **1.18** in the body (Figure 1.13) and is used to treat breast, liver and skin cancers.[46] This analogue binds covalently and irreversibly to the active site of the thymidylate synthase, an enzyme that catalyses the conversion of 2'-deoxyuridylic acid (dUMP) to deoxythymidine-5-phosphate (dTMP, Figure 1.13) terminating synthesis of thymidine and in turn the synthesis of DNA.

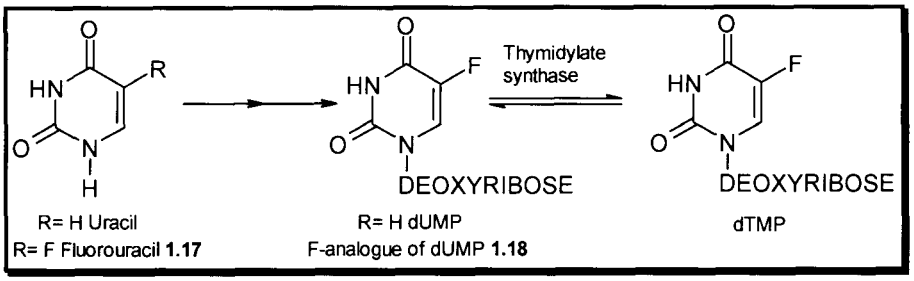

Figure 1.13: Biosynthesis of dTMP[46]

Topoisomerase inhibitors prevent topoisomerase enzymes from reattaching the cleaved ends of DNA during replication. This causes DNA strand breaks in cells that are dividing, resulting in cell death. Alkylating agents are highly electrophilic compounds that form strong covalent bonds with nucleophilic groups in DNA "building blocks". This disruption produces defects in the normal double helical structure of DNA such as breaks and incorrect links between or within strands. If these defects are not repaired, apoptosis will be triggered. *Cis*-diammonia dichloroplatinum (II), known as cisplatin **1.19**, is an alkylating agent used for the treatment of testicular and ovarian tumors (Figure 1.14). Cisplatin forms links within DNA strands, thus inhibiting transcription.[46] The last family of chemotherapeutic agents are those derived from plants that can prevent cell division by binding to the protein tubulin. Tubulin polymerizes in the cell cytoplasm to form microtubles that have various functions within the cell such as exocytosis, release of neurotransmitters, and maintenance of shape and mobility of cells. Tubulin has crucial functioning in the mitotic phase of the cell cycle. Upon initiation of cell division, microtubules depolymerize to tubulin, which repolymerize to form spindles that act as a framework on which duplicate chromosomes are transferred to the daughter cell.

Drugs such as vinblastine **1.20** and vinblastine **1.21** (Figure 1.14) bind to tubulin and prevent this polymerization/depolymerization cycle, inhibiting tumor growth.

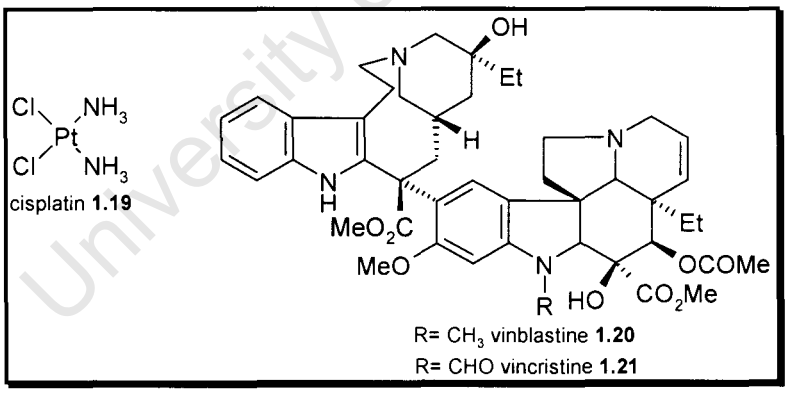

Figure 1.14: Chemical structures of cisplatin, vinblastine and vicristine

The available chemotherapeutic agents often bring on serious side effects that limit the doses physicians can administer, and many of the most common cancers are not yet curable with chemotherapy alone and thus also involve surgery and radiation. Some of the current chemotherapy has another fundamental weakness, that being drug resistance to structurally and functionally unrelated chemotherapeutic agents.

References

1. Bruce-Chwatt, L. J. *Chemotherapy of Malaria*, 2nd ed. Geneva, World Health Organization, **1981**.
2. Poser, C.M.;Bruyn, G.W. *An illustrated History of Malaria*, 1st ed. London, The Parthenon publishing Group, **1999**.
3. "Malaria" Microsoft®Encarta® Online Encyclopedia, **2001**. http://encarta.msn.com ©1997 – 2001 Microsoft Corporation.
4. Gardner, M.J.; Hall, N.; Fung, E.; White, O.; Berriman, M.; Hyman, R.W.; Carlton, J.M.; Pain, A.; Nelson, K.E.; Bowman, S.; Paulsen, I.T.; James, K.; Eisen, J.A.; Rutherford, K.; Salzberg, S.L. *et al*: *Nature*, **2002**, *419*, 498.
5. Phillips, R.S. *Studies in Biology no. 152 Malaria*, 1st ed., London, Edward Arnold Ltd, **1983**.
6. WHO: *The World Health Report 2000. Health Systems: Improving Performance*, World Health Organization, Geneva, **2000**.
7. http://www.rbm.who.int/wmr2005/html/map1.htm
8. Kumar, A.; Katiyar, S. B.; Agarwal, A.; Chauhan, P. M. S. *Curr. Med. Chem.*, **2003**,*10*, 1137.
9. Trager, W.; Jensen, J.B. *Science*, **1976**, *193*, 673.
10. http://www.tiscali.co.uk/lifestyle/healthfitness
11. Rosenthal, P.J.; Meshnick, S.R. *Mol. Biochem. Parasitol.*, **1996**, *83*, 131.
12. Sherman, I.W.; Tanigoshi, L. *Int. J. Biochem.*, **1970**, *1*, 635.
13. Loria, P.; Miller, S.; Foley, M.; Tilley, L. *Biochem. J.*, **1999**, *339*, 363.
14. Ginsburg, H.; Famin, O.; Zhang, F.; Krugliak, M. *Biochem. Pharmacol.*, **1998**, *56*, 1305.
15. Krugliak, M.;Zhang, F.;Ginsburg, H. *Mol. Biochem.Parasitol.*, **2002**, *119*, 249
16. Lew, V.L.; Tiffert, T.; Ginsburg, H. *Blood*, **2003**, *101*, 4189.
17. Ginsburg, H. *Blood Cells*, **1990**, *16*, 225.
18. Egan, T.J.; *Drug Design Reviews Online*, **2004**, *1*, 93.
19. Eggleson,K.K.; Duffin, K.L.; Goldberg D.E. *J. Biol. Chem.*, **1999**, *274*, 32411.
20. Gluzman, I.Y.; Francis, S.E.; Oksman, A.; Smith, C.E.; Duffin, K.L.; Goldberg, D.E., *J. Clin. Invest.*, **1994**, *93*, 1602.
21. Banerjee, R.; Liu, J.; Beatty, W.; Pelosof, L.; Klemba, M.; Goldberg, D.E. *Proc. Natl. Acad. Sci. USA*, **2002**, *99*, 990.

22. Rosenthal, P.J.; Sijwali, P.S.; Singh, A.; Shenai, B.R. *Curr. Pharm. Des.*, **2002**, *8*, 1659.

23. http://www.tula.ed.

24. Salas, F.; Fichmann, J.; Lee, G.K.; Scott, M.D.; Rosenthal, P.J. *Infect. Immun.*, **1995**, *63*, 2125.

25. (a) Bailley, E.; Jambou, R.; Savel, J.; Jaureguiberry, G. *Protozol*, **1992**, *39*, 593; (b) Rosenthal, P.J. *Exp Parasitol*, **1995**, *80*, 272.

26. Hanspal, M.; Dua, M.; Takakuwa, Y.; Chishti, A.H.; Mizuno, A. *Blood*, **2002**, *100*, 1048.

27. Brown, W.J. *Exp. Med.*, **1911**, *13*, 290.

28. Hay, S.I.; Guerra, C.A.; Tatem, A.J.; Noor, A.M.; Snow, R.W. *The Lancet infectious diseases*, **2004**, *4*, 327.

29. http://www.micro.msb.le.ac.uk

30. Fidock, D.A.; Rosenthal, P.J.; Croft, S.L.; Brun, R.; Nwaka, S. *Nature Reviews*, **2004**, *3*, 509.

31. Ridley, R.G. *Nature*, **2002**, *415*, 686.

32. Chauhan, P.M.S.; Srivastava, S.K. *Curr. Med. Chem.*, **2001**, *8*, 1535.

33. Frederich, M.; Dogne, J-M.; Angenot, L.; Mol, P. D. *Curr. Med. Chem.*, **2002**, *9*, 1435.

34. Kumar, A.; Katiyar, S. B.; Agarwal, A.; Chauhan, P. M. S. *Curr. Med. Chem.*, **2003**, *10*, 1137.

35. Cohen, S.N.; Phifer, K.O.; Yielding, K.L. *Nature*, **1964**, *202*, 805.

36. Winstanley, P. *The Lancet Infectious Diseases*, **2001**, *1*, 242.

37. White, N.J.; Nosten, F.; Looareesuwan, S. *Lancet*, **1999**, *353*, 1965.

38. Borstnik, K.; Paik, I.H.; Posner, G.H. *Mini Rev. Med. Chem.*, **2002**, *2*, 573.

39. Aldieri, E.; Atragene, D.; Bergandi, L.; Riganti, C.; Costamagna, C.; Bosia, A.; Ghigo, D. *FEBS Lett.*, **2003**, *552*, 141.

40. de Dominguez, G.N.D.; Rosenthal, P.J. *Blood*, **1996**, *87*, 4448.

41. Rosenthal, P.J. *Emerging Infect.* Dis., **1998**, *4*, 1.

42. Rosenthal, P. J.; Lee, G. K.; Smith, R. E. *J. Clin. Invest.*, **1993**, *91*, 1052.

43. Olson, J. E.; Lee, G. K.; Seemenov, A.; Rosenthal, P. J. *Bioorg. Med. Chem.*, **1999**, *7*, 633.

44. http://www.nci.nih.gov/

45. Scientific American, *What you need to know about cancer*, 1st ed., USA,**1997**.

46. Patrick, G.L., *An Introduction to Medicinal Chemistry*, 2nd ed., New York, Oxford University Press, **2001**.

CHAPTER 2

4-AMINOQUINOLINE-BASED CHALCONES AND MANNICH BASE DERIVATIVES

2.1 Introduction

In this MSc project, one of the main objectives is to develop single agents that provide both inhibition of the growth of malaria parasites and of tumour cells. The strategy was to hybridize chalcone moieties and their Mannich base derivatives with the 4-aminoquinoline moiety. This dual drug concept uses the basic structure of various known antimalarial or anticancer pharmacophores and/or bioactiphores, with different modes of action, in order to exert maximum activity and overcome or prevent drug resistance. The following chapter describes the known antimalarial and anticancer activities of the aforementioned organic scaffolds and the concept of cyclodextrin inclusion complexes in an attempt to render these dual drugs water-soluble.

2.2 4-Aminoquinolines in Malaria

2.2.1 Introduction

Of all the current clinically established antimalarials, the 4-aminoquinolines have proven to be the most significant and efficacious for the treatment and prophylaxis of malaria. The most important of the 4-aminoquinolines, chloroquine was as a result of a rigorous antimalarial research program in the United States during World War II and has been the basis of antimalarial chemotherapy for over 50 years. Chloroquine is one of the most successful chemotherapeutic agents ever synthesized based on its safety, affordability and high efficacy. However, the spread of drug resistant parasites has reduced the efficacy of 4-aminoquinoline antimalarial drugs. Nonetheless, there remains a great deal of interest in 4-aminoquinolines, the sub-structural moiety of chloroquine vital for antimalarial activity, in the hope that new derivatives with similar properties, but that can circumvent resistance, could be developed.

2.2.2 Mechanism of Action

Despite many years of use and study, the exact mode of action of chloroquine and other 4-aminoquinoline antimalarials remain to be elucidated. It has been known since the 1960s that chloroquine and other 4-aminoquinolines form complexes with haematin[1] and there is now considerable evidence that "haem" [either in the form of free haematin, histidine rich protein 2 (HRP-2) bound haematin or haemozoin] is the target of these drugs. Some of evidence leading to this conclusion includes the following:

i. Chloroquine is only active against the blood stages of the *Plasmodium* parasite, and in particular against the trophozoite stage during which haemoglobin degradation is maximal.[2]
ii. Plasmepsin inhibitors, which reduce the release of haematin from haemoglobin, are antagonists of quinoline antimalarials.[3]
iii. Although chloroquine is chiral, both enantiomers are active, signifying an achiral target, consistent with haematin.[4]
iv. The biological activity of chloroquine and 4-aminoquinoline derivatives are directly proportional to the degree of inhibition of β-haematin.[5]

In this view, the commonly accepted hypothesis of the observed antimalarial activity of the 4-aminoquinolines is interaction with haematin in the food vacuole of the parasite, inhibiting haemozoin formation and so interfering with the detoxification of haematin.

Selective accumulation of chloroquine in the food vacuole can be explained by its weak base properties, and occurs by passive diffusion. At neutral pH, chloroquine can diffuse freely through membranes, and upon entering the acidic food vacuole, chloroquine is protonated and trapped within the food vacuole. The precise manner in which the 4-aminoquinoline derivatives inhibit haemozoin formation and how this leads to parasite death is unresolved. One possibility is that the drugs form π-π complexes with free haematin, preventing its incorporation into haemozoin and so causing an accumulation of haem, which is toxic to the parasite. The chloroquine-haematin complex itself is also toxic to the parasite. However, the presence of haem does not seem to be fatal to the parasite as it can be disposed of by diffusion out of the cell or by degradation by reduced glutathione.[6] Thus it is presumably the formation of

the haem-chloroquine complex that is the toxic event as it protects haem from degradation by glutathione. The accumulation of haem or haem-chloroquine complex in the cytosol and membranes of the parasite causes or at least contributes to cell death. It is likely that these drugs inhibit parasite growth by a number of additive effects. The uncertainty over the mode of action of chloroquine and other 4-aminoquinolines is a serious obstacle in the rational design of novel drugs of this type

2.2.3 Mechanism of Chloroquine Resistance

Drug resistance in the case of malaria can be defined as "the ability of a strain of the malaria parasite to multiply or survive in the presence of normal dose or up to the maximum tolerated concentration of an antimalarial drug".[7] Resistance to chloroquine was first reported in 1959 in South America and since then has spread to most malaria endemic areas of the world. The fact that chloroquine resistance appeared many years after its use suggests the resistance has a mutagenic basis. Chloroquine-resistant parasites accumulate less drug in the food vacuole than the chloroquine-sensitive strains, excluding the drug from its site of action.[8] This could be a result of enhanced efflux, reduced uptake or a combination of both. Chloroquine resistance has been attributed to enhanced efflux, a mechanism known to operate in multi-drug resistant cancer cells. Resistance in these multi-drug resistant cancer cells can be reversed *in vitro* by the chemosensitiser verapamil and it has been confirmed that verapamil could improve the sensitivity of chloroquine resistant parasites to chloroquine, suggesting a similar mechanism of resistance. Multi-drug resistance (MDR) in cancer cells is brought about through the action of an ATP-dependent transport protein called P-glycoprotein (Pgp), which pumps the drugs away from its site of action.[9] *P. falciparum* possesses a transmembrane glycoprotein, P-glycoprotein homologue 1 (Pgh1), coded for by the gene *pfmdr1* which resembles the mammalian protein Pgp.[10] Based on the current evidence available, chloroquine resistance cannot be conferred by Pgh1 alone and requires mutations in other genes. Recently, resistance is strongly linked to mutations in the *pfcrt* gene, which codes for the protein PfCRT (*P. falciparum* chloroquine resistance transporter) located on the food vacuole membrane of the intraerythrocytic parasite.[11,12] A common mutation across chloroquine resistant strains is K67T, with PfCRT possibly being the primary protein responsible for the resistance.

Hypotheses for reduced drug accumulation due to altered uptake rate include mutations in the Na^+/H^+ exchanger[13], change in vacuolar pH[14] and alteration in membrane permeability.

2.2.4 Overcoming Chloroquine Resistance

Chloroquine resistance may be reversed by two possible methods; that is with the use of chemosensitisers or by making structural changes to the drug. Ideally, chemosensitisers are structurally and functionally distinct compounds without any inherent cytotoxicity, which can completely reverse the resistance of cells to the action of the drug. Since the initial demonstration of verapamil chemosensitisation of chloroquine-resistant parasites, many other agents have been identified that are capable of reversing resistance *in vitro* to some extent.[15] All of these compounds contain a protonatable nitrogen and sensitise resistant *P. falciparum* to chloroquine by increasing drug accumulation. The phenomenon of chemosensitisation has been extended to other quinoline type drugs that show resistance and future prospects for the use of quinoline compounds have thus improved considerably.

There are a significant number of review articles reporting on the antimalarial properties of 4-aminoquinolines.[5,15-18] Studies reporting on the structural modifications to chloroquine and the resultant effect on activity against chloroquine resistant parasites are also numerous. Chloroquine analogues that retain the 4-amino-7-chloroquinoline moiety but in which the aminoalkyl side chain is changed are active against chloroquine resistant parasites. This is observed in compounds with shortened (2-3 carbon) and lengthened (10-12 carbon) side chains,[19] those with shortened side chains with methyl branches and bulky groups attached to the terminal amine[20] and those with bulky groups such as ferrocene in the side chain.[21] Modifications to the aminoquinoline nucleus such as replacement of the 7-chloro group or substitutions on the aminoquinoline ring had only moderate effects or no effect at all.[19] Removal of the 7-chloro group actually resulted in a marked decrease in antiplasmodial activity and is thus crucial for activity. Due to the likelihood that these structurally modified compounds act against the same target as chloroquine, this target remains a useful one in the design of novel drugs. There are also a number of examples in the literature of

dual acting drugs incorporating the 4-aminoquinoline moiety. Some examples include:

i. The 4-aminoquinoline hydroxamate-based1,4-bis(3-aminopropyl) piperazines **2.1** (Figure 2.1) which potentially target the *Plasmodium falciparum* aminopeptidase of the M1 family of metalloproteases (PfA-M1) as well as inhibiting haemozoin formation.[22]

ii. The 4-aminoquinoline-based glyoxylylhydrazones **2.2** (Figure 2.1), which may act as cysteine protease inhibitors and metal chelating agents, thus potentially targeting the falcipains and the metalloproteases falcilysin and PfA-M1.[23]

iii. The isatin-based 4-aminoquinoline thiosemicarbazones **2.3** (Figure 2.1), which have activity against the cysteine protease falcipain 2 and are also capable of metal chelation and inhibition of haemozoin formation.[24]

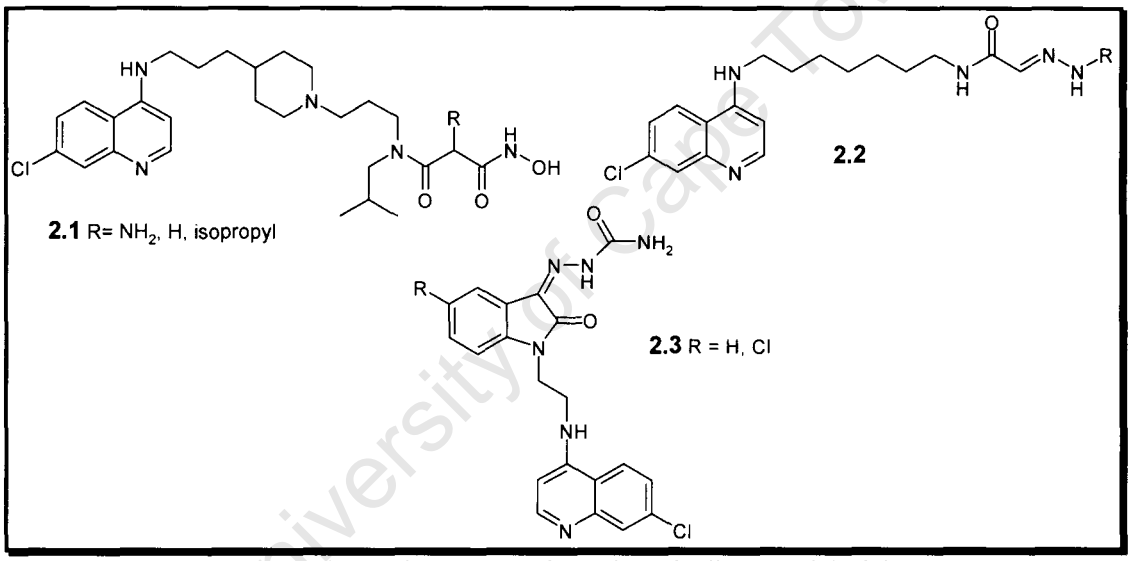

Figure 2.1: Chemical structures of 4-aminoquinoline-based dual drugs

2.3 Quinoline Derivatives in Cancer Therapy

2.3.1 Background

Chloroquine and other quinolines have demonstrated the ability to act as multi-drug resistance reversal agents.[25-28] A number of quinolines including chloroquine have also been reported to act as differentiating-inducing agents, that modulate gene expression to control tumor growth.[29] A series of quinoline derivatives have been reported as potent and selective cytotoxic agents.[30,31] Recently, chloroquine has been reported to inhibit cell growth and induce cell death.[32] These activities of chloroquine and other quinoline derivatives are discussed below.

2.3.2 Multi-drug Resistance Reversal Agents

Multi-drug resistance (MDR) is a major obstacle in cancer chemotherapy. As discussed in the previous section (2.2.3), it is generally believed that the most common mechanism of resistance is P-glycoprotein-mediated MDR. Increased expression of P-glycoprotein (Pgp), which is expressed on the plasma membrane of drug-resistant tumor cells, lowers the intracellular concentration of cytotoxic agents by effluxing them out of the cells. MDR reversal agents are thought to compete with anticancer drugs in binding to Pgp, or block the efflux mechanism, thus resulting in a decrease of drug efflux.[9,33] Chloroquine and various quinoline derivatives were studied *in vitro* and shown to act as multi-drug resistance reversal (MDRR) agents for vincristine-resistant and vinblastine-resistant cancer cell lines.[25] It was found that some derivatives were more effective MDRR agents than verapamil and showed very low toxicity.[34] Quinine and its derivatives have shown activity *in vitro* and *in vivo* as a MDR reverters in non-Hodgkin's lymphoma, vinblastine-resistant and hormone-refractory prostate cancer cells.[26-28] The structural requirements important for MDR activity in quinoline derivatives are the presence of a nitrogen atom, a hydrophobic moiety, two or more planar aromatic rings and a positive charge at physiological pH.[25,33] When the quinoline ring is replaced by a naphthyl or phenyl ring, activity decreases considerably. Thus the quinoline moiety plays an important role in drug activity.[25]

2.3.3 Differentiation-inducing Quinolines

Differentiation therapy entails the use of chemotherapeutic agents that modulate gene expression to control tumor growth.[29] The therapeutic effect of most current differentiation-inducing agents is not strong when compared to conventional chemotherapeutic agents and are used in combination with conventional chemotherapy or radiation therapy to potentiate the effect.[35] In a study conducted by Strobel *et al* it was demonstrated *in vitro* that various quinoline derivatives stimulated cell differentiation at growth inhibitory concentrations in MCF-7 human breast tumor cells.[29] Among the compounds tested, quinolines with a 4-substitution such as chloroquine, hydroxychloroquine, amodiaquine, quinidine and quinine, were most active in differentiation assays.

Three potential mechanisms are proposed to account for the observed cell growth inhibition and differentiation: (i.) E2F1 suppression, (ii.) DNA damage and (iii.) histone deacetylase (HDAC) inhibition.[29]

i. The transcription factor E2F1 is a cell regulatory protein that promotes cell growth by stimulating the G1-S cell cycle transition. It also plays a role in cell differentiation, with down- regulation necessary for differentiation of cells, as well as having the potential to initiate apoptosis in cells, making E2F1 an excellent molecular target. Strong suppression of E2F1 alone inhibits growth by preventing cell cycle progression. The data in the study demonstrated that suppression of E2F1 by the quinoline derivatives is characteristic of *in vitro* activity and is thus consistent with these hypotheses.

ii. Moderate suppression of E2F1, together with generation of DNA damage, also promotes differentiation through activation of the p53-Rb pathway. The quinoline derivatives screened exhibited variable capacities to induce DNA damage and apoptosis.

iii. Histone deacetylases are a common target of tumor differentiation agents[36] and interestingly many of the HDAC inhibitors were initially used as antiprotozoal agents.[37] Histones are proteins that form a scaffold around which a cell's DNA is wrapped. Modification of these histone proteins by acetylation controls the tightness of the DNA around the histone proteins and, consequently, controls the expression of the genes. In cancer, increased HDAC expression results in deacetylation of histone proteins, which causes the DNA to be wrapped too tightly around the histones, thereby inhibiting gene expression. The inappropriate deacetylation of tumor suppressor genes, a molecular defect, may silence these genes, resulting in the progression of cancer. HDAC inhibitors selectively switch on these tumor suppressor genes, something traditional chemotherapy may not do.

2.3.4 Anti-tumor Activity of Quinoline Derivatives

Quinoline derivatives have been evaluated *in vitro* as anti-tumor agents in comparison to available drugs such as adriamycin and vincristine. Abel *et al* reported a series of azoylylalkylquinolines that were more cytotoxic on KB cells (human nasopharyngeal carcinoma) and L1210 cells (murine lymphocytic leukemia) in comparison to

adriamycin.[30] Another study conducted evaluated the anticancer activity of another series of quinoline derivatives against the human breast cancer T47D cell line, with some compounds showing a growth inhibitory effect greater than that of vincristine and similar to that of adriamycin.[31] Recently chloroquine has demonstrated the ability to inhibit cell growth and induce cell death, depending on the concentration administered, in A549 lung cancer cells.[32] It was found at concentrations from 0.25 - 32 μM, chloroquine inhibited A549 lung cancer proliferation by increasing lysosomal volumes and thus enlarging the plasma membrane surface. Apoptosis and necrosis occurred at chloroquine concentrations above 32 μM. Chloroquine thus may be of use in lung cancer therapy by careful dosage administration. Therefore, from the evidence mentioned above, potential anti-tumor agents containing a quinoline ring are good candidates for further investigation.

2.4 Justification for Research into Aminoquinolines

As it has been demonstrated in sections 2.2 and 2.3, future research into aminoquinoline derivatives is still warranted and justified on the basis of several considerations:

- Aminoquinolines have proven to be the most successful class of compounds for the treatment and prophylaxis of malaria
- Drug resistance is due to reduced drug accumulation and there is no change in the structure of the drug target
- Analogues of chloroquine have shown activity against chloroquine resistant strains of the parasite
- Haemoglobin degradation pathway has a proven history of being an excellent therapeutic target
- 4-Aminoquinolines have acceptable toxicity profiles and are well tolerated
- Shown to act as multi-drug resistance (MDR) reversal agents of certain cancer cell lines
- Quinoline derivatives have demonstrated the ability to act as anti-tumor and differentiation-inducing agents.
- Chloroquine and other quinoline derivatives have shown inhibition of cell growth and induction of cell death in certain cancer cells.

2.5 Bioactivities of Chalcones

2.5.1 Introduction

Chalcone is a broad term given to compounds that have a 1,3-diphenylprop-2-en-1-one scaffold (Figure 2.2) and occur naturally in plants as precursor compounds for synthesis of different classes of flavonoids. There has been a resurgence of scientific interest in this group of natural products due to a wide range of beneficial biological activities, which are reliant on the structural modifications made to the chalcone scaffold. Some examples include substituents on the aromatic rings A and B,[38] replacement of the phenyl rings with various heterocyclic and polyaromatic rings,[39] substitution on the enone linker[40] and cyclisation of the chalcone.[41]

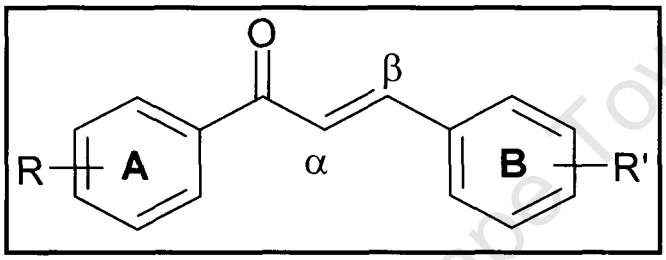

Figure 2.2: General structure of chalcones indicating rings A and B

The presence of the reactive α-β-unsaturated system and the relative flexibility of chalcones allow interactions with a diverse range of enzymes and receptors, thus chalcones are recognized as a "privileged structure" in drug design. Pharmacological activities cited in the literature include anti-inflammatory,[42] antileishmanial,[38,43] anti-invasive,[44] nitric oxide inhibition[45] and modulation of P-glycoprotein-mediated multi-drug resistance,[46] to name but a few. In the context of this project, antimalarial, anti-proliferative and tumour-reducing properties are known and will be discussed in the sections that follow. The multiple activities and structural diversity of chalcones make this class of compounds a good candidate as dual acting drugs, to provide inhibition of both the malaria parasite and tumour growth.

2.5.2 Antimalarial Activity of Chalcones

Interest in the antimalarial activity of chalcones was encouraged by the discovery of licochalcone A (Figure 2.3), an oxygenated chalcone isolated from the roots of Chinese liquorice, which showed significant antimalarial activity *in vitro* and *in vivo*.[47] At about the same time, a separate study confirmed the antimalarial activity of

chalcones and their derivatives using both molecular modelling and *in vitro* testing, with malarial cysteine protease acting as the most likely target.[39]

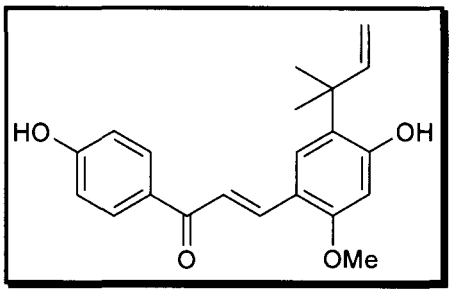

Figure 2.3: Chemical structure of licochalcone A

Most of the activity of chalcones is due to the α-β-unsaturated system, which is a Michael acceptor and is capable of undergoing conjugate addition with the sulfhydryl group of the cysteine side chain (Figure 2.4). In addition, this conjugated linker generates a linear, almost planar structure, that has been demonstrated by modelling programs to have favourable interactions with the long cleft of the active site of malarial cysteine protease.[39]

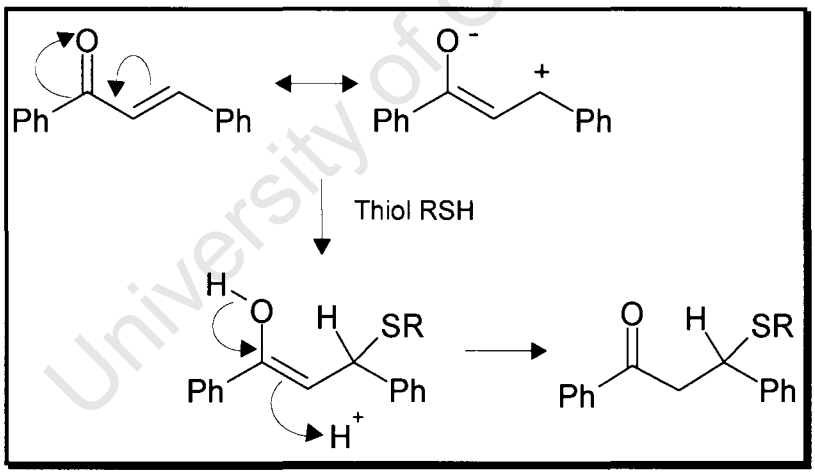

Figure 2.4: Reaction of a representative chalcone (Michael acceptor) and a nucleophilic thiol (RSH)[48]

However, investigations into cysteine protease inhibition as the mode of action has established that antimalarial activity is not always correlated with inhibition of malarial cysteine protease[49] and this comes as no surprise due to the wide range of pharmacological properties of chalcones.[50] A more recent target investigated for antimalarial chalcones are the parasite-induced new permeability pathways.[51] New permeability pathways (NPP), that are absent from the uninfected erythrocyte membrane, are induced by the malaria parasite and cause the infected erythrocyte to

have a higher permeability to a range of low molecular weight solutes, inorganic and organic ions, amino acids, sugars and nucleosides. The primary role of NPP is thought to be acquisition of nutrients but there is evidence that shows that they may have a bifunctional role and are also required for the removal of metabolic waste from the infected cells,[52] making these pathways an attractive drug target. A series of chalcones with known antimalarial activity were screened as inhibitors of new permeability pathways and a significant number had good activity.[51] The structural requirements for antimalarial activity in chalcones will be discussed in section 3.1.1.

2.5.3 Cytotoxic and Chemoprotective Properties of Chalcones

Chalcones have been identified as cytotoxic and chemoprotective agents by various research groups, and have exhibited anticancer activity against a variety of cancer cell lines and animal cancer models. The recognition of these broad anticancer properties have resulted in a sustained interest in chalcones and in understanding how they exert their cytotoxic or chemoprotective activity.

2.5.3.1 Cytotoxic Chalcones

Chalcones have displayed cytotoxic activity against many different tumour cell lines in the low micromolar range (IC_{50} < 50μM).[48] Most of the reports of anticancer activity are focused on the anti-mitotic activity of chalcones. Edwards *et al* proposed that chalcones interact with the thiol residue present at the binding site of tubulin,[53] interfering with the dynamics of tubulin polymerisation and depolymerisation, leading to mitotic arrest. This hypothesis was based on the structure-activity relationships of colchicine-tubulin binding and the observation of preferential reactivity of the enone moiety of chalcones towards thiols, thus implying chalcones should interact in a similar way to colchicine. This hypothesis has been backed up by a subsequent study in which an alkoxylated chalcone was shown by cell cytometry to cause an accumulation of cells in the G2/M phase, which is an indication of disruption of the mitotic spindle.[54] Chalcones also react readily with glutathione (GSH), a protein thiol important for detoxification of xenobiotics. This chalcone-GSH interaction has been widely investigated[55] and has shown to increase the toxicities of chalcones. Indeed, depletion of intracellular GSH is associated with pathways leading to apoptosis and growth arrest.[56] Chalcone derivatives are capable of antagonizing interactions

between the human oncoprotein MDM2 and p53.[57] The MDM2 oncogene, which is over-expressed in a variety of tumours, inhibits the tumour suppressor protein p53 by binding to its transactivation domain and thus allowing cell cycle progression of defective cells. Chalcones have shown to bind in or near the tryptophan pocket of the p53 binding cleft of MDM2 and promote dissociation of the complex, releasing the tumour suppressor protein p53. There are numerous series of hydroxylated chalcones that have shown potent cytotoxic activities against tumour cell lines such as B16 murine melanoma, HCT 116 human colon cancer, A31 human epidermoid carcinoma as well as a non-tumour endothelial cell line (human umbilical venous endothelial cells or HUVEC).[58] Due to the fact that these cancers differ significantly in their genetic source as well as the observation of selective cytotoxicity towards the HUVEC cell line, the authors proposed that these chalcones act as angiogenesis inhibitors.[59] Other proposals for activity of hydroxychalcones include the induction of apoptosis,[60] and induction of mitochondrial uncoupling and membrane collapse.[61]

2.5.3.2 Chemoprotective Chalcones

Cancer is the culmination of years of genetic and biochemical changes in cells, rather than a single, fixed event and there is the possibility for intervention at several biological levels. Chemoprotection is an approach that uses natural or synthetic compounds to prevent, halt or reverse carcinogenesis. Chalcones were initially considered as chemoprotectants due to their structural similarity to stilbene, a motif found in anti-estrogen drugs such as tamoxifen, that has demonstrated the ability to prevent breast cancer in women who are at increased risk.[34,38] Secondly, the α-β-unsaturated system of chalcones can bind to certain receptors leading to either inhibition of enzymes important for a carcinogenic event or induction of phase II enzymes, a widely recognized chemoprotective mechanism.[48] The chemoprotective roles of chalcones are mainly due to their antioxidant properties and their ability to scavenge free radicals, which are involved in various stages of carcinogenesis.[48] A single antioxidant pharmacophore may not exist in chalcones but phenolic hydroxyl groups have been found important for antioxidant activity. Chalcones are potential inducers of phase-2 enzymes such as glutathione S-transferase and quinone reductase, which are involved in the metabolism of xenobiotics.[49] Chalcones can also exert an anti-invasive effect[44] and reduce nitric oxide production.[45]

2.6 Mannich Bases

2.6.1 The Mannich reaction

The Mannich (aminomethylation) reaction involves condensation of a substrate possessing a reactive hydrogen atom with a nonenolizable aldehyde, usually formaldehyde, and a primary or secondary amine (Scheme 2.1). The product of this multi-component condensation reaction is known as a Mannich base, in which an aminomethyl group replaces the active hydrogen of the substrate. Since the initial studies by Carl Mannich of the chemistry of this reaction, Mannich bases have been the subject of numerous mechanistic studies[62-64] and have received attention for their synthetic utility,[62,63,65] pharmaceutical activities and numerous other applications in polymer chemistry such as surface active agents, paints and dyes.[66]

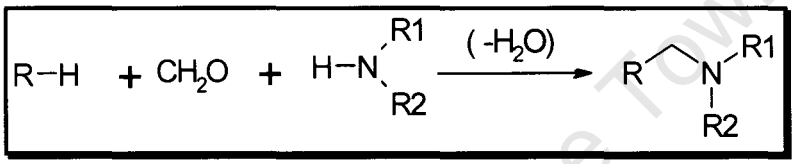

Scheme 2.1: Representation of the Mannich reaction

The interest in Mannich base derivatives of target compounds in this project is two-fold. Firstly, the Mannich reaction introduces a basic function that can increase the water-solubility via salt formation, which is important for bioavailability of target compounds. The basicity also ensures target compounds could potentially accumulate in the acidic food vacuole of the malaria parasite. Secondly, Mannich base derivatives of target compounds will be very reactive and at a lower pH associated with tumour cells or the acidic food vacuole, can undergo deamination leading to the formation of vinyl ketones. These generated vinyl ketones can potentially react with various cellular thiols important for parasite or tumour growth (described in sections 2.5.2 and 2.5.3). This change in pH may therefore be used as a prodrug concept whereby the cytotoxic agent is released at its site of action.

2.6.2 Antimalarial Mannich Bases

Since amodiaquine **1.2** (Figure 1.6, p11), a Mannich base derivative of chloroquine, was shown to be an effective antimalarial against chloroquine-resistant parasites, there have been numerous studies of structural analogues of amodiaquine that may potentially evade drug-resistance and yet maintain activity.[67-70] Amodiaquine however

has a low bioavailability and is rapidly metabolised to a bis-deethylated metabolite[71] or excreted as the 5'-glutathionyl ester.[72] Investigations into Mannich base compounds with structurally modified side chains that are less susceptible to metabolism led to antimalarials such as amopyroquine **2.4**, tebuquine **2.5** and the *tert*-butyl analogue **2.6** (Figure 2.5). All of these analogues were found to be more active against chloroquine-resistant strains of the *P. falciparum* parasite than amodiaquine and chloroquine.[67-70]

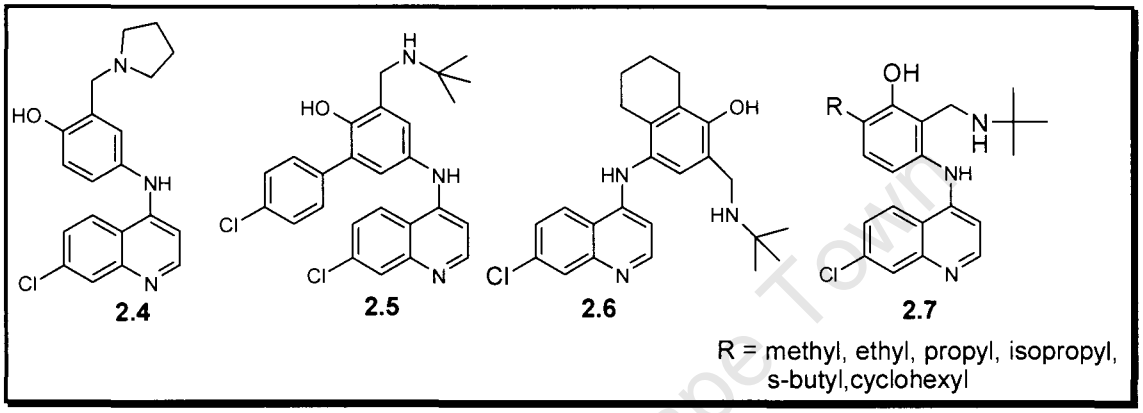

Figure 2.5: Chemical structures of amodiaquine analogues

Ward *et al* undertook a structure-activity investigation on *N-tert*-butylamino derivatives of amodiaquine **2.7** (Figure 2.5) to determine factors important for antimalarial activity.[69] The results indicated that replacement of the diethylamino group with a *N-tert*-butylamino group led to a substantial increase in activity in both chloroquine-resistant and chloroquine-sensitive strains. Drug lipophilicity and the type of alkyl side chain (especially a propyl or isopropyl group) at the 5' position were found to be important for activity. More recently, a high-throughput screening of compounds identified Mannich bases exemplified by the unsaturated Mannich base **2.8** (Figure 2.6) as a new set of thioredoxin reductase (TrxR) mechanism-based inhibitors.[73] An α-α-dimethyl-β-amino ketone **2.9** for which deamination is blocked and the saturated Mannich base 3-(dimethylamino)propiophenone **2.10** (Figure 2.6) were designed in order to determine the importance of two electrophilic sites for activity.

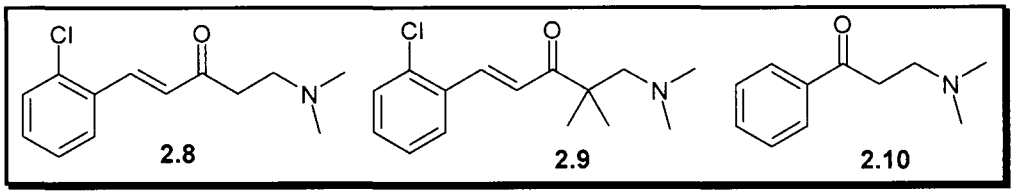

Figure 2.6: Mannich bases used for inactivation studies of TrxR

Thioredoxin reductase catalyses the reduction of the protein thioredoxin disulfide (Trx) to the dithiol in the presence of NADPH (equation 2.1).

$$NADPH + Trx(S)_2 \rightleftharpoons NADP^+ + Trx(SH)_2 \quad \text{(equation 2.1)}$$

TrxR shows potential as a drug target as it protects the parasite against oxidative stress and is essential for survival of the parasite.[74] Another favourable factor of TrxR as a antimalarial drug target is that the protein sequences at the C-terminal cysteine residue of parasitic TrxR differ significantly from human TrxR and thus inhibitors may be designed to interact specifically with the parasite enzyme.[73] Davioud-Charvet *et al*[73] hypothesised that the Mannich bases containing electrophilic centres could inactivate TrxR by interacting with the C-terminal cysteine residues, Cys 540' and Cys 535'. It was found that Mannich base **2.8**, which is capable of bisalkylation, was the most effective in comparison to **2.9** and **2.10** which only have one electrophilic centre capable of alkylation. The proposed mechanism for TrxR inactivation by the unsaturated Mannich base **2.8** is outlined in Scheme 2.2.

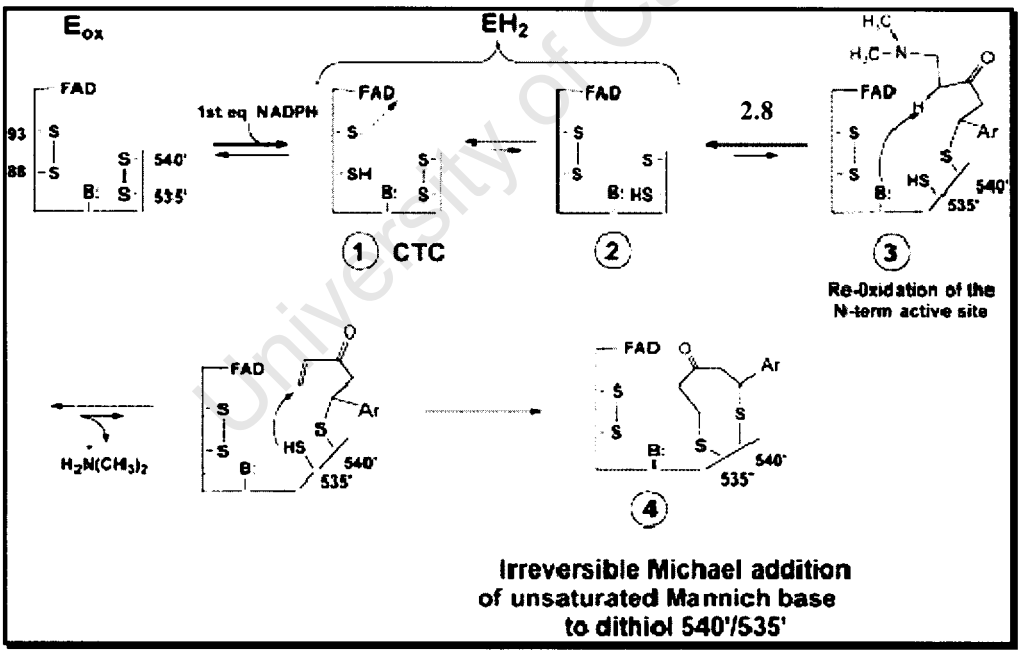

Scheme 2.2: The proposed mechanism for TrxR inactivation by **2.8**[73]

Inhibition of TrxR can only occur when the oxidized enzyme, (E_{ox}), is converted by NADPH to its predominant reduced form, EH_2. This two-electron-reduced form, which is characterized spectroscopically by the charge transfer complex (CTC)

observed at approximately 540 nm, makes the thiols at Cys 540' and Cys 535' available to attack the olefinic bond. The Mannich base **2.8** undergoes a Michael addition with the most exposed thiol Cys 540', and then His509' catalyses deamination of **2.8**, which is followed by addition of the thiol Cys535' to the generated double bond. The formation of the macrocyclic species **4** results in irreversible inactivation of the TrxR.

2.6.3 Anticancer Properties of Mannich Bases

Dimmock and collaborators have performed investigations into the anticancer and cytotoxic properties of Mannich bases.[55,75,76] Interest in Mannich bases was spurred by the fact that these compounds could act as prodrugs of α,β-unsaturated ketones since Mannich bases can undergo deamination at physiological pH. This deamination has been demonstrated *in vivo* and simulated *in vitro*.[75] There are several reasons for the evaluation of α,β-unsaturated ketones as anticancer agents. Firstly, these compounds react preferably as thiol alkylators and have an insignificant affinity for amino or hydroxy nucleophiles.[77] Hence shortcomings of certain alkylating agents such as mutagenicity[78] and carcinogenicity[79] due to interactions with nucleic acids are avoided. The mode of action of these compounds also differs from current alkylating agents such as melphalan, which is useful in overcoming resistance that has developed towards this drug. Indeed it has been demonstrated that these α,β-unsaturated ketones display cytotoxicity towards melphalan-resistant and melphalan-sensitive tumour cell lines.[80] Furthermore, these compounds have selective toxicity towards rapidly growing tumour cells compared with normal cells due to a higher demand of cellular thiols necessary in various processes of cell division and growth, as well as their involvement in detoxification mechanisms. Examples include inhibition of the mitotic phase of the cell cycle and inhibition of the enzyme TrxR and GSH necessary for detoxification of reactive oxygen species and xenobiotics. Results from numerous studies by Dimmock *et al* revealed that conversion of α,β-unsaturated ketones into their Mannich base derivatives, thus possessing two sites for thiol alkylation, was accompanied by an increase in bioactivity both *in vitro* and *in vivo*.[75] This was attributed to the concept of sequential toxicity[81] and several series of Mannich bases have been designed in light of this concept.[55,75,76] Of note are the Mannich base derivatives of chalcones that had significant activity towards murine P388 and L1210

as well as various other cancer cell lines.[55] The hypothesis of sequential cytotoxicity is shown in Scheme 2.3 for a representative chalcone Mannich base derivative. Initially there is a nucleophilic attack by the cellular thiol at the β-carbon of the olefinic bond (intermediate **A**), followed by deamination of the monothiol adduct (intermediate **B**) and attack by a second thiol at the generated double bond to give bisalkylated product **C**. This process of deamination and alkylation can occur again giving product **E**. Thus increased cytotoxic activity is not only due to the greater number of electrophilic sites available for nucleophilic attack by cellular thiols but also due to the successive release of two or more cytotoxic agents, which is more damaging to tumour cells than normal cells.[55]

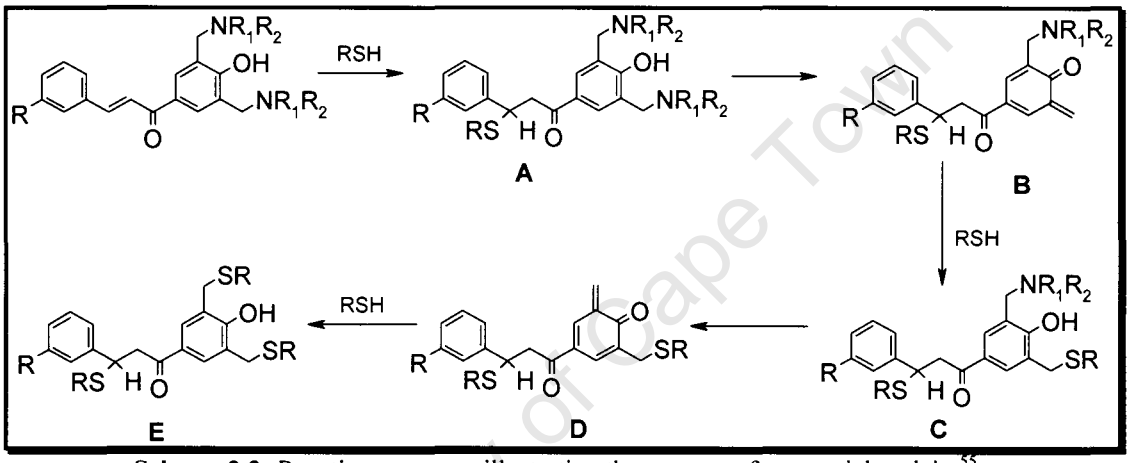

Scheme 2.3: Reaction sequence illustrating the concept of sequential toxicity[55]

The increased reactivity of Mannich base derivatives of compounds containing an α,β-unsaturated system may also be due to the stabilization effect of the reaction intermediate shown in Figure 2.7. This stabilization is aided by the inductive effect of the quadrivalent nitrogen atom and hydrogen bonding.

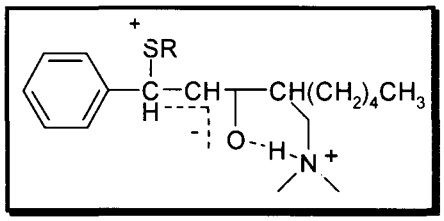

Figure 2.7: Stabilization of reaction intermediate[75]

Thus, Mannich base derivatives of chalcones are novel alkylating agents that display significant cytotoxic activity as well as being free mutagenic effects, making these compounds potentially valuable chemotherapeutic agents.

2.7 Cyclodextrins

2.7.1 Chemical and Physical Properties of Cyclodextrins

Cyclodextrins (CDs) are cyclic, toroidal shaped oligosaccharides that are the products of the enzymatic degradation of starch. Due to the unspecificity of the glucosyltransferase enzyme, the cyclic oligosaccharides are composed of *D*-glucopyranose units of various lengths linked by α-1,4-glycosidic bonds.[82] There are three major or parent cyclodextrins and several minor, rare ones that differ from each other by the number of glucopyranose units. The α-, β- and γ-cyclodextrins are made up of 6, 7 and 8 glucose units respectively and are crystalline, homogenous and nonhygroscopic substances[83] (Figure 2.8).

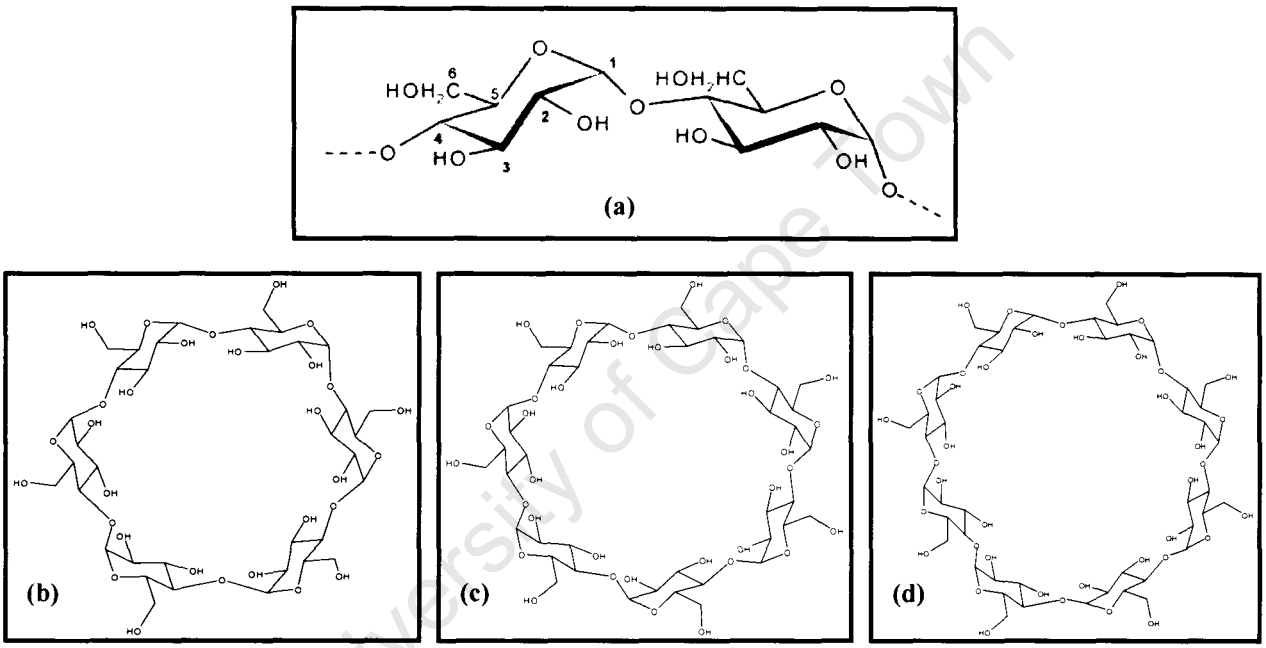

Figure 2.8: Schematic diagram of (a) conformation and labelling of glucopyranose unit, (b) α-CD, (c) β-CD and (d) γ-CD

As a consequence of the rigid ^{4}C1-chair conformation of the glucopyranose units and intramolecular hydrogen bonding between O2-H···O3` and O2...H-O3`, the CDs have overall shape reminiscent of a 'truncated cone.' Intramolecular, interglucose hydrogen bonds stabilize the conformation of the CD macrocycles. Cyclodextrins have a hydrophobic cavity and a hydrophilic exterior. The hydrophobicity arises due to the cavity containing hydrogen atoms from the C3-H and C5-H methane groups, the C6-H_2 methylene groups and the glycosidic oxygens (O4). The hydrophilic exterior is due to the primary hydroxyl groups (O6) on the narrower side of the cone and the secondary hydroxyl groups (O2, O3) on the wide side of the cone. As a consequence,

cyclodextrins are soluble in aqueous media and are capable of encapsulating hydrophobic guest molecules within their cavities. In order to improve solubility's of parent cyclodextrins, especially β-CD, the hydroxyl groups can be chemically modified. For this purpose, the O2 and O6 positions of β-CD have been methylated to form heptakis(2,6-di-O-methyl)-β-cyclodextrin (DIMEB) and additionally at the O3 position to form heptakis(2,3,6-tri-O-methyl)- β-cyclodextrin (TRIMEB). Some of the characteristics of the parent cyclodextrins are summarized in Table 3.

Table 3: Characteristics of α-CD, β-CD and γ-CD[83]

	α-CD	β-CD	γ-CD
No. of glucose units	6	7	8
Mol. wt	972	1135	1297
Cavity diameter/Å	4.7 5.3	6.0 6.5	7.5 – 8.3
Height of torus/ Å	7.9 ± 0.1	7.9 ± 0.1	7.9 ± 0.1
Approx. volume of cavity/ $Å^3$	174	262	427
Solubility in water/ g $100ml^{-1}$ at 25°C	14.5	1.85	23.2
Crystal forms of water	Hexagonal plates	Monoclinic prisms	Monoclinic prisms

2.7.2 Cyclodextrin Inclusion Complexes

The most important feature of cyclodextrins is their ability to form inclusion complexes with various guest molecules. The cavity allows the CD to act as a host molecule to a variety of guest compounds. The inclusion of guest molecules can occur in two modes: molecular inclusion and lattice inclusion. Molecular inclusion involves encapsulation of a guest molecule within a single CD cavity. In lattice inclusion, the host molecules form solid lattices that contain voids that are capable of inclusion. Due to the size and hydrophobic nature of the cyclodextrin cavity, complexes are formed when the included molecule is compatible with the dimensions of the cavity and orientated in such a way as to achieve maximal contact between the hydrophobic part of the guest and the apolar CD cavity. Complex formation with larger molecules is also possible, with only certain groups or side chains fitting into the cavity. The inclusion of a guest in a CD cavity is essentially a substitution of the included water molecules by a less polar guest. The driving force of complexation is not fully understood with several factors contributing to the process.[84] An initial contributing factor was thought to be the replacement of 'high-enthalpy' water with a more

hydrophobic guest molecule (Figure 2.9),[83] which lowers the energy of the system (unfavoured polar/apolar interaction to more favoured apolar/apolar interaction). Additional factors such as van der Waals forces, hydrogen bonding and hydrophobic interactions as well as CD strain release have also been found to be important driving forces behind complexation.

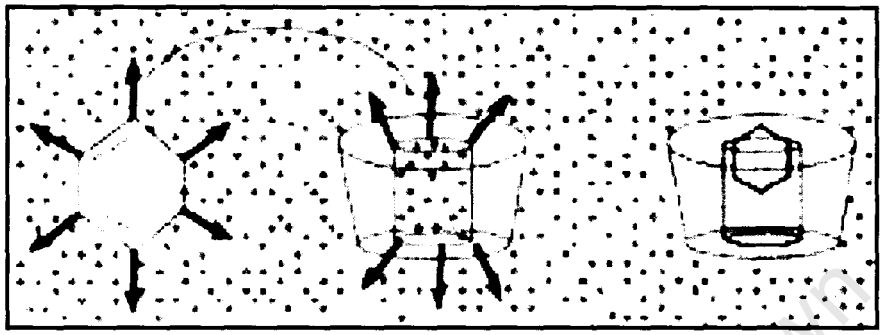

Figure 2.9: Hypothetical schematic representation of CD inclusion complex formation, where the small circles represent molecules of water[83]

The ability of cyclodextrins to form inclusion complexes has applications in food, cosmetics and pharmaceutical industries and for analytical purposes. *In the context of this project, the interest in cyclodextrins is due to their ability to act as solubilisers, stabilisers and carriers of poorly soluble drug molecules.*[85]

Cyclodextrins are true drug carriers, bringing the hydrophobic drug into solution, keeping it in a dissolved state, and transporting it to the lipophilic cell membrane. Due to the fact that the cell has a higher affinity for the drug than the CD, it remains in the aqueous phase and the bulk of the CD is metabolised in the colon by the colon microflora.[83] The primary metabolites (acyclic maltose, maltose and glucose) as with starch, are then further metabolised, absorbed and finally excreted as CO_2 and H_2O. The pharmaceutical use of cyclodextrin inclusion complexes requires that they are structurally characterised in order to verify complexation, so that regulatory requirements are met as well as to validate patent claims of novelty.[85] A number of analytical techniques may be used such as UV, IR and Raman spectroscopy, thin-layer chromatography, NMR spectroscopy, mass spectroscopy, X-ray diffraction, thermogravimetry and differential scanning calorimetry.[83,86] A convenient and relatively fast technique for determination of complexation is that based on the isostructurality of cyclodextrin inclusion complexes. Isostructurality is the

phenomenon whereby two or more crystalline phases have identical or quasi-identical packing motifs[87] and thus have similar unit cell dimensions and similar internal arrangement of molecules. This implies that common atoms of these phases have approximately the same co-ordinates.[88] Caira and co-workers have systematically classified the majority of the structurally characterized CD complexes obtained from the Cambridge Structural Database into distinct isostructural series.[85] The powder X-ray diffraction (PXRD) patterns within a series are essentially the same, regardless of the nature of the included guest.[85] Thus, comparisons of gross peaks can be made between experimental PXRD patterns and reference patterns of parent cyclodextrins and their complexes to determine if inclusion took place. Successful matching of the experimental pattern with the computed reference pattern not only establishes inclusion of the guest molecule but also generates important structural information such as crystal packing arrangement and space group.[85] *This technique served as the primary analytical tool for determination of inclusion complex formation within this project.*

2.8 AIMS AND OBJECTIVES

Overall Objective:

The main objective of this MSc study is to develop single agents that provide inhibition of both the growth of tumour cells and malaria parasites. This multi-therapeutic strategy is achieved by hybridising various known anti-malarial and anti-cancer pharmacophores and/or bioactiphores together with the 4-aminoquinoline moiety. For this purpose, hybrid molecules **1**, **2** and **3** (Figure 2.10) were designed as potential dual acting drugs.

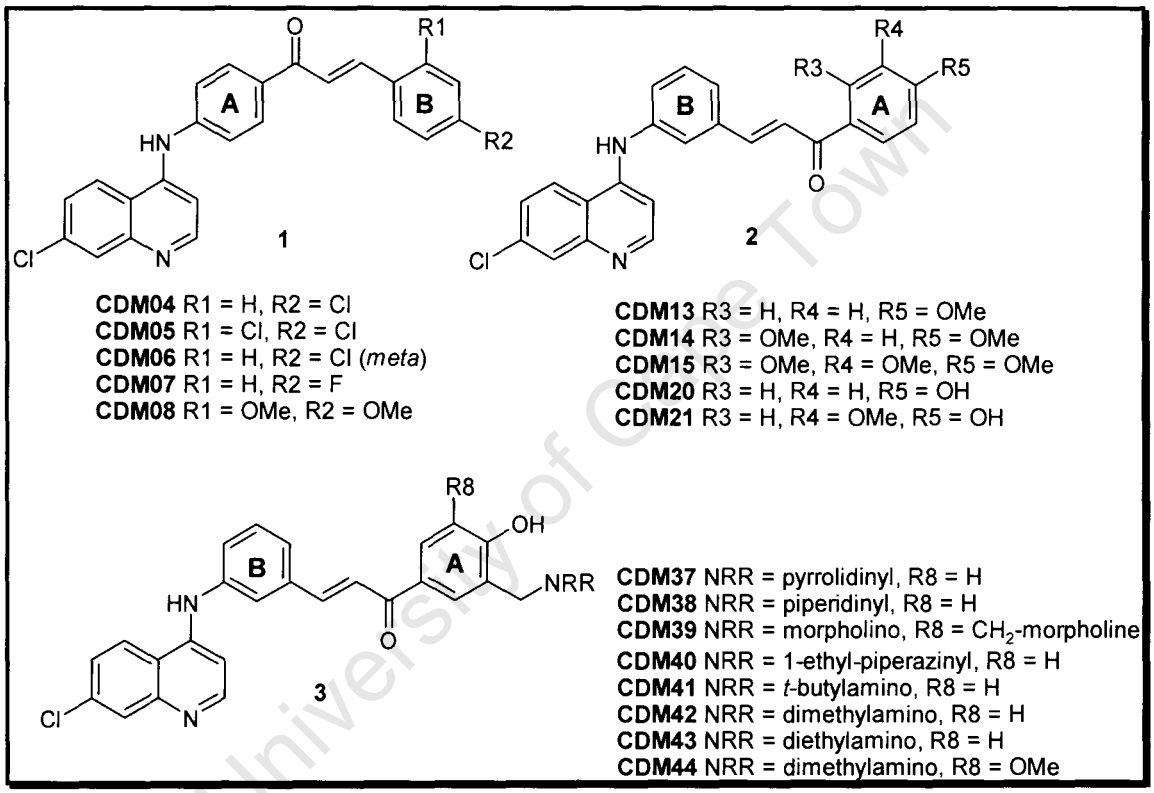

Figure 2.10: Chemical scaffold of target compounds

Specific Aims:

1. To synthesise novel exploratory libraries of 4-aminoquinoline-based chalcones and their Mannich base derivatives.
2. To improve water solubility properties of selected compounds by cyclodextrin inclusion and preparation of salt derivatives.
3. In collaboration with appropriate laboratories, to evaluate synthesised compounds *in vitro* in appropriate cancer and malaria disease models.

References

1. Cohen, S.N.; Phifer, K.O.; Yielding, K.L. *Nature*, **1964**, *202*, 805.
2. Slater, A.F.G. *Pharmac. Ther.*, **1993**, *57*, 203.
3. Mungthin, M.; Bray, P.G.; Ridley, R.G.; Ward, S.A. *Antimicr. Agents Chemother.*, **1998**, *42*, 2973.
4. Webster, R.V.; Craig, J.C.; Shyamala, V.; Kirby, G.C.; Warhurst, D.C. *Biochem. Pharmacol.*, **1991**, *42S*, S225.
5. Egan, T.J.; *Drug Design Reviews Online*, **2004,** *1*, 93.
6. Ginsburg, H.; Famin, O.; Zhang, F.; Krugliak, M. *Biochem. Pharmacol.*, **1998**, *56*, 1305.
7. Phillips, R.S. *Studies in Biology no. 152 Malaria*, 1st ed., London, Edward Arnold Ltd, **1983**.
8. Rosenthal, P. J.; Lee, G. K.; Smith, R. E. *J. Clin. Invest.*, **1993**, *91*, 1052; Olson, J. E.; Lee, G. K.; Seemenov, A.; Rosenthal, P. J. *Bioorg. Med. Chem.*, **1999**, *7*, 633; Yayon, A.; Cabantchik, Z.I.; Ginsburg, H. *EMBO J.*, **1984**, *3*, 2690.
9. O' Neill, P.M.; Bray, P.G.; Hawley, S.R.; Ward, S.A.; Park, B.K. *Pharmacol. Ther.*, **1998**, *77*, 29.
10. Foote, S. J.; Kyle, D. E.; Martin, R. K.; Oduola, A. M. J.; Forsyth, K.; Kemp, D. J.; Cowman, A. F. *Nature*, **1990**, *345*, 255 .
11. (a) Johnson, D. J.; Fidock, D. A.; Mungthin, M.; Lakshman, V.; Sidhu, A. B. S.; Bray, P. G.; Ward, S. A. *Mol. Cell*, **2004**, *15*, 867 – 877; (b) Bray, P. G.; Martin, E.R.; Tilley, L.; Ward, S. A.; Kirk, K.; Fidock, D. A. *Mol. Microbiol.*, **2005**, *56*, 323.
12. Fiddock, D. A.; Nomura, T.; Talley, A. K.; Cooper, R. A.; Dzekunov, S. M.; Ferdig, M. T.; Ursos, L. M. B.; Sidhu, A. B. S.; Naude, B.; Deitsch, K. W.; Su, X.-Z.;Wootton, J. C.; Roepe, P. D.; Wellems, T. E. *Mol. Cell*, **2000**, *6*, 861.
13. Sanchez, C.P.; Wűnsch, S.; Lanzer, M., *J. Biol. Chem.*, **1997**, *272*, 2652.
14. Geary, T. G.; Jensen, J. B.; Ginsburg, H. *Biochem. Pharmacol.*, **1986**, *35*, 3805– 3812; (b) Ginsburg, H.; Stein, W. D. *Biochem. Pharmacol.*, **1991**, *41*, 1463 –1470; (c) Bray, P. G.; Howells, R. E.; Ward, S. A. *Biochem. Pharmacol.* **1992**, *43*,1219.
15. Bray, P.G.; Ward, S.A. *Pharmacol. Ther.*, **1998**, *77*, 1.

16. Biot, C.; Chibale, K. *Infectious Disorders-Drug Targets*, **2006**, *6*, 173.
17. Deprez-Poulain, R.; Melnyk, P. *Comb. Chem. High Throughput Screen*, **2005**, *8*, 39.
18. Biagini, G.A.; O'Neill, P.M.; Nzila, A.; Ward, S.A.; Bray, P.G. *Trends Parasitol.*, **2003**, *19*, 479.
19. De, D.; Krogstad, F.M.; Byers, L.D.; Krogstad, D.J. *J. Med. Chem.*, **1998**, *41*, 4918.
20. Ridley, R.G.; Hofheinz, W.; Matile, H.; Jaquet, C.; Dorn, A.; Masciadri, R.; Jolidon, S.; Richter, W.F.; Guenzi, A.; Girometta, M.A.; Urwyler, H.; Thaithong, S.; Peters, W. *Antimicr. Agents Chemother.*, **1996**, *40*, 1846.
21. Chibale, K.; Moss, J.R.; Blackie, M.; van Schalkwyk, D.; Smith, P. J. *Tetrahedron Lett.*, **2000**, *41*, 6231.
22. Allary, M.; Schrevel, J.; Florent, I. *Parasitology*, **2002**, *125*, 1.
23. Ryckebusch, A.; Fruchart, J.-S.; Cattiaux, L.; Rousselot-Paillet, P.; Leroux, V.; Melnyk, P.; Grellier, P.; Mouray, E.; Sergheraert, C.; Melnyk, P. *Bioorg. Med. Chem. Lett.*, **2004**, *14*, 4439.
24. Chiyanzu, I.; Clarkson, C.; Smith, P.J.; Lehman, J.; Gut, J.; Rosenthal, P.J.; Chibale, K. *Bioorg. Med. Chem.*, **2005**, *13*, 3249.
25. (a) Zamora, J.M.; Beck, W.T. *Biochem. Pharmacol.*, **1986**, *35*, 4303; (b) Zamora, J.M.; Pearce, H.L.; Beck, W.T. *Mol. Pharmacol.*, **1988**, *33*, 454; (c) Suzuki, T.; Fukuzawa, N.; San-nohe, K.; Sato, W.; Yano, O.; Tsuruo, T. *J. Med. Chem.*, **1997**, *40*, 2047.
26. Miller, T.P.; Chase, E.M.; Dorr, R.; Dalton, W.S.; Lam, K.S.; Salmon, S.E. *Anti-Cancer Drugs*, **1998**, *9*, 135.
27. Solary, E.; Caillot, D.; Chauffert, B.; Casasnovas, R.O.; Dumas, M.; Maynadie, M.; et al. *J. Clin. Oncol.*, **1992**, *10*, 1730.
28. de Souza, P.L.; Castillo, M.; Myers, C.E. *Br. J. Cancer*, **1997**, *75*, 1593.
29. Martirosyan, A.R.; Rahim-Bata, R.; Freeman, A.B.; Clarke, C.D.; Howard, R.L.; Strobl, J.S. *Biochem. Pharmacol.*, **2004**, *68*, 1729.

30. (a) Abel, M.D.; Luu, H.T.; Micetich, R.G.; Nguyen, D.Q.; Nukatsuka, M.; Oreski, A.B.; Tempest, M.L.; Daneshtalab, M. *Drug Des. Discov.*, **1996**, *14*, 15; (b) Abel, M.D.; Ha, C.M.; Luu, H.T.; Micetich, R.G.; Nguyen, D.Q.; Oreski, A.B.; Tempest, M.L.; Daneshtalab, M. *Drug Des. Discov.*, **1996**, *14*, 31.

31. Rasoul-Amini, S.; Khalaj, A.; Shafiee, A.; Daneshtalab, M.; Madadkar-Sobhani, A.; Fouladdel, S.; Azizi, E. Intl. *J. Cancer Res.*, **2006**, *2*, 102.

32. Fan, C.; Wang, W.; Zhao, B.; Zhang, S.; Miao, J. *Bioorg. Med. Chem.*, **2006**, *14*, 3218.

33. Kawase, M.; Motohashi, N. *Current Drug Targets*, **2003**, *4*, 31.

34. Scientific American, a Special Issue, *What you need to know about cancer*, 1st ed., USA, **1997**.

35. Hitoshi, K.; Masatsugu, T.; Takahiro, F.; Yutaka, I. *Curr. Pharm. Des.*, **2006**, *12*, 379.

36. Marks, P.A.; Rifkind, R.A.; Richon, V.M.; Breslow, R. *Clin. Cancer Res.*, **2001**, *7*, 759.

37. Darkin-Rattray, S.J.; Gurnett, A.M.; Myers, R.M.; Dulski, P.M.; Crumley, T.M.; Allocco, J.J.; et al. *Proc. Natl. Acad. Sci. USA*, **1996**, *93*, 13143.

38. Nielsen, S.F.; Christensen, S.B.; Cruciani, G.; Kharazmi, A; Liljefors, T. *J. Med. Chem.*, **1998**, *41*, 4819.

39. Li, R.; Kenyon, G.; Cohen, F.E.; Chen, X.; Gong, B.; Dominguez, J.N.; Davidson, E.; Kurzban, G.; Miller, R.E.; Nuzum, E.O.; Rosenthal, P.J.; Mckerrow, J.H. *J. Med. Chem.*, **1995**, *38*, 5031.

40. Nielson, S.F.; Kharazmi, A.; Christensen, S.B. *Bioorg. Med. Chem.*, **1998**, *6*, 937.

41. Dimmock, J.R.; Zello, G.A.; Oloo, E.O.; Quail, J.W.; Kraatz, H.B.; Perjesi, P.; Aradi, F.; Takacs-Novak, K.; Allen, T.M.; Santos, C.L.; Balzarini, J.; De Clercq, E.; Stables, J.P. *J. Med. Chem.*, **2002**, *45*, 3103.

42. Herencia, F.; Ferrandiz, M.L.; Ubeda, A.; Dominguez, J.N.; Charris, J.E.; Lobo, G.M.; Alcaraz, M.J. *Bioorg. Med. Chem. Lett.*, **1998**, *8*, 1169.

43. Liu, M.; Wilairat, P.; Croft, S.L.; Tan, A. L-C.; Go, M-L. *Bioorg. Med. Chem.*, **2003**, *11*, 2729.

44. Mukherjee, S.; Kumar, V.; Prasad, A.K.; Raj. H.G.; Bracke, M.E.; Olsen, C.E.; Jain, S.C.; Parmar, V.S. *Bioorg. Med. Chem.*, **2001**, *9*, 337.

45. Rojas, J.; Paya, M.; Dominguez, J.N.; Ferrandiz, M.L. *Bioorg. Med. Chem. Lett.*, **2002**, *12*, 1951.

46. Bois, F.; Boumendjel, A.; Mariotte, A.; Conseil, G.; Di Petro, A. *Bioorg. Med. Chem.*, **1999**, *7*, 2691.

47. Chen, M.; Theander, T.G.; Christensen, S.B.; Hviid, L.; Zhai, L.; Kharazmi, A. *Antimicrob. Agents Chemother.*, **1994**, *38*, 1470.

48. Go, M.L.; Wu, X.; Liu, X.L. *Curr. Med. Chem.*, **2005**, *12*, 483.

49. Dominguez, J.N.; Charris, J.E.; Lobo, G.; de Dominguez, N.G.; Moreno, M.M.; Riggione, F.; Sanchez, E.; Olson, J.; Rosenthal, P.J. *Eur. J. Med. Chem.*, **2001**, *36*, 555.

50. Dimmock, J.R.; Elias, D.W.; Beazely, M.A.; Kandepu, N.M. *Curr. Med. Chem.*, **1999**, *6*, 1125.

51. Go, M-L.; Liu, M.; Wilairat, P.; Rosenthal, P.J.; Saliba, K.J.; Kirk, K. *Antimicrob. Agents Chemother.*, **2004**, *48*, 3241.

52. Saliba, K.J.; Martin, R.E.; Staines, H.M.; Kirk, K.A. In: Kozlowski, R.Z., editor. *Chloride channels*. Oxford: Isis Medical Media; **1999**, p. 137-48; Kirk, K. *Physiol. Rev.* **2001**, *81*, 495-537.

53. Edwards, M.L.; Stemerick, D.M.; Sunkara, P.S. *J. Med. Chem.*, **1990**, *33*, 1948.

54. Lawrence, N.J.; McGown, A.T.; Ducki, S.; Hadfield, J. A. *Anticancer Drug Des.*, **2000**, *15*, 135.

55. Dimmock, J.R.; Kandepu, N.M.; Hetherington, M.; Quail, J.W.; Pugazhenthi, U.; Sudom, A.M.; Chamankhah, M.; Rose, P.; Pasa, E.; Allen, T.M.; Halleran, S.; Szydlowski, J.; Mutus, B.; Tannous, M.; Manavathu, E.K.; Myers, T.G.; De Clercq, E.; Balzarini, J. *J. Med. Chem.*, **1998**, *41*, 1014;

56. Domenicotti, C.; Marengo, B.; Nitti, M.; Verzola, D.; Garibotto, G.; Cottalasso, D.; Poli, G.; Melloni, E.; Pronzato, M.A.; Marinari, U.M. *Biochem. Pharmacol.*, **2003**, *66*, 1521.

57. Stoll, R.; Renner, C.; Hansen, S.; Palme, S.; Klein, C.; Belling, A.; Zeslawski, W.; Kamionka, M.; Rehm, T.; Mühlhahn, P.; Schemacher, R.; Hesse, F.; Kaluza, B.; Voelter, W.; Engh, R.A.; Holak, T.A. *Biochemistry*, **2001**, *40*, 336.

58. Nam, N.H.; You, Y.J.; Kim, Y.; Hong, D.H.; Kim, H.M.; Ahn, B.Z. *Arch. Pharm. Res.*, **2002**, *25*, 590.

59. Nam, N.H.; You, Y.J.; Kim, Y.; Hong, D.H.; Kim, H.M.; Ahn, B.Z. *Eur. J. Med. Chem.*, **2003**, *38*, 179.

60. De Vincenzo, R.; Ferlini, C.; Distefano, M.; Gaggini, C.; Riva, A.; Bombardelli, E.; Morazzoni, P.; Valenti, P.; Belluti, F.; Ranelletti, F.O.; Mancuso, F.; Scambia, G. *Cancer Chemother. Pharmcol.*, **2000**, *46*, 305; Saydam, G.; Hakan Aydin, H.; Sahin, F.; Kueukoglu, O.; Ereiyas, E.; Terzioglu, E.; Buyukkececi, F.; Omay, S.D. *Leukemia Res.*, **2003**, *27*, 57.

61. Sabzevari, O.; Galati, G.; Moridani, M.Y.; Siraki, A.; O'Brien, P.J. *Chemico-Biological Interactions*, **2004**, *148*, 57.

62. Tramontini, M. *Synthesis*, **1973**, 703.

63. Tramontini, M.; Angiolini, L. *Tetrahedron,* **1990**, *46,* 1791.

64. Thompson, B.B. *J. Pharm. Sci.*, **1968**, *57*, 715.

65. Tramontini, M.; Angiolini, L. *Mannich Bases: Chemistry and Uses*, CRC Press: Boca Raton, **1994**.

66. Tramontini, M.; Angiolini, L.; Ghedini, N. *Polymer*, **1988**, *29*, 771.

67. Pussard, E.; Verdier, F.; Faurisson, F.; Clavier, F.; Simon, F.; Gaudebout, C. *Antimicrob. Agents Chemother.*, **1988**, *32*, 568.

68. Werbel, L.M.; Cook, P.D.; Elslager, E.F.; Hung, J.H.; Johnson, J.L.; Keston, S.J.; McNamara, D.J.; Ortwine, D.F.; Worth, D.F. *J. Med. Chem.*, **1985**, *29*, 924.

69. Raynes, K.J.; Stocks, P.A.; O' Neill, P.M.; Park, B.K.; Ward, S.A. *J. Med. Chem.*, **1999**, *42*, 2747.

70. Pang, X.; Wang, G.; Xing, Q. *Chin. J. Parasitol. Parasitic Dis.*, **1999**, *17*, 20.

71. Laurent, F.; Salvin, S.; Chretien, P.; Magnaval, J.F.; Peyron, F.; Sqalli, A.; Tufenkji, A.E.; Coulais, Y.; Baba, H.; Campistron, G.; Regis, H.; Ambrose-Thomas, P. *Arzneim.-Forsch. Drug. Res.*, **1993**, *43*, 612.

72. Harrison, A.C.; Kitteringham, N.R.; Clarke, J.B.; Park, B.K. *Biochem. Pharmacol.*, **1992**, *43*, 1421.

73. Davioud-Charvet, E.; McLeish, M.J.; Veine, D.M.; Giegel, D.; Arscott, L.D.; Andricopulo, A.D.; Becker, K.; Müller, S.; Schirmer, R.H.; Williams, Jr., C.H.; Kenyon, G.L. *Biochemistry*, **2003**, *42*, 13319.

74. Becker, K.; Gromer, S.; Schirmer, R.H.; Müller, S. *Eur. J. Biochem.*, **2000**, *267*, 6118; Krnajski, Z.; Gilberger, T.W.; Walter, R.D.; Cowman, A.F.; Müller, S. *J. Biol. Chem.*, **2002**, *277*, 25970.

75. Dimmock, J.R.; Kumar, P. *Curr. Med. Chem.*, **1997**, *4*, 1.

76. Dimmock, J.R.; Vashishtha, S.C.; Quail, J.W.; Pugazhenthi, U.; Zimpel, Z.; Sudom, A.M.; Allen, T.M.; Kao, G.Y.; Balzarini, J.; De Clercq, E. *J. Med. Chem.*, **1998**, *41*, 4012.

77. Baluja, G.; Municio, A.M.; Vega, S. *Chem. Ind.*, **1964**, 5053; Dimmock, J.R.; Raghavan, S.K.; Logan, B.M.; Bigam, G.E. *Eur. J. Med. Chem.*, **1983**, *18*, 248.

78. Cairns, J. *Nature*, **1980**, *286*, 176.

79. Farmer, P.B. *Chem. Brit.*, **1982**, *18*, 790.

80. Dimmock, J.R.; Kumar, P.; Quail, J.W.; Pugazhenthi, U.; Yang, J.; Chen, M.; Reid, R.S.; Allen, T.M.; Kao, G.Y.; Cole, S.P.C.; Batist, G.; Balzarini, J.; De Clercq, E. *Eur. J. Med. Chem.*, **1995**, *30*, 209.

81. Dimmock, J.R.; Sidhu, K.K.; Chen, M.; Reid, R.S.; Allen, T.M.; Kao, G.Y.; Truitt, G.A. *Eur. J. Med. Chem.*, **1993**, *28*, 313.

82. Szejtli, J. *Topics of Inclusion Science- Cyclodextrin Technology*, Davies, J.E.D. (Eds), Dordrecht, The Netherlands, Kluwer Academic Publishers, **1988**.

83. Szejtli, J.; Fromming, K.H. *Topics in Inclusion Science- Cyclodextrins in Pharmacy*, Dordrecht, The Netherlands, Kluwer Academic Publishers, **1994**.

84. Bender, M.I.; Komiyama, M. *Cyclodextrin Chemistry*, Berlin, Springer-Verlag, **1976**.

85. Caira, M.R. *Rev. Roum. Chim.*, **2001**, *46*, 371.

86. Szente, L. *Comprehensive Supramolecular Chemistry*, Atwood, J.L.; Davies, J.E.D.; MacNicol, D.D; Vögtle, F. (Eds.), UK, Pergamon, Ch.8, Vol.3, **1996**.

87. Kàlmán, A.; Pàrkányi, L. *Advances in Molecular Structure Research*, JAI Press Inc., **1997**, 189.

88. Fábiàn, L.; Kàlmán, A. *Acta Crystallogr.*, **1999**, *B55*, 1039.

CHAPTER 3

Synthesis and Characterization of Target Compounds

3.1 4-Aminoquinoline-based Chalcones

3.1.1 Rationale of Drug Design

The well-known antimalarial and anticancer properties of both chalcones and the 4-aminoquinoline unit, presented in the previous chapter, led to the design and synthesis of an exploratory group of 4-aminoquinoline-based chalcones. The rationale in this regard is based on a multi-therapeutic strategy in which the presence of two known antimalarial and anticancer pharmacophores should provide maximal inhibition of both the malaria parasite and tumour growth. These hybrid compounds may also potentially overcome or slow down drug resistance, as compounds aimed at multiple targets are less likely to be rendered ineffective compared to those aimed at a single target. The rationale for the design of target compounds is summarized in Figure 3.1.

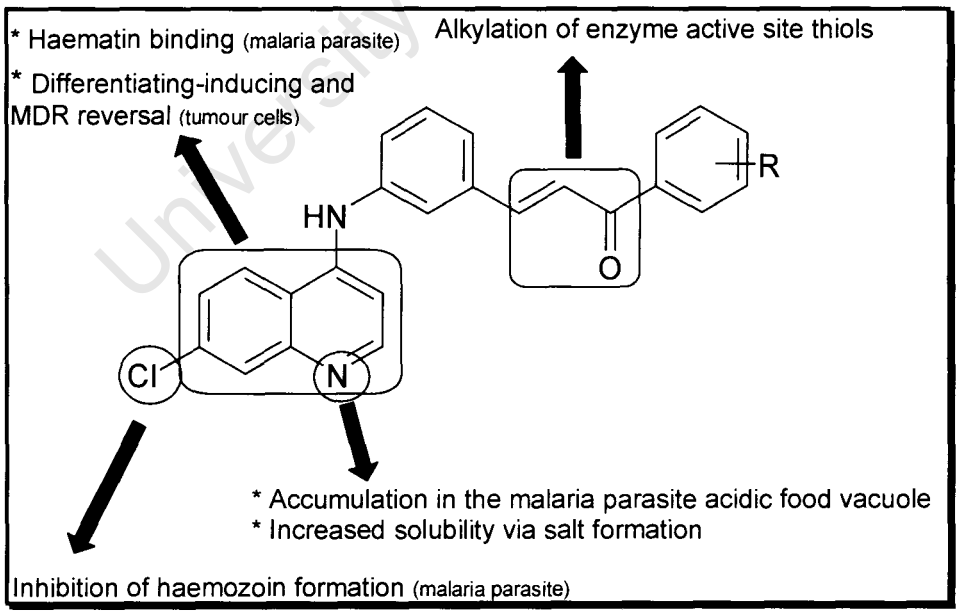

Figure 3.1: Rationale for design of target compounds

Various studies have been done on 4-aminoquinoline-haematin interactions in both aqueous and non-aqueous solutions using different analytical methods.[1] Although

there is dispute over the stoichiometry of interactions between the drug and haematin, it is generally considered that these complexes occur through pi-stacking of the aromatic ring of the drug over the porphyrin ring. This coplanar, hydrophobic interaction is the major source of stability of these π-π complexes. Structure-activity relationship studies have revealed that not only hydrophobic interactions but also electronic factors are important for haematin binding and thus inhibition of haemozoin formation.[2] The position of the electron-donating amino group on the aminoquinolines determines the extent of complexation, with only the 2- and 4-aminoquinolines forming strong complexes with haematin. This is due to an increase in electron density within the pyridine ring, which favours stacking over the electron poor region of the porphyrin ring.[1] Another electronic factor contributing to strong association of 4-aminoquinolines to haematin may be due to the resonance interaction between the amino group and the quinoline nitrogen atom. This means that 4-aminoquinolines have lower pKa values than other aminoquinolines and can be protonated and are thus cationic.[1] This cation-π interaction has been demonstrated to be of significant importance for complexation.[3] Modification of substituents on the quinoline ring are of less importance, however, moving the chloro group from the 7-position appears to destabilize the complex. Finally, the weak base properties of these 4-aminoquinolines are a requirement for accumulation of these drugs in the food vacuole of the malaria parasite through pH trapping. The structural features of importance for MDR-reversal activity include a quinoline ring, a hydrophobic moiety and the presence of a nitrogen atom, charged at physiological pH.[4-6] Compounds contributing to antiproliferative activities lacked a discernible common chemical feature other than the quinoline ring.[7]

Target compounds **1** and **2** (Figure 3.2), which differ in the position of attachment of the 4-aminoquinoline moiety, were designed and synthesized in order to determine whether there is a potentially favourable substitution pattern. Chemically, the reactivity of chalcones is dependent on the electrophilicity of the β-carbon. In this view, **CDM04-CDM07** (target hybrid **1**) were synthesised with ring **B** having electron-withdrawing substituents, such as halogens, which serve to enhance the electron deficiency of the β-carbon, and thus its reactivity towards nucleophiles.[8] Based on literature findings, oxygenated chalcones, especially those substituted on ring **A**, serve to enhance cytotoxic activity and chemoprotective properties of chalcones.[9]

This oxygen functionality is also a structural feature associated with good antimalarial activity.[8,10] **CDM13-15** and **CDM20-CDM21** (target hybrid **2**) were synthesized for this purpose, with methoxy and hydroxy substituents on ring **A**.

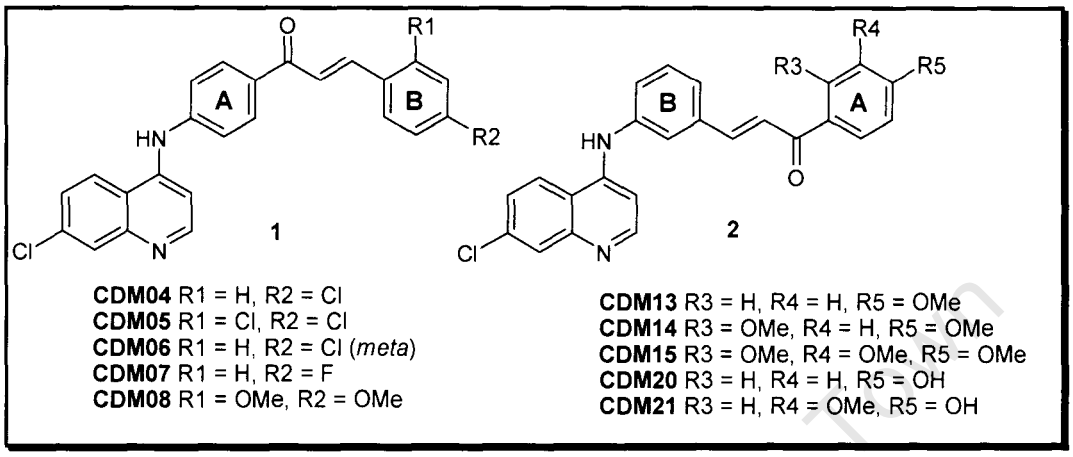

Figure 3.2: Chemical scaffold of target compounds **1** and **2**

In addition **CDM21** shows structural resemblance to curcumin, a plant extract showing a wide array of pharmacological activities (Figure 3.3).

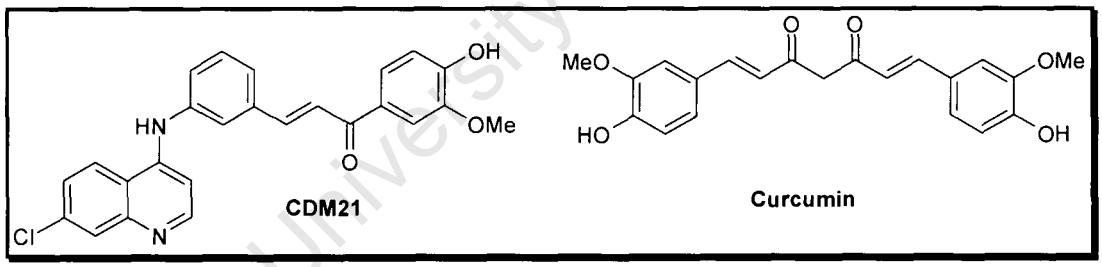

Figure 3.3: Chemical structures of **CDM21** and curcumin, depicting structural similarities

CDM08 (target hybrid **1**) was designed with a dimethoxy substitution on ring **B** for comparison purposes. Besides, the reactivity of the enone linker towards cellular thiols, the presence of the α,β-unsaturated system is also important to make the chalcones adopt a more rigid, extended conformation. From modelling studies, this linear, almost planar structure fits well in the long cleft of the active site of the malarial cysteine protease.[10] Finally, the chemical synthesis of the 4-aminoquinoline-based chalcones is relatively simple as well as being versatile, with many functional groups compatible with the reaction conditions.

3.1.2 Synthesis and Characterization of 4-Aminoquinoline-Chalcone Hybrid 1

3.1.2.1 Retrosynthetic Analysis (CDM04-CDM08)

The retrosynthesis of target compounds **CDM04-CDM08** is shown in Scheme 3.1 and involves two simple disconnections. An α,β disconnection leads to the aminoquinoline acetophenones **CDM01-CDM03**, which have the *para, meta* and *ortho* relationships respectively, and the commercially available aromatic aldehydes. Further analysis of aminoquinoline acetophenones **CDM01-CDM03** leads to the commercially available 4,7-dichloroquinoline and the 2-,3- or 4-aminoacetophenones.

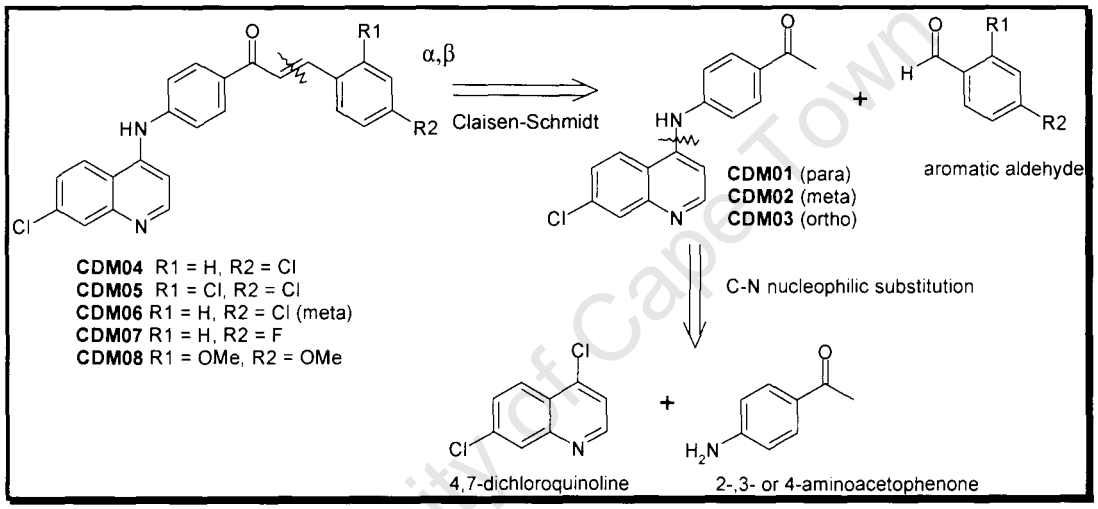

Scheme 3.1: Retrosynthetic analysis of 4-aminoquinoline-chalcone hybrid **1**

3.1.2.2 Synthesis of Aminoquinoline Acetophenones CDM01-CDM03

The 4-amino-7-chloroquinoline-acetophenones **CDM01-CDM03** were prepared following a modified literature procedure described by Raynes *et al*, Scheme 3.2.[11]

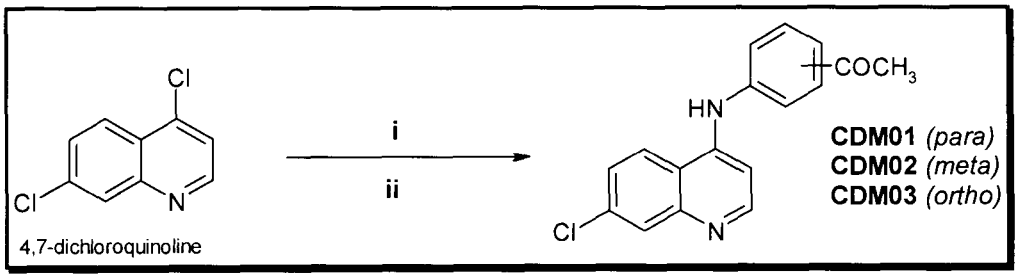

Scheme 3.2: *Reagents and conditions* i.) Aminoacetophenone, ethanol, 80-85°C, 2-4 h ii.) NH_4OH

These compounds were synthesized via a nucleophilic substitution reaction by refluxing the aminoacetophenone and an equimolar equivalent of 4,7-dichloroquinoline in ethanol for 2-4 hours, followed by neutralization with aqueous ammonia. The crude products were purified by recrystallization from ethanol to give 1-[4-(7-chloro-4-quinolinyl)amino]phenyl]-ethan-1-one(**CDM01**),1-[3-(7-chloro-4-quinolinyl)amino] phenyl]-ethan-1-one (**CDM02**) and 1-[2-(7-chloro-4-quinolinyl)amino]phenyl]-ethan-1-one (**CDM03**) in 79%, 94% and 60% yields respectively. The structures of these compounds were confirmed using ^{1}H and ^{13}C NMR.

3.1.2.2.1 Mechanistic Details

The nitrogen atom within the quinoline ring makes this aromatic system π-electron deficient by mesomeric and inductive effects, which is more pronounced at the C-2 and C-4 positions (Figure 3.4).

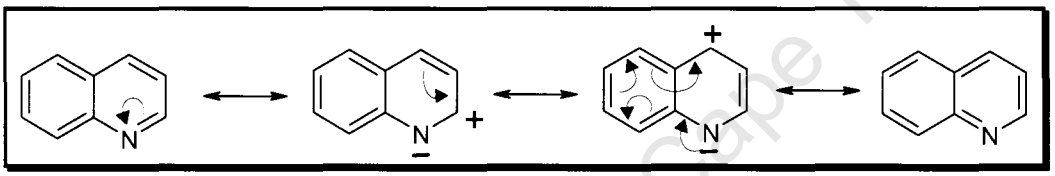

Figure 3.4: Canonical structures depicting inductive and mesomeric effects of N-atom in the quinoline ring

The C-4 position of 4,7-dichloroquinoline is further enhanced towards nucleophilic attack due to the close proximity to the nitrogen atom and the presence of the electron-withdrawing chloro group. The nucleophilic amine group of aminoacetophenone attacks the quinoline ring at the C4 position, dearomatising the ring with the quinoline nitrogen acting as an'electron sink'. The chloride is displaced when the electron pair on the nitrogen is returned to the ring and regains aromaticity (Scheme 3.3). The driving forces behind this regioselective attack are thus the resonance stabilization that occurs and the close proximity of C-4 to the N-atom.

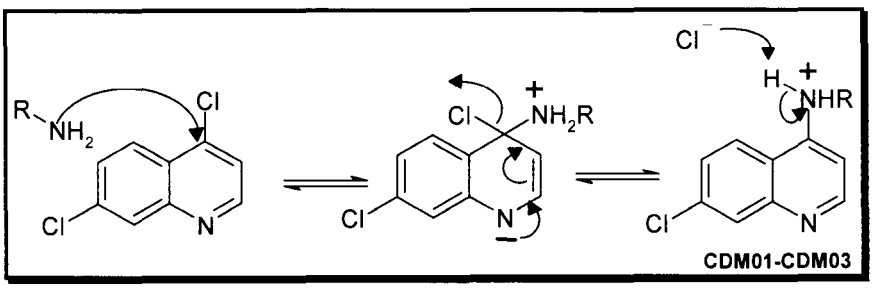

Scheme 3.3: Mechanism of formation of 4-amino-7-chloroquinoline-acetophenones

3.1.2.3 Synthesis of 4-Aminoquinoline Chalcones CDM04-CDM08

Chalcone derivatives **CDM04-CDM08** were synthesized by a base-catalyzed Claisen-Schmidt condensation of an aromatic aldehyde with the appropriate 4-aminoquinoline-derived acetophenones. In order to determine optimum reaction conditions, the condensation reaction was attempted using $Ba(OH)_2$, KOH and NaOH as catalysts as well as using $KF\text{-}Al_2O_2$ under ultrasonic irradiation. A literature procedure detailed by Go *et al*[8] using a 3% w/v methanolic solution of NaOH provided the most convenient and high yielding reaction conditions and was thus the general procedure used for preparation of the target chalcones (Scheme 3.4). The product was obtained as a yellow precipitate after a short period of stirring but required 24 h to go to completion. A minimum amount of methanol must be used to ensure formation of a solid product. Formation of the *ortho*-product, with respect to the position between the carbonyl and the nitrogen atom, was unsuccessful presumably due to steric factors.

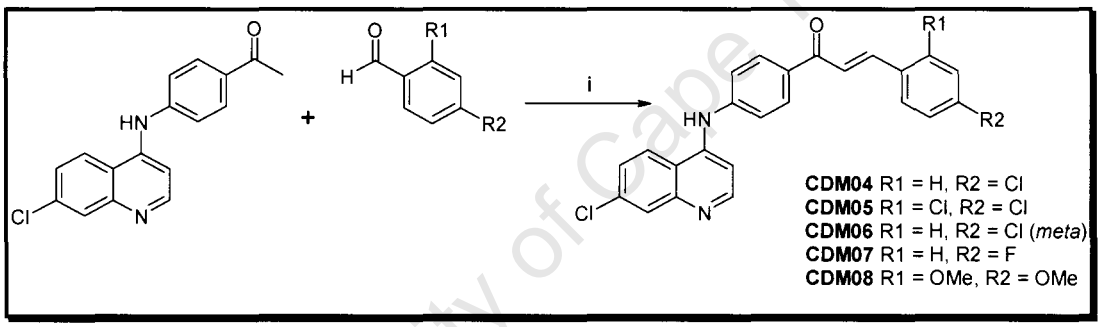

Scheme 3.4: *Reagents and conditions* i.) 3% w/v NaOH, MeOH, reflux, 24 h

3.1.2.3.1 Mechanistic Details

The mechanism of the Claisen-Schmidt condensation is shown in Scheme 3.5. It involves a base-mediated enolization of the 4-aminoquinoline-derived acetophenone, in which the base removes an acidic proton adjacent to the carbonyl group. This is followed by nucleophilic attack by the resulting enolate ion on the aromatic aldehyde to form the aldol product. This β-hydroxy ketone then undergoes a base-catalysed elimination (E1cB) to give the more stable conjugated chalcone system.

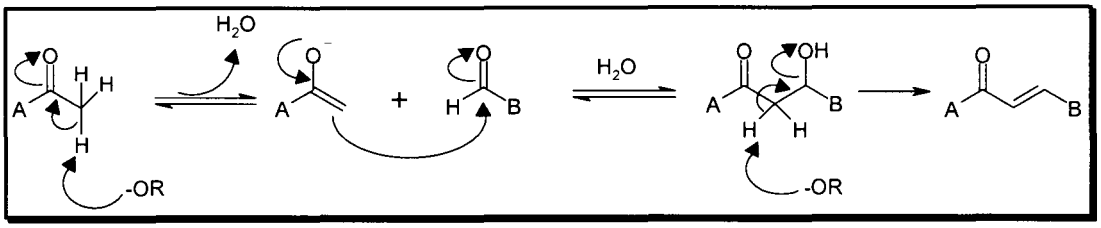

Scheme 3.5: Mechanism of Claisen-Schmidt condensation reaction

The yields of the synthesized compounds and their respective melting points are given in Table 4.

Table 4: 4-Aminoquinoline-based chalcone hybrid 1 with their respective yields and melting points

Product Structure	Code	Yield (%)	Mp (°C)
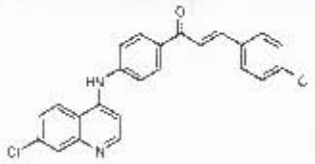	**CDM04**	66	230-233
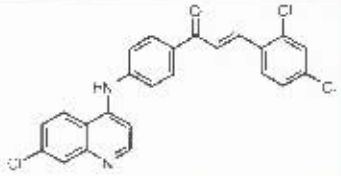	**CDM05**	74	229-233
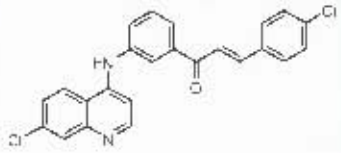	**CDM06**	75	218-220
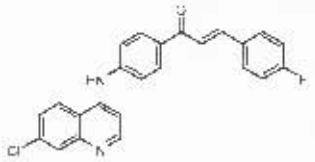	**CDM07**	30	189-192
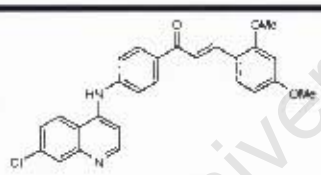	**CDM08**	54	239-242

The filtered precipitates of **CDM04** and **CDM05** were washed with cold methanol to yield pure products. The filtered precipitates of **CDM06**, **CDM07** and **CDM08** still contained trace amounts of unreacted methyl ketone and further purification was needed. Hybrids **CDM06** and **CDM08** were recrystallized from ethyl acetate and methanol, respectively. **CDM07** was very insoluble and was purified by column chromatography. Purity was checked by TLC before characterization by ^{1}H and ^{13}C NMR, IR, mass spectrometry and elemental analysis.

3.1.2 Synthesis and Characterization of 4-Aminoquinoline-Chalcone Hybrid 2

3.1.2.1 Retrosynthetic Analysis (CDM13-CDM15 and CDM20-CDM21)

Generation of the 4-aminoquinoline-chalcone hybrid **2** was achieved by considering the retrosynthetic analysis shown in Scheme 3.6.

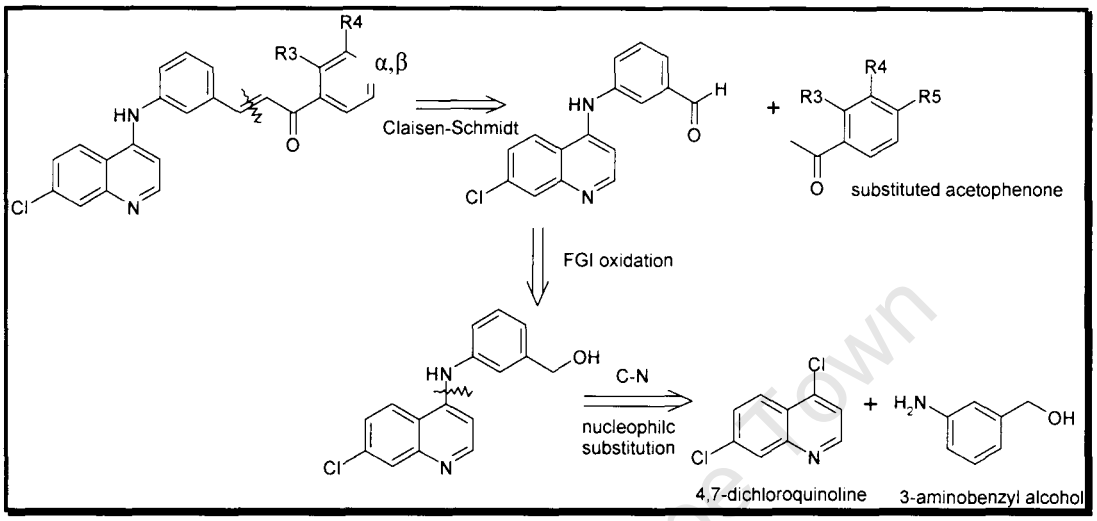

Scheme 3.6: Retrosynthetic analysis of 4-aminoquinoline-chalcone hybrid **2**

Retrosynthesis of target compounds **2** follow similar disconnections to target compounds **1,** with the difference being that the 3-aminobenzaldehyde was not commercially available for nucleophilic aromatic substitution with 4,7-dichloroquinoline, and the 3-aminobenzyl alcohol was thus used. The intermediate 4-aminoquinoline-derived benzyl alcohol was then oxidised to the appropriate aldehyde.

3.1.2.2 Synthesis of 4-Aminoquinoline Chalcones CDM13-CDM15

The intermediate 4-aminoquinoline-based benzyl alcohol was synthesised via a nucleophilic aromatic substitution reaction between 4,7-dichloroquinoline and 3-aminobenzyl alcohol, as described in section 3.1.2.2, to give [3-(7-chloro-quinolin-4-ylamino)-phenyl]-methanol (**CDM09**) in 98% yield (Scheme 3.7). The *ortho*-product [2-(7-chloro-quinolin-4-ylamino)-phenyl]-methanol (**CDM10**) was synthesised in low yield (33%), however attempts at synthesising the *para*-product failed, with ^{1}H NMR spectra of the isolated product showing only the starting material, 4-aminobenzyl alcohol and other impurities.

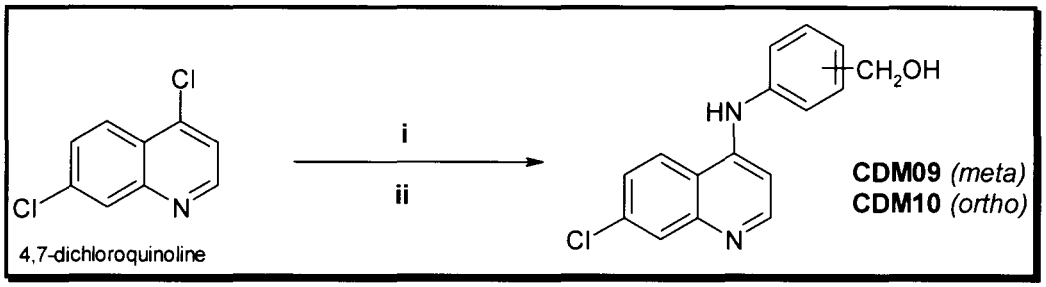

Scheme 3.7: *Reagents and conditions* i.) Aminobenzyl alcohol, ethanol, 80-85°C, 2-4 h ii.) NH_4OH

The next step in the synthesis involved oxidation of the intermediate benzyl alcohol (**CDM09** or **CDM10**) to the appropriate aldehyde, (**CDM11** or **CDM12**) by the Parikh-Doering oxidation method,[12] a modification of the method originally developed by Pfitzner and Moffat.[13] **CDM09** and **CDM10** were stirred with Et_3N in DMSO, followed by the addition of the sulfur trioxide pyridine complex to afford the aldehydes **CDM11** and **CDM12** in yields of 97% and 81% respectively (Scheme 3.8). These intermediates were characterised by ^1H NMR and ^{13}C NMR, with the disappearance of the CH_2 and OH group in the region of δ4.50 ppm and δ5.20 ppm, respectively and the appearance of aldehyde proton at around δ10.0 ppm confirming their formation.

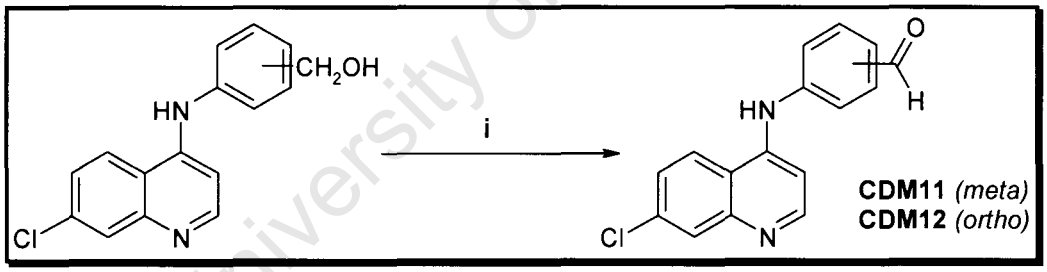

Scheme 3.8: *Reagents and conditions i.)* SO_3.Pyr complex, Et_3N, DMSO, rt, 72 h

3.1.3.2.1 Mechanistic Details

The mechanism of Parikh-Doering oxidation reaction (Scheme 3.9) is similar to that of the Swern oxidation. The charged oxygen atom of DMSO attacks the sulfur atom of the SO_3.pyr complex to give an electrophilic sulfur compound. The alcohol then reacts with this sulfonium ion that is formed to give a new sulfonium salt. This compound is stable enough to be deprotonated by Et_3N, forming a sulfonium ylide that fragments to form the aldehyde (**CDM11-CDM12**) and dimethyl sulfide.

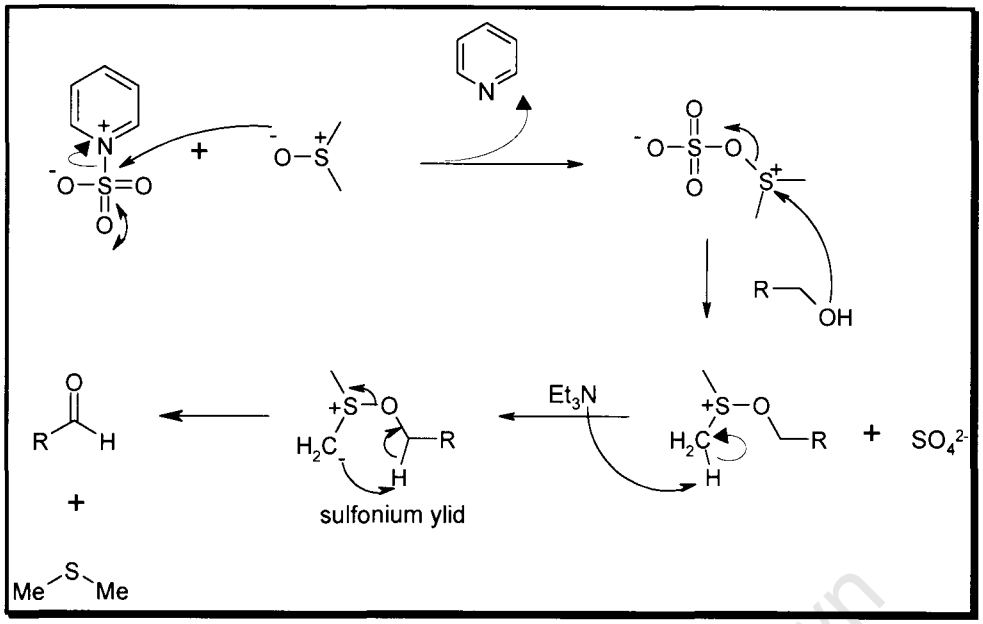

Scheme 3.9: Mechanism of Parikh-Doering oxidation

After work-up of the above reaction, the product was isolated without further purification. The final step in the synthesis is the base-catalyzed Claisen-Schmidt condensation reaction between the 4-aminoquinoline-derived aldehyde **CDM11** or **CDM12** and a series of methoxylated acetophenones to afford **CDM13-CDM15** in 75%, 70% and 70% yields respectively (Scheme 3.10). Condensation of the *ortho*-aldehyde **CDM12** with a methoxy acetophenone was unsuccessful, most likely due to steric hindrance.

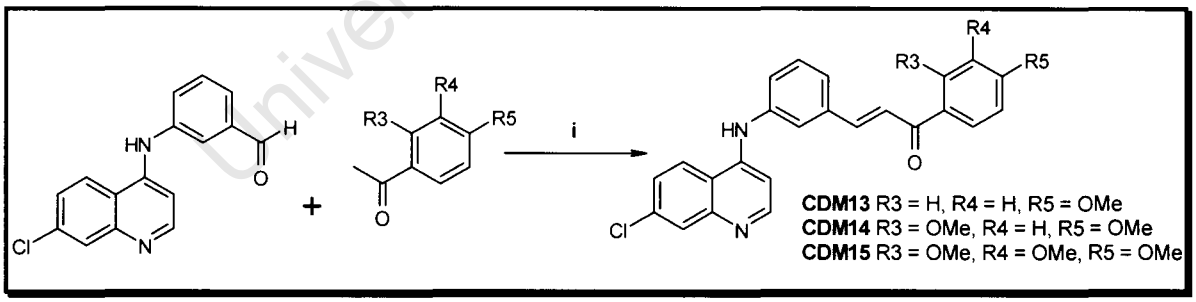

Scheme 3.10: *Reagents and conditions* i.) 3% w/v NaOH, MeOH, Reflux, 24 h

3.1.3.3 Synthesis of 4-Aminoquinoline Chalcones CDM20-CDM21

For the synthesis of hydroxylated chalcones, **CDM20** and **CDM21**, it was necessary to protect the phenolic group on the substituted acetophenones before condensation, in order to improve product yields. Phenolic protons are relatively acidic (pKa ~10) in comparison to methyl ketone protons (pKa > 20) and will be deprotonated more rapidly due to the formation of a more stabilized intermediate (Figure 3.5).

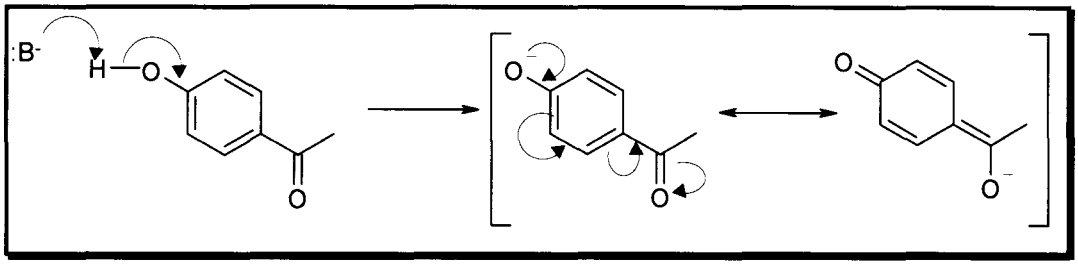

Figure 3.5: Deprotonation of phenolic proton to give resonance stabilized phenoxide anion

This results in limited conversion of methyl ketone into enolate ions and it thus becomes necessary to protect the hydroxy group of the starting materials, 4-hydroxyacetophenone and acetovanillone, as tetrahydropyranyl ethers. This was accomplished by stirring the hydroxylated starting materials, pyridinium *p*-toluenesulfonate and 3,4-dihydro-2H-pyran in methylene chloride for 72 h to afford 1-(4-tetrahydro-2H-pyran-2-yloxy-phenyl)ethanone **CDM16** and 1-[3-methoxy-4-(tetrahydro-pyran-2-yloxy)-phenyl]-ethanone **CDM17** in 99% and 95% yields, respectively. **CDM16** and **CDM17** then underwent a Claisen-Schmidt condensation with the 4-aminoquinoline-derived aldehyde **CDM11** to give the intermediate products **CDM18** and **CDM19**. Finally, removal of the THP protecting group under mild acidic conditions gave the final products **CDM20** and **CDM21** in good yields. This approach used is depicted in Scheme 3.11.

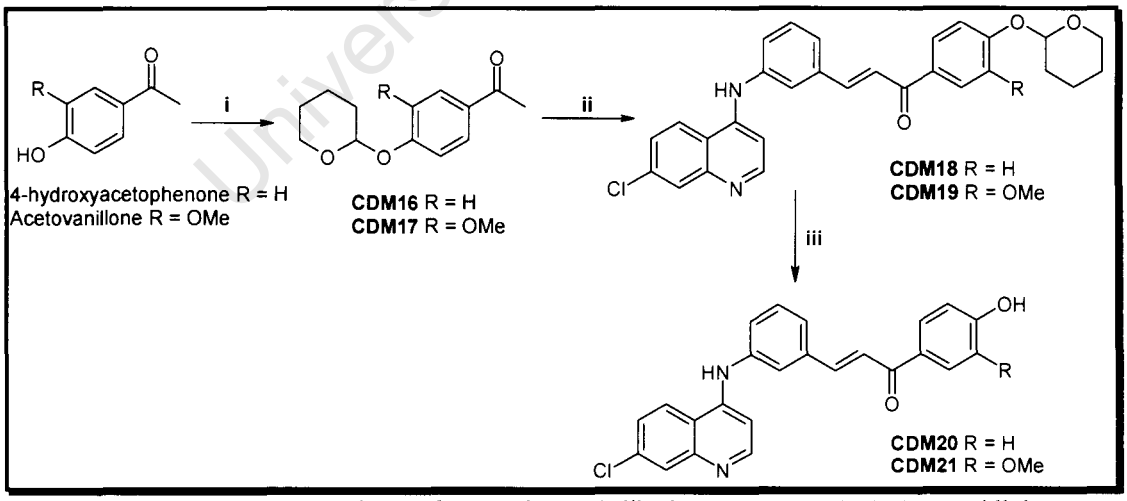

Scheme 3.11: *Reagents and conditions* i.) 3,4-dihydro-2H-pyran (1.6eq), pyridinium *p*-toluenesulfonate (0.1eq), CH_2Cl_2, rt, 72 h ii.) 3% w/v NaOH, MeOH, Reflux, 24 h iii.) 4M HCl, MeOH, rt, 4 h.

The structures, isolated yields and respective melting points of the resultant 4-aminoquinoline-based chalcone hybrid **2** are depicted in Table 5.

Table 5: 4-Aminoquinoline-based chalcone hybrid **2** with their respective yields and melting points

Product Structure	Code	Yield (%)	Mp (°C)
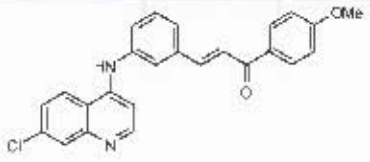	**CDM13**	75	254-257
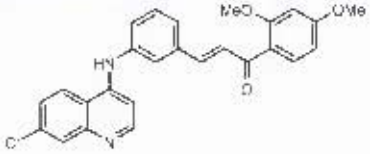	**CDM14**	70	175-179
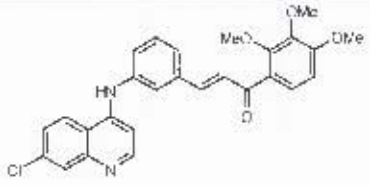	**CDM15**	70	179-182
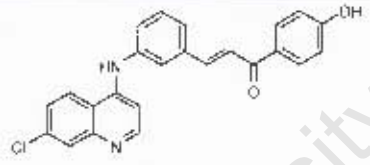	**CDM20**	40	328-333
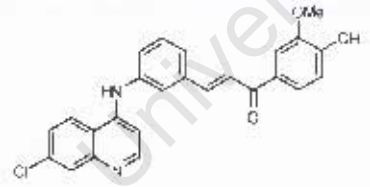	**CDM21**	58	225-227

3.1.4 Characterisation of Target Compounds

All the ^{1}H NMR spectra of the resultant products displayed two common diagnostic doublets around δ 8 ppm and δ 7 ppm, integrating for 1 proton each, and have coupling constant values between 15-16 Hz. These peaks correlate to the methine protons on the double bond of the α,β-unsaturated system and also confirm that the *trans*-isomer is formed preferentially. The formation of the proposed products was also confirmed by the disappearance of the methyl ketone peak present in the starting material ^{1}H NMR spectra at approximately δ 2.5 ppm for target hybrid **1** and the

aldehyde proton at ~ δ 10 ppm for target hybrid **2**. The ^{13}C NMR spectra that were obtained are also consistent with the proposed structures, with the carbonyl carbon (C=O) of the α,β-unsaturated system observed in the region of δ 187 ppm in comparison to the methyl ketone carbonyl group of the starting material which appears at δ 196ppm or the aldehyde carbonyl group at ~ δ 190 ppm. A representative ^1H NMR spectrum is shown of compound **CDM04** from target hybrid **1** (Figure 3.6) and of compound **CDM13** from target hybrid **2** (Figure 3.7).

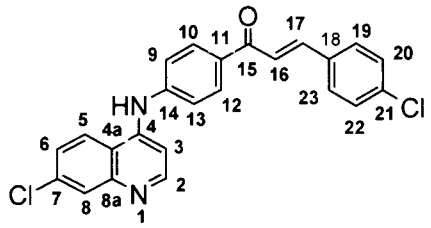

δ/ppm	Multiplicity	J/Hz	H
9.43	s	-	NH
8.62	d	5.1	H2
8.41	d	8.8	H5
8.21	d	8.8	H10, H12
8.0	d	15.6	H17
7.97	d	2.4	H8
7.92	d	8.8	H19, H23
7.73	d	15.6	H16
7.64-7.61	dd	2.4, 9.2	H6
7.53	d	8.4	H9, H13
7.50	d	8.8	H20, H22
7.32	d	5.2	H3

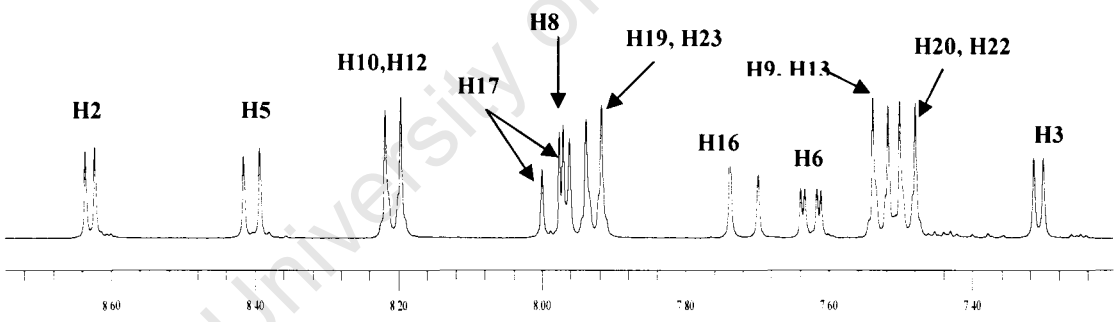

Figure 3.6: ^1H NMR spectrum of **CDM04** in d_6-DMSO at 400MHz

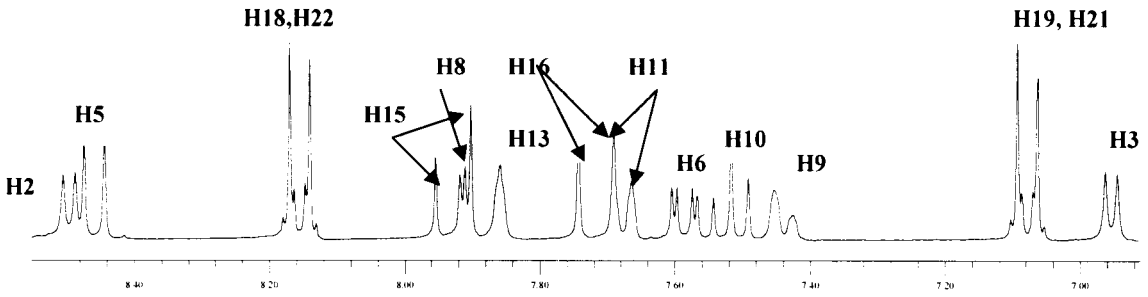

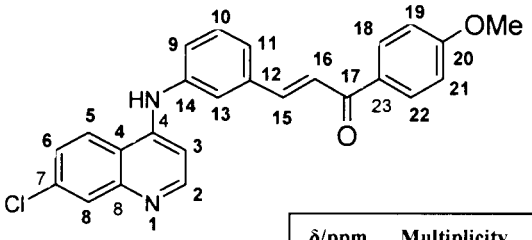

δ/ppm	Multiplicity	J/Hz	H
9.20	s	-	NH
8.48	d	5.1	H2
8.45	d	9.0	H5
8.16	d	8.7	H18, H22
7.95	d	15.6	H15
7.89	d	2.0	H8
7.84	s	-	H13
7.73	d	15.6	H16
7.65	d	8.0	H11
7.59-7.55	dd	2.1, 9.0	H6
7.53-7.48	t	8.1	H10
7.43	d	8.1	H9
7.08	d	8.7	H19, H21
6.94	d	5.1	H3
3.82	s	-	OCH_3

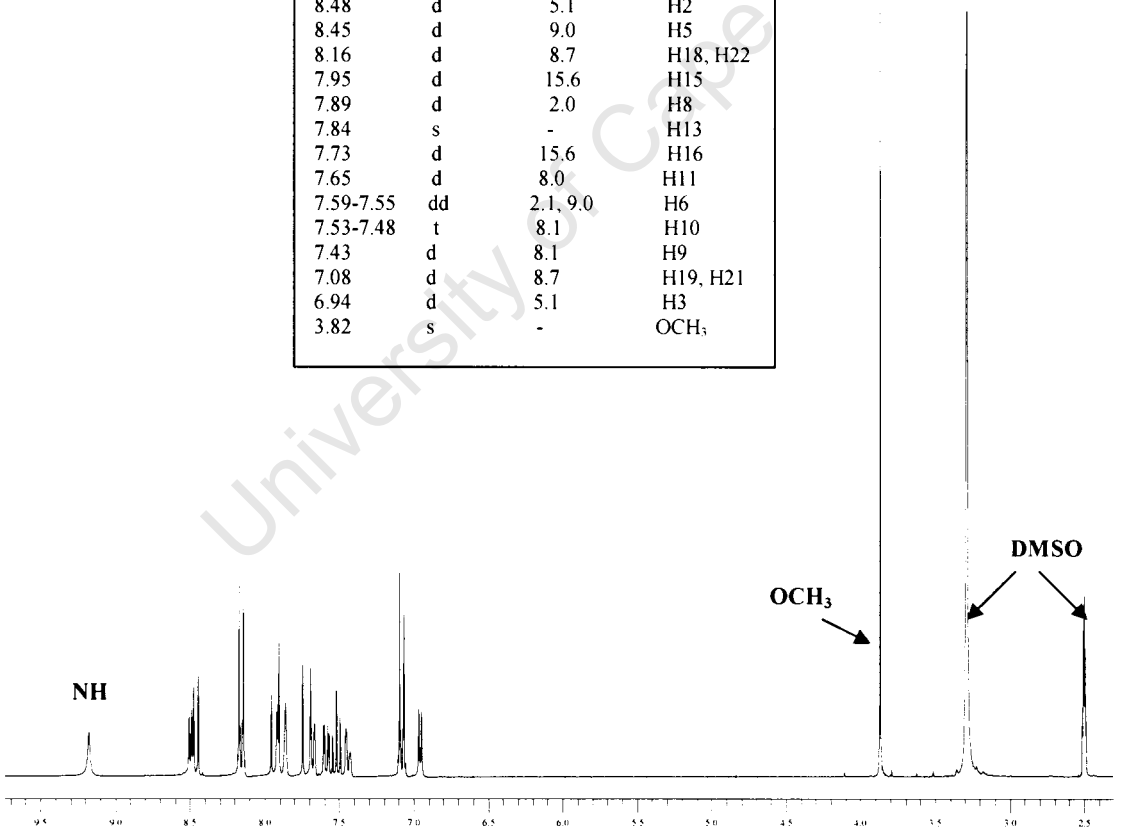

Figure 3.7: ^{1}H NMR spectrum of **CDM13** in d_6-DMSO at 400MHz

Characteristic IR bands included the peaks around 3300 cm^{-1} and ~1670 cm^{-1} due to NH and C=O stretches respectively. All compounds depicted the presence of the other functional groups with ArH and C=C stretches appearing around ~1560 cm^{-1} and ~1600 cm^{-1} respectively. Elemental analysis confirmed the molecular formula and purity of the compounds.

3.1.5 Crystallographic Analysis

Within this project, single crystal X-ray crystallography was a tool used primarily for elucidation and confirmation of target compound structures, but the accurate molecular structures determined using this method may also be of potential use in molecular modelling studies. Guided by the X-ray structure, molecular modelling may be used to obtain a better understanding of structural factors that contribute to activity as well as to investigate potential structural modifications of target compounds important for optimising activity. Single crystals obtained for **CDM06** (target hybrid **1**) and **CDM14** (target hybrid **2**) were coated with Paratone N oil and mounted on a goniometer head and their diffraction intensities collected on a Nonius Kappa CCD diffractometer. Crystals were cooled in a stream of N_2 using a Cryostream cooler (Oxford Cryosystems, UK). The program XPREP[14] was used to determine the space groups of **CDM06** and **CDM14**. **CDM06** crystallized in the orthorhombic system in the space group $Pca2_1$ and **CDM14** crystallized in the triclinic system in the space group P-1 (based on $|E^2 - 1| = 0.999$). This choice was confirmed by successful refinement of the structures in the aforementioned space groups. Both structures were solved using SHELXS-97,[15] which revealed the position of all non-hydrogen atoms which were then refined isotropically on F^2 using full-matrix least-squares in the program SHELXL-97.[16] All non-hydrogen atoms were then refined anisotropically. Hydrogen atoms were placed in idealised positions using a riding model and refined isotropically with temperature factors 1.2 times those of their parent atoms. The crystal and refinement data for **CDM06** and **CDM14** are listed in Table 6.

Table 6: Crystal and refinement data of **CDM06** and **CDM14**

Parameter	CDM06	CDM14
Molecular Formula	$C_{24}H_{16}Cl_2N_2O$	$C_{24}H_{16}ClN_2O \cdot CH_4O$
Formula Weight / g.mol^{-1}	419.29	476.94
Crystal System	Orthorhombic	Triclinic
Space Group	$Pca2_1$	P-1
a / Å	12.9251(1)	8.3116(3)
b / Å	5.5871(1)	9.0714(4)
c / Å	26.7880(3)	15.9988(8)
α / °	90	85.668(2)
β / °	90	88.376(2)
γ / °	90	77.608(3)
Volume / Å^3	1934.46(4)	1175.42(9)
Z	4	2
D(calc) / g.cm^{-3}	1.440	1.348
μ(MoKα) / mm^{-1}	0.354	0.200
F(000)	864	500
Temperature / K	173	113
Range scanned θ / °	3.9< θ <25.7	3.4≤ θ ≤25.4
No. of measured reflections	24498	20971
No. unique reflections	3642	4254
No. of reflections I > 2σ (I)	3275	2728
R(int)	0.052	0.102
No. of parameters	262	311
S	1.04	1.04
R_1	0.0310	0.0606
wR_2 (all reflections)	0.0760	0.1569
Δρ excursions / e Å^3	-0.28, 0.29	-0.29, 0.28

The structures of the asymmetric units of **CDM06** and **CDM14** and the atomic numbering are shown in Figure 3.8 and Figure 3.9 respectively. The hydrogen atoms are named after their parent atoms. The crystal structures further confirmed that the olefinic bond in these compounds adopted the *E* configuration.

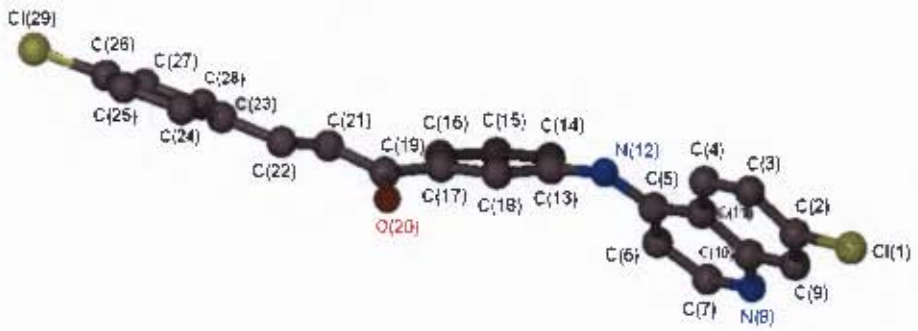

Figure 3.8: Crystal structure of **CDM06** depicting labelling and conformational aspects H atoms have been omitted for clarity

The crystal structure depicted in Figure 3.8 shows that the two ring systems deviate from planarity with regard to the α,β-unsaturated system. Ring **B** containing the Cl (29) atom lies slightly above the plane of the α,β-unsaturated system with the torsion angle of 17. 5(1)° between ring C(13)-C(14)-C(15)-C(16)-C(17)-C(18) and ring C(23)-C(24)-C(25)-C(26)-C(27)-C(28). The quinoline ring lies below the plane of the α,β-unsaturated system with the orientation of the two rings, C(13)-C(14)-C(15)-C(16)-C(17)-C(18) and C(2)-C(3)-C(4)-C(11)-C(5)-C(6)-C(7)-N(8)-C(10)-C(9), with respect to each other described by the torsion angle of 47.83(8)°. The latter deviation is due to steric interactions between the hydrogen atom H6 on the quinoline ring and the hydrogen atom H14 on the aromatic ring **A**.

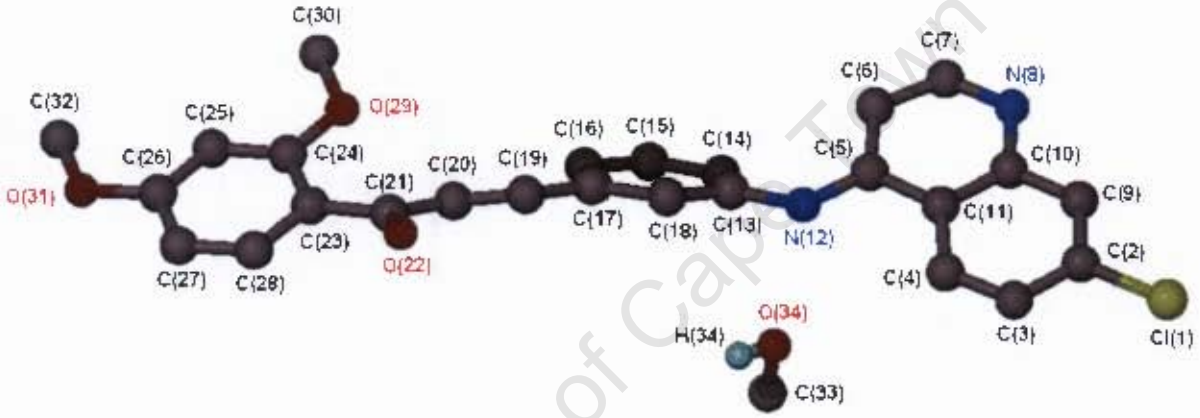

Figure 3.9: Crystal structure of **CDM14** depicting labelling and conformational aspects H atoms have been omitted for clarity

The three ring systems in the crystal structure of **CDM14** depicted in Figure 3.9 are not coplanar, with the terminal rings, C(23)-C(24)-C(25)-C(26)-C(27)-C(28) and C(2)-C(3)-C(4)-C(11)-C(5)-C(6)-C(7)-N(8)-C(10)-C(9), being nearly coplanar with a torsion angle between them being 11.9(1)°. The nonplanarity between the α,β-unsaturated ring system and the adjacent rings is due to steric interactions. As with **CDM06** there is a steric interaction between the hydrogen atom H6 on the quinoline ring and the aromatic hydrogen H14 of the middle ring system causing a torsion angle C(6)-C(5)-N(12)-C(13) of 42.7(1)°. The torsion angle O(29)-C(24)-C(23)-C(21) between the methoxy-substituted aromatic ring and ring C13-C18 is 34.3(2)°. The middle ring, C13-C18, however, is coplanar with the α,β-unsaturated system. The nonplanarity between the α,β-unsaturated system and the methoxy-substituted aromatic ring is due to intramolecular hydrogen bonding between the oxygen atom

O29 of the C24 methoxy group and the hydrogen atom H20 of the α,β-unsaturated system. The torsion angle formed through this intramolecular hydrogen bonding is 106°, typical of a six-membered ring. If the methoxy-substituted ring is rotated to be planar with the α,β-unsaturated system, there will be a repulsion between the methoxy group and the hydrogen atom of the α,β-unsaturated system and thus this nonplanarity, with a torsion angle C(24)-C(23)-C(21)-C(20) of -32.8(5)°, limits repulsive interactions.

The crystal structure of **CDM06** shows no intermolecular hydrogen bonding and the crystal lattice is stabilized by hydrophobic interactions. The zigzag packing motif of **CDM06** is depicted in Figure 3.10 showing hydrophobic interactions and four molecules of **CDM06** per unit cell.

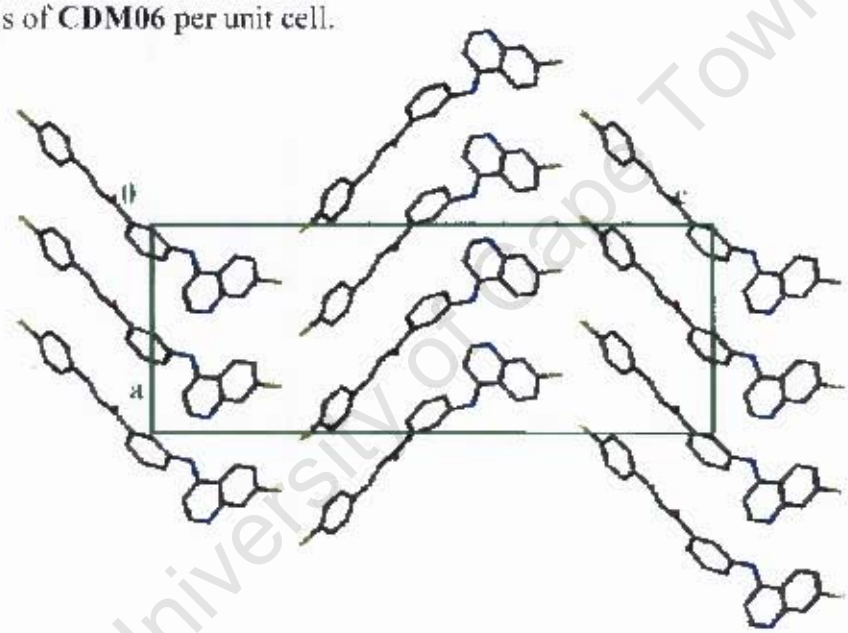

Figure 3.10: Packing diagram of **CDM06**, viewed along [010].

CDM14 packs in such a way to form channels in which solvent molecules may reside (Figure 3.11). Indeed this is the case, with **CDM14** being solvated with methanol.

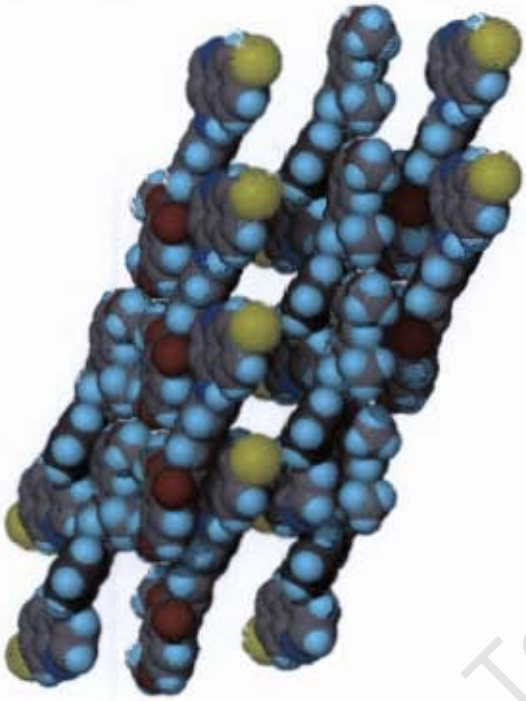

Figure 3.11: View of packing down [100], depicting formation of channels

There are two molecules of **CDM14** per unit cell, with the oxygen atom O(34) of methanol hydrogen bonding to the aniline type hydrogen H12 of **CDM14** and the methyl hydrogen of methanol hydrogen bonding to N8 of another molecule of **CDM14**. These interactions and the intramolecular bonding discussed previously between the oxygen atom O29 of the C24 methoxy group and the hydrogen atom H20 of the α,β-unsaturated system are depicted in Figure 3.12.

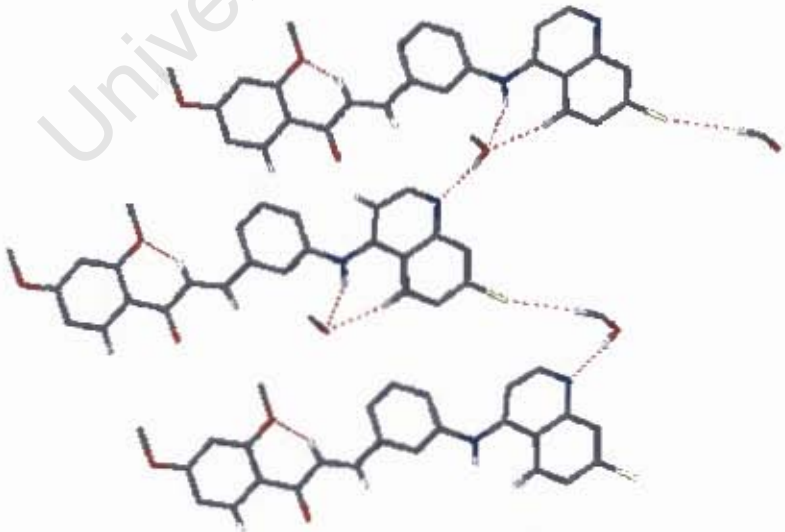

Figure 3.12: Hydrogen bonding (represented in red) between the MeOH and **CDM14**

These intermolecular and intramolecular hydrogen bonds stabilize the crystal structure and their distances and related angles are given in Table 7 as calculated by PLATON[17], where *a* denotes symmetry related position x, 1+y, z and *b* denotes symmetry related position 1+x, -1+y, z.

Table 7: Hydrogen bond distances and angles of **CDM14**

Atoms (Donor-H...acceptor)	D - H (Å)	H...A (Å)	D...A (Å)	D- H...A(°)
N(12) --H(12) ..O(34)	0.88	2.12	2.916(3)	149
O(34) --H(34) ..N(8)^{a}	0.84	1.92	2.750(3)	167
C(4) --H(4) ..O(34)	0.95	2.39	3.330(3)	168
C(20) --H(20) ..O(29)	0.95	2.36	2.777(4)	106
C(33) --H(33B) ..Cl(1)^{b}	0.98	2.74	3.692(4)	163

Figure 3.13 shows the packing of **CDM14** molecules linked by the solvent molecule. The packing consists of a ribbon-like repeating motif A-B-A-B, where A is the molecule positioned with the Cl group pointing upwards and B is the molecule positioned with Cl group pointing downwards.

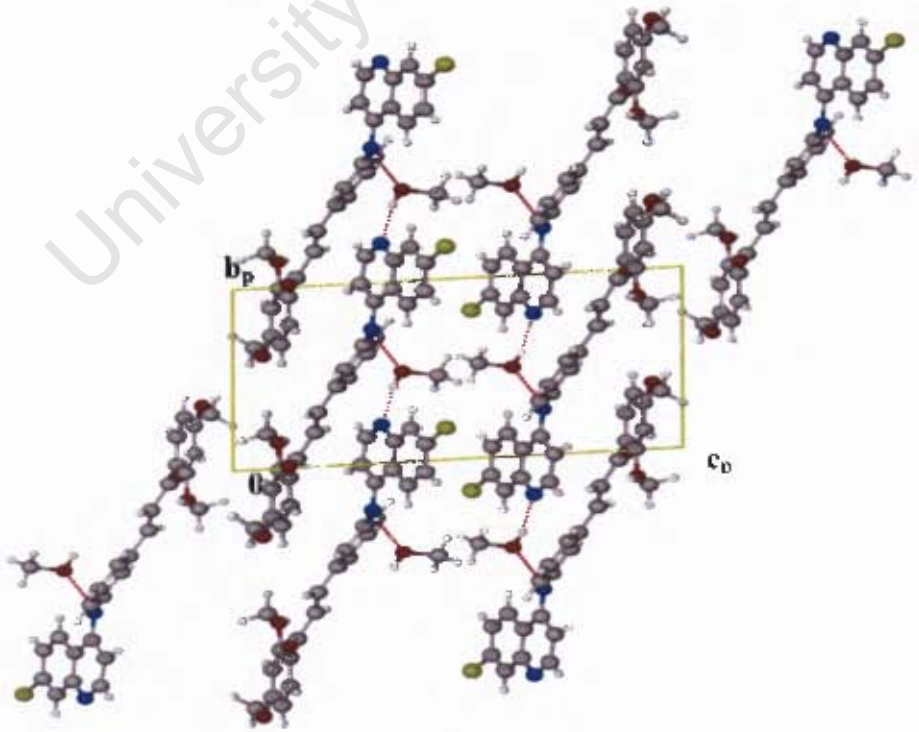

Figure 3.13: Packing diagram of **CDM14**, viewed down [100].

The two thermal analytical methods used for analysing the single crystals **CDM06** and **CDM14** were Hot Stage Microscopy (HSM) and Differential Scanning Calorimetry (DSC). Hot stage microscopy experiments with crystal immersed in silicone oil were used to determine whether these crystals contained solvent of crystallisation. Images captured for **CDM06** confirmed that the crystals were not solvated and the melt onset was at 218°C (Figure 3.14).

Figure 3.14: HSM photos of **CDM06** at (a) 25°C and (b) 220°C

HSM experiments showed that **CDM14** contained solvent with desolvation starting at 111°C (bubble formation) and melt onset temperature at 175°C (Figure 3.15).

Figure 3.15: HSM photos of **CDM14** at (a) 25°C, (b) 111°C and (c) 177°C

Differential scanning calorimetry is used to measure the rate of heat absorbed or evolved by a sample, during a temperature programme. DSC was used to confirm the melting point of **CDM14** and the onset temperature of desolvation of methanol. The DSC curve showed a broad endotherm with an onset temperature of desolvation at 110°C. The broad peak has a shoulder corresponding to the desolvation of methanol and the highest point of the peak corresponds to the melting of **CDM14** at 141°C (Figure 3.16). This temperature differs from that recorded from the hot stage due to the fact the DSC sample holder is within a closed environment.

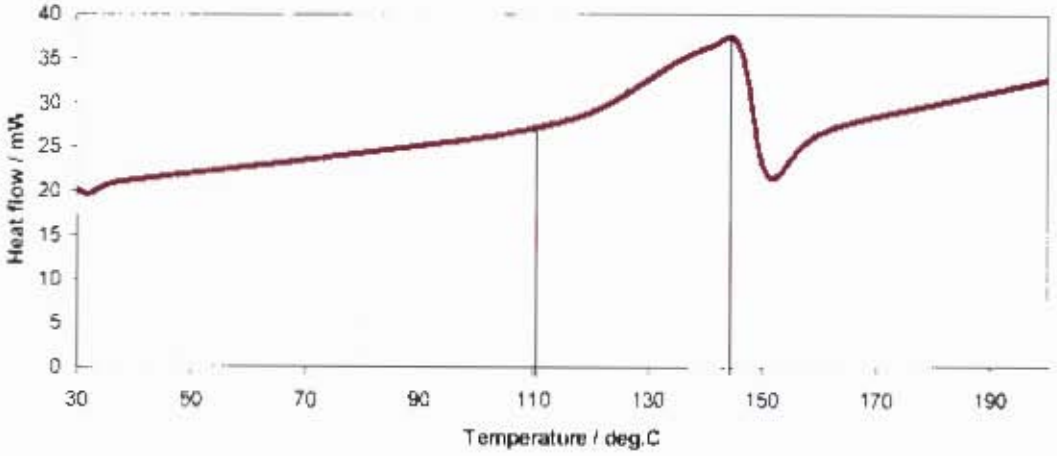

Figure 3.16: DSC trace of **CDM14**

The temperature at which the methanol desolvates in comparison to its normal boiling point (T_b = 64.7°C) is an indication of the relative stability of the solvated crystal. A value of T_{on}/T_b greater than one indicates a relatively stable structure; the T_{on}/T_b value of the system is 1.6 indicating that the solvated crystal is stable. The TGA trace shows a mass loss of 7.2 % at 110°C, which is consistent with a 1:1 methanol solvate of **CDM14** (theorectical value = 6.7 %).

3.1.6 Improving Solubility

One of the limiting factors involved in bioavailability and thus the efficacy of these hydrophobic target compounds is their insolubility in aqueous media. *In this project, two methods were used in order to potentially improve water solubility properties of target compounds, those being formation of salt derivatives and inclusion into cyclodextrins.*

3.1.6.1 Salt Formation

The citrate salt derivatives of all the 4-aminoquinoline-based chalcone target compounds were prepared via a simple procedure involving protonation of the quinoline nitrogen with citric acid. Citrate salts were prepared due to their well-known low toxicity and the ready availability of citric acid. An equimolar equivalent of citric acid was dissolved in a minimum amount of acetone and added dropwise to the heated acetone solution of the target compound. The citrate salts precipitated out of solution when cooled at 4°C overnight and the resulting precipitates were filtered to give the salt derivatives with good yields (Table 8). The ^{1}H NMR spectrum confirmed the formation of the citrate salts, with the appearance of two doublets between δ 2-3 ppm that integrate for two protons each, arising from geminal coupling of each pair of the CH_2 protons of citric acid. The chemical shifts of the other protons remained relatively unchanged, except for those correlating to the quinoline ring, which showed a downfield shift. This trend confirms salt formation via protonation of the quinoline nitrogen. This method of salt formation only improved the solubility of target compounds very slightly. This could be attributed to the fact there is only one charged centre, which may be insufficient to overcome the strong non-polar character of the large target compounds. It may be of interest to produce salt derivatives of mineral acids such as hydrochlorides or phosphates, which are highly polar and may improve water solubility.

Table 8: Citrate salt derivatives of 4-aminoquinoline-chalcone hybrids

Product Structure	Code	Yield (%)	Mp (°C)
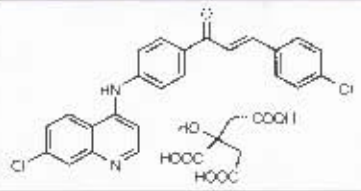	**CDM22**	93	197-198
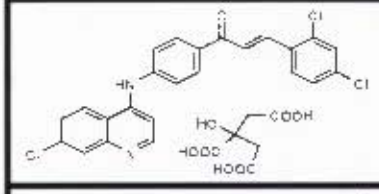	**CDM23**	62	208-211
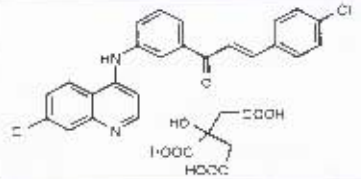	**CDM24**	60	219-221
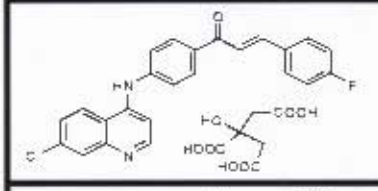	**CDM25**	92	226-228
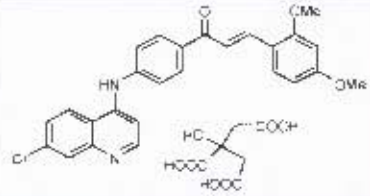	**CDM26**	63	224-228
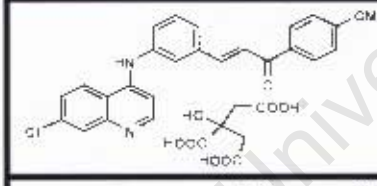	**CDM27**	47	250-254
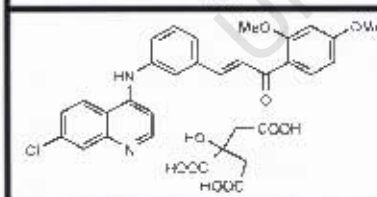	**CDM28**	42	89-94
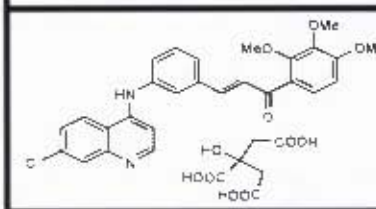	**CDM29**	97	158-160

3.1.6.2 Cyclodextrin Inclusion Complexes

Target compounds **CDM13-CDM15** and their citrate salt derivatives **CDM27-CDM29** were selected for cyclodextrin inclusion based on their observed activity *in vitro*, especially in cancer cell models. Kneading, co-precipitation and co-solvent methods were employed using β-CD and γ-CD in both 1:1 and 2:1 (CD: drug) molar ratios. All co-precipitation and co-solvation experiments were unsuccessful, yielding only native-CD single crystals which were confirmed on the X-ray diffractometer by comparison of known unit cell dimensions of native-CD and its complexes with the experimental unit cell dimensions. The powder X-ray diffraction (PXRD) patterns obtained from kneading experiments were compared with the computed PXRD patterns, known as isostructural series, to determine if complexation had occurred. The PXRD patterns (Figure 3.17) of the kneaded material of **CDM14** (1:1 β-CD:drug ratio) and **CDM15** (2:1 β-CD:drug ratio) did not match the PXRD pattern for native β-CD and thus indicated that inclusion complexes had formed. The patterns however did not match any previously identified isostructural series,[18,19] but were isostructural with each other, with the conclusion that new β-CD inclusion complexes of **CDM14** and **CDM15** had probably been formed. Recrystallization of the kneaded complex failed to give X-ray grade single crystals needed in order to confirm inclusion.

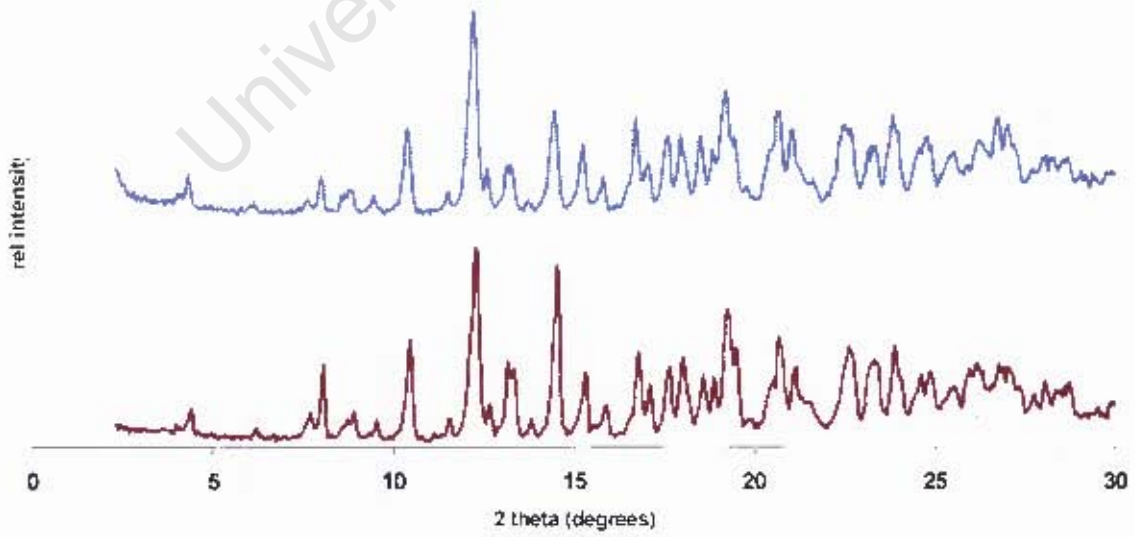

Figure 3.17: Experimental PXRD traces of (a) β-CD-**CDM14** complex and (c) 2β-CD-**CDM15** complex

The PXRD patterns of kneaded materials for the other target compounds attempted for inclusion in β-CD showed that no inclusion complex had formed as the patterns matched that of native β-CD.

γ-CD is a more likely candidate to form inclusion complexes with the compounds in this study due to the cavity of the CD being larger than that of β-CD. Three kneading experiments were attempted with γ-CD and **CDM13**, **CDM14** and **CDM15** in a 1:1 host:drug ratio. The PXRD traces of two of the γ-CD complexes, **CDM14** and **CDM15**, were in reasonable agreement with the PXRD pattern for isostructural series 17, confirming that complexation has occurred (Figure 3.18).

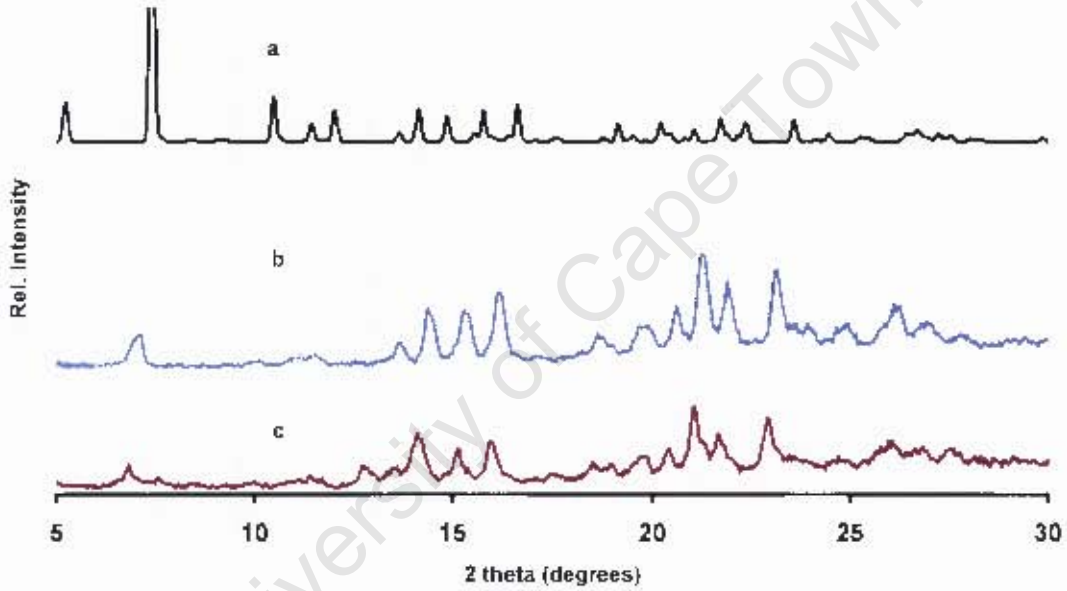

Figure 3.18: a) Computed PXRD trace for known γ-CD complex and experimental PXRD traces of (b) γ-CD-**CDM14** complex and (c) γ-CD-**CDM15** complex

All observed γ-CD complexes containing guest molecules have the same packing arrangement and thus a considerable amount of structural information can be inferred.[18] These complexes crystallize in the tetragonal space group $P42_12$ with channel packing. The channels have three γ-CD molecules in one asymmetric unit stacked together in head-to-head (A and B), tail-to-tail (B and C) and head-to-tail (C and A') packing modes (Figure 3.19). While the level of agreement between pattern 'a' and the experimental ones may not appear to be convincing, it must be noted that

pattern 'a' is a reference pattern, obtained by averaging those for all known γ-CD inclusion complexes. The intensities registered are therefore artificial and one does not expect them to correspond exactly with those for the prepared complexes. Similarly, peak positions may vary depending on the unit cell size variation, a function of the nature of the guest and crystal water content.

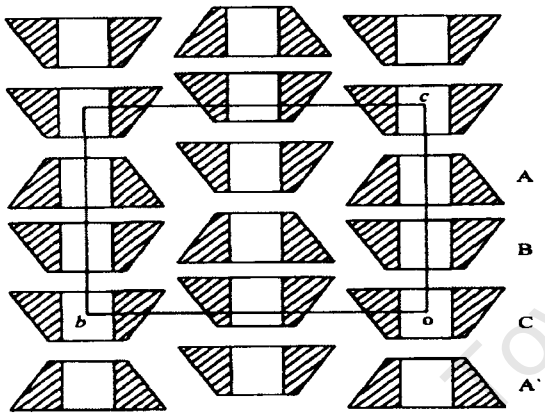

Figure 3.19: The packing arrangement of γ-CD complexes

The γ-CD molecules possess four-fold crystallographic symmetry and this requires guest molecules to be disordered. Due to this disorder, details of the geometry of the guest inclusion cannot generally be ascertained by crystallographic analysis.

Although from the above experiments four inclusion complexes were obtained, subsequent recrystallization did not yield single crystals intended for full X-ray structure determination, which is essential for pharmaceutical use of cyclodextrin inclusion complexes. Consequently the strategy of improving the water-solubility and hence the bioavailability of target compounds through cyclodextrin inclusion could not be fully explored.

3.2 Mannich Base Derivatives of 4-Aminoquinoline-Chalcones

3.2.1 Rationale of Drug Design

The rationale for the design of 4-aminoquinoline-based chalcones has been discussed previously in section 3.1.1. Mannich base derivatives of the target hybrid **2** were synthesized due to their superior biological activity in comparison to target hybrid **1**. In particular, Mannich base derivatives of **CDM20** and **CDM21** (Figure 3.2, p54)

were synthesized due to the previously discussed biological activity of hydroxylated chalcones (sections 2.5.2 and 2.5.3). Both acyclic and cyclic amines were used in order to explore preliminary structure-activity relationships of these hybrid compounds. Conversion of the 4-aminoquinoline-derived chalcones into their Mannich base derivatives was done due to the following considerations. Firstly, the presence of an additional protonatable nitrogen would increase the compounds' water-solubility properties via salt formation and also enhance accumulation in the acidic food vacuole of the malaria parasite via pH trapping. Secondly, at the lower pH associated with tumour cells or the acidic food vacuole, these phenolic Mannich base derivatives can undergo deamination to give very reactive intermediate enones that can potentially react with various cellular thiols important for parasite or tumour growth. These phenolic Mannich base derivatives may therefore be used as prodrugs whereby the cytotoxic agent is released at its site of action. Despite the numerous examples of antimalarial Mannich bases and wide interest in chalcones, antimalarial Mannich base derivatives of chalcones remain an unexplored field. Investigations of cytotoxic activity of phenolic Mannich base derivatives of chalcones by Dimmock *et al*[20] revealed that these compounds are a promising new class of cytotoxic agents due to good biological activity and absence of mutagenic effects. These Mannich bases were designed using the concept of sequential toxicity. Figure 3.20 summarises the chemical features of phenolic Mannich base derivatives of the 4-aminoquinoline-based chalcones and their potential biological action.

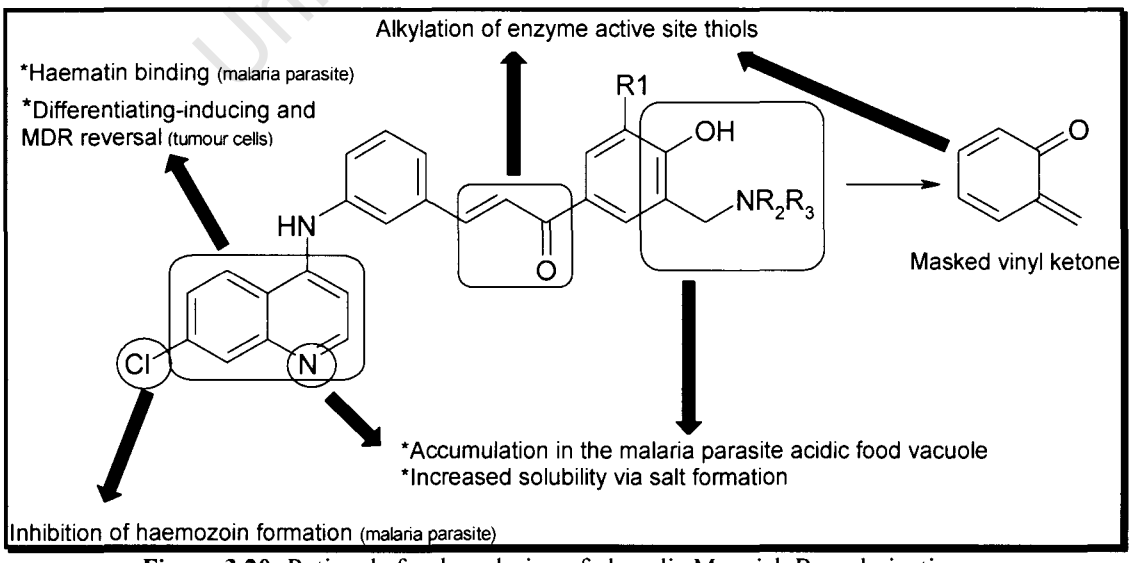

Figure 3.20: Rationale for drug design of phenolic Mannich Base derivatives

3.2.2 Retrosynthetic Analysis

The synthesis of the Mannich base derivatives was envisaged via two synthetic routes depicted in Scheme 3.12: **path a**, in which the starting material undergoes a Mannich reaction followed by a Claisen-Schmidt condensation reaction and, **path b**, involving the aminomethylation of the 4-aminoquinoline-based chalcone.

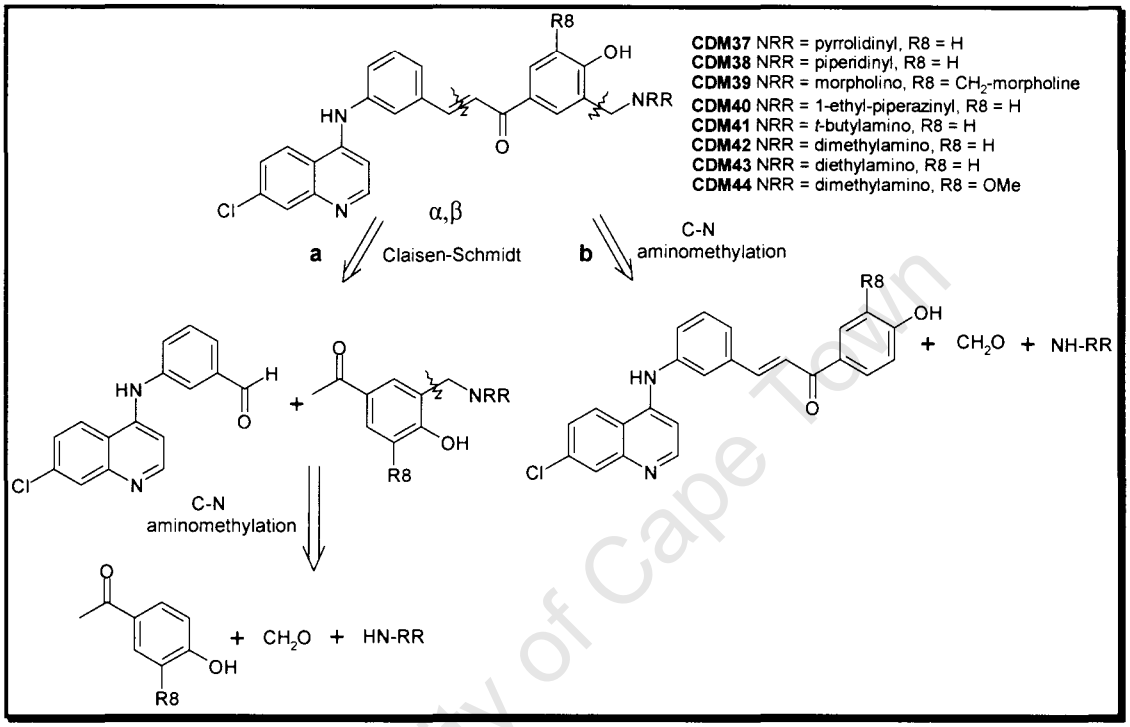

Scheme 3.12: Retrosynthetic analysis of Mannich base derivatives of target hybrid **2**

3.2.3 Synthesis of Phenolic Mannich Base Derivatives

The starting point in the synthesis of Mannich base derivatives via **path a** involved an aminomethylation reaction of 4-hydroxyacetophenone to yield the respective phenolic Mannich base derivative. This was performed using traditional methodology, i.e., heating the substituted amine with equimolar equivalents of paraformaldehyde in methanol for 2 h. Upon condensation of the amine and aldehyde, the resulting reactive intermediate was treated with the substrate to afford the phenolic Mannich base derivatives **CDM30-CDM36**, after purification by column chromatography. The second step in the synthesis involves a base-catalyzed Claisen-Schmidt condensation reaction of **CDM30-CDM36** with the 4-aminoquinoline-derived aldehyde to yield the Mannich base derivatives **CDM36-CDM41** in moderate yields. This approach used is depicted in Scheme 3.13.

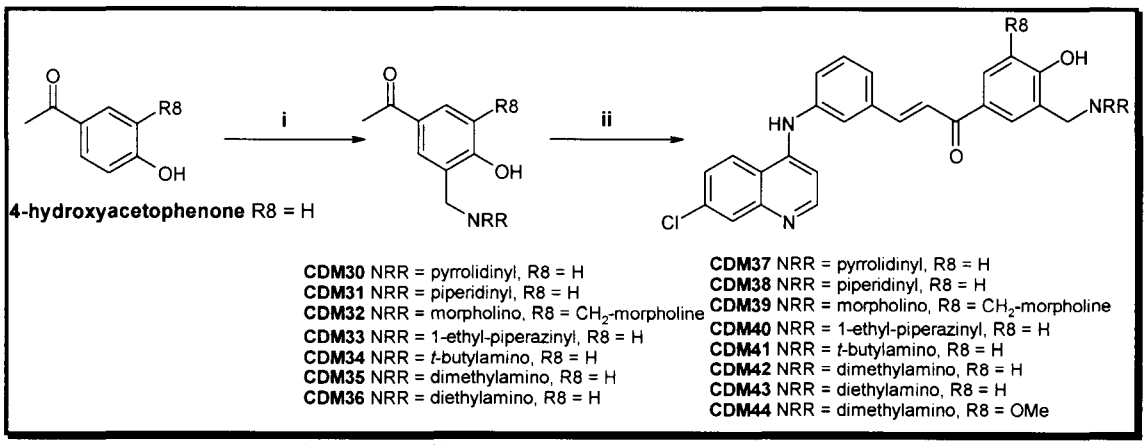

Scheme 3.13: *Reagents and conditions* i.) R_1R_2NH (2eq), CH_2O (2eq), MeOH, 65°C, 2 h then addition of substrate ii.) 3% w/v NaOH, MeOH, Reflux, 72 h.

Synthesis of the target compounds via **path b**, that is aminomethylation of the hydroxylated chalcones **CDM20** and **CDM21**, was attempted using various reaction conditions. The amine both as it free base and as hydrochlorides, formaldehyde either as an aqueous solution or paraformaldehyde and various solvents such as ethanol, methanol, acetonitrile and NMP were used in order to improve reaction times and yields. These attempts, however, were unsuccessful except for the formation of **CDM44**, which was achieved by heating dimethylamine hydrochloride and paraformaldehyde in NMP for 2 h, followed by addition of **CDM21** and further stirring for 4 d (Scheme 3.14). The long reaction times and low yields deemed this path undesirable.

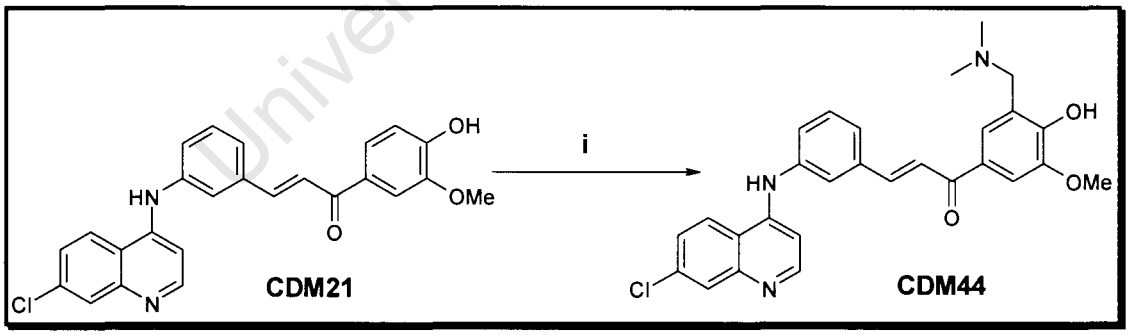

Scheme 3.14: *Reagents and conditions* i.) $(CH_3)_2NH.HCl$, CH_2O, NMP, 70°C, 4 days.

The structures, isolated yields and respective melting points of the resultant Mannich base derivatives of the 4-aminoquinoline-based chalcones are depicted in Table 9. The low yields observed may be due to factors such as the competing reaction of deprotonation of the phenolic proton (Fig. 3.5, p62) as well as difficulty in purification by column chromatography as a result of fractions 'co-running'.

Table 9: Mannich base derivatives of 4-Aminoquinoline-based chalcones with their respective yields and melting points

Product Structure	Code	Yield (%)	Mp (°C)
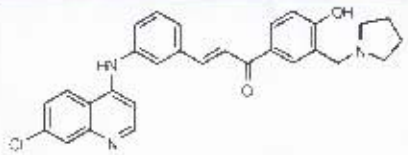	**CDM37**	17	209-211
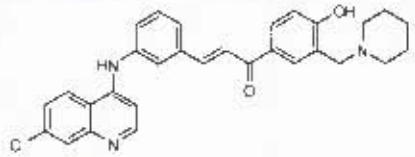	**CDM38**	38	223-225
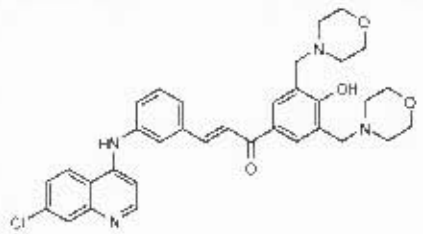	**CDM39**	15	233-235
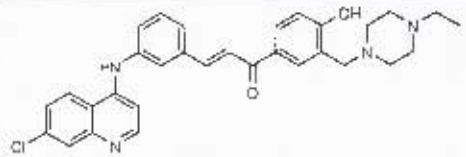	**CDM40**	12	214-216
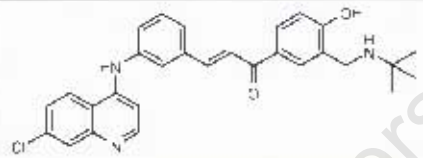	**CDM41**	11	232-234
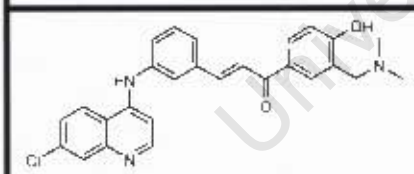	**CDM42**	34	216-218
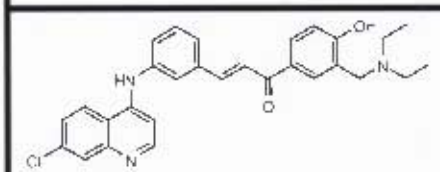	**CDM43**	20	207-210
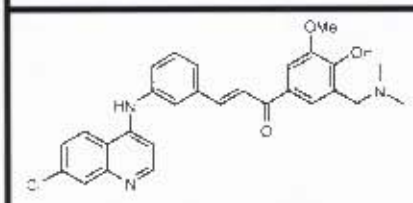	**CDM44**	20	280-282

3.2.4 Mechanistic Details

The mechanism of the Mannich reaction has been well investigated[21,22] and is thought to proceed through either of the two pathways depicted in Scheme 3.15.

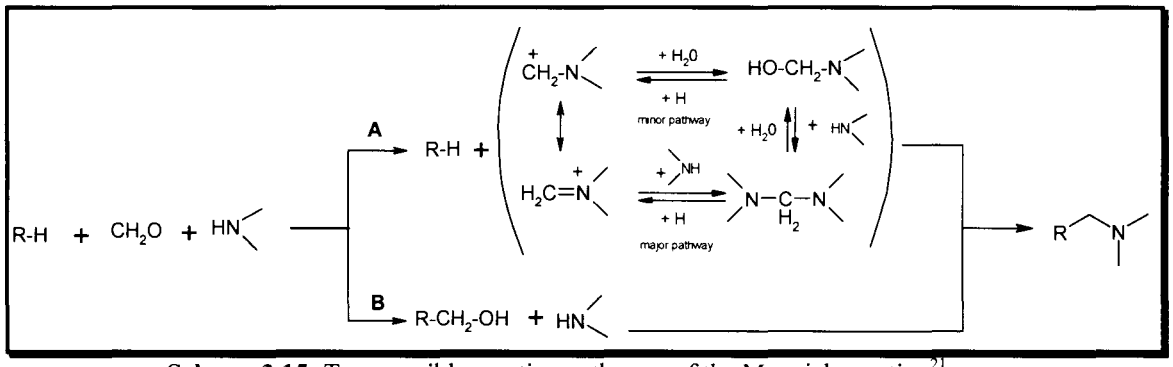

Scheme 3.15: Two possible reaction pathways of the Mannich reaction[21]

The preferred pathway depends on the nature of the reactants and the reaction conditions employed. Pathway **A** is widely accepted as the favoured route in which the nucleophilic amine attacks the more electrophilic substrate, which is formaldehyde, to give the condensation product, an imine salt. The electrophilic salt can now add to the phenol group of the substrate to give the product of the reaction, a Mannich base in which an aminomethyl group replaces the active hydrogen of the substrate. The proposed mechanism is given in Scheme 3.16.

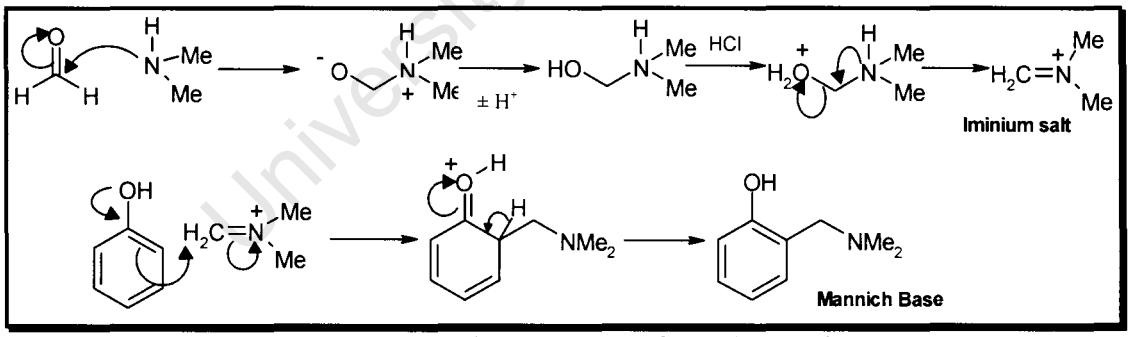

Scheme 3.16: Reaction mechanism of Mannich reaction

Phenols undergo aminomethylation at the *ortho* and *para* positions due to activation at these positions by the hydroxyl group. The regioselectivity is influenced by the nature and position of substituents on the phenol ring. The *ortho* position is usually preferred, although *para*-substitutions can occur when the *ortho* positions are blocked or have large substituents, as the attacking species shows considerable steric requirements.[22] This preferred *ortho*-substitution may also be explained by a

postulated mechanism involving a hydrogen-bonded complex depicted in Figure 3.21. For the Mannich bases in this study, the *para* position was blocked and thus aminomethylation occurred vicinal to the hydroxy group. The aminomethylation of the 4-hydroxyacetophenone starting material is also chemoselective, as this substrate has two sites for reaction with the aminomethylating agent. This chemoselectivity can be accounted for by comparing the transition states for both possible functional groups that may undergo attack, that is, the phenol group and the alkyl keto group. Aminomethylation at the active hydrogen of the phenol yields a more resonance-stabilized intermediate and is thus favoured (Figure 3.21). Reaction conditions are also important for chemoselectivity, with the alkyl keto group reacting under acidic conditions and phenols under neutral or basic conditions.

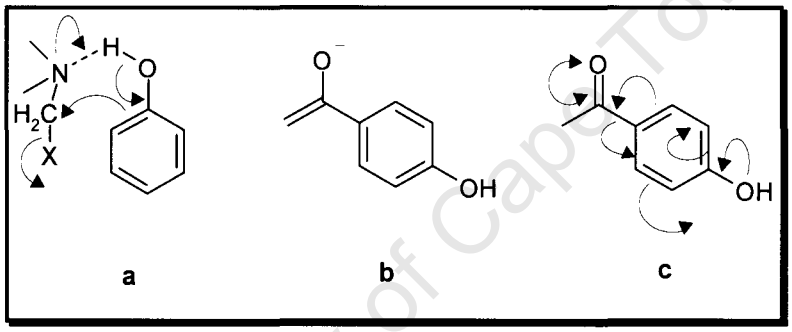

Figure 3.21: Chemical structures depicting regioselectivity due to a.) Hydrogen-bonded complex and reaction intermediates explaining chemoselectivity between the b.) alkyl keto group and c.) phenol group.

3.2.5 Characterization of Target Compounds

All Mannich base derivatives were characterized by ^{1}H and ^{13}C NMR, IR, mass spectrometry and elemental analysis. As for the ^{1}H NMR of the 4-aminoquinoline-based chalcones, resultant products displayed two common diagnostic doublets around δ 8 ppm and δ 7 ppm, correlating to the methine protons on the double bond of the α,β-unsaturated system. Additional ^{1}H NMR spectroscopic evidence for confirmation of the proposed structures came from the appearance of a singlet, integrating for two hydrogens at ~ δ 3.7 ppm which is consistent with the expected CH_2 of the aminomethyl group. This was confirmed in the ^{13}C NMR spectrum with a diagnostic peak appearing ~ δ 54 ppm.

Figure 3.22 shows a ^{1}H NMR spectrum of representative compound **CDM43**.

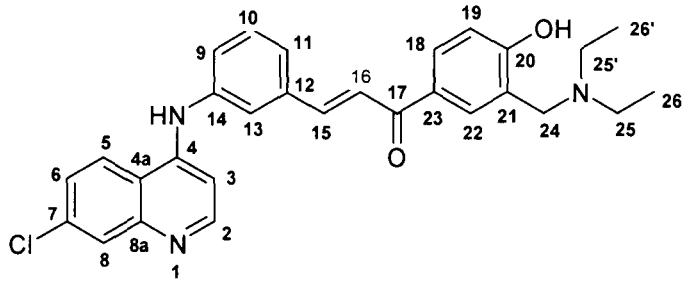

δ/ppm	Multiplicity	J/Hz	H
9.15	s	-	NH
8.48	d	5.2	H2
8.45	d	9.2	H5
7.98-7.96	dd	2.4, 8.4	H18
7.93	d	2.1	H7
7.90	d	15.0	H15
7.89	d	2.4	H22
7.82	s	-	H13
7.69	d	15.6	H16
7.65	d	7.6	H11
7.58-7.56	dd	2.4, 9.2	H6
7.50	t	8.0	H10
7.42	d	8.0	H19
6.94	d	5.6	H3
6.78	d	8.4	H9
3.85	s	-	H24 (CH_2)
2.62-2.56	q	7.2	H25+25'
1.03	t	7.2	H26+26'

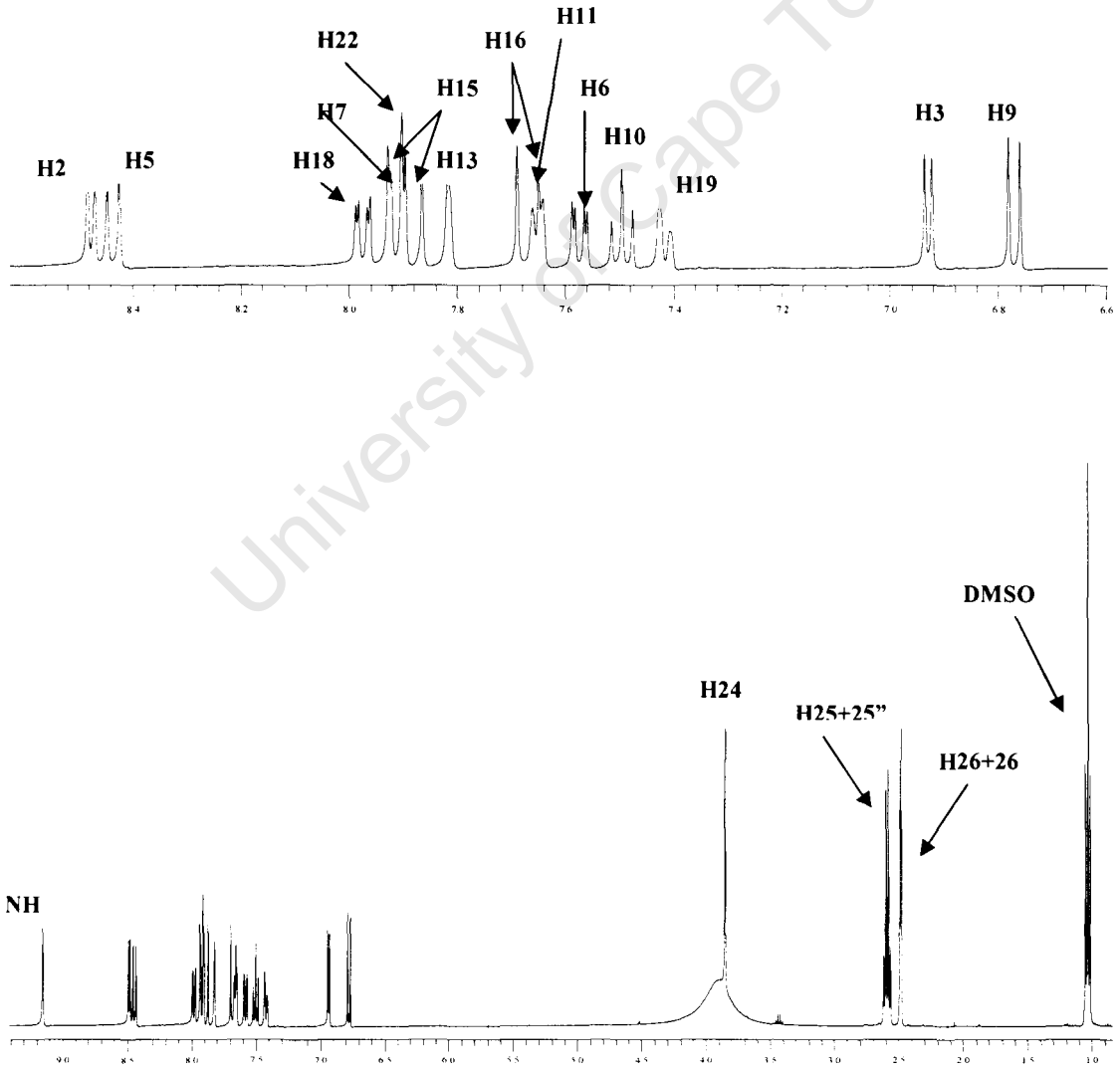

Figure 3.22: ^{1}H NMR spectrum of **CDM43** in d_6-DMSO at 400MHz

3.2.6 Cyclodextrin Inclusion Complexes

Preparation of cyclodextrin inclusion complexes was attempted using **CDM38** based on its biological activity and availability of material. Kneading and co-precipitation methods were employed using β-CD in both 1:1 and 2:1 (CD: guest) molar ratios and all attempts were unsuccessful, with the experimental PXRD patterns matching those of native β-CD. However, a γ-CD complex was prepared by the kneading method using a 1:1 molar ratio, with the PXRD pattern of the kneaded material matching that of the isostructural series 17, confirming that complexation has occurred (Figure 3.23).

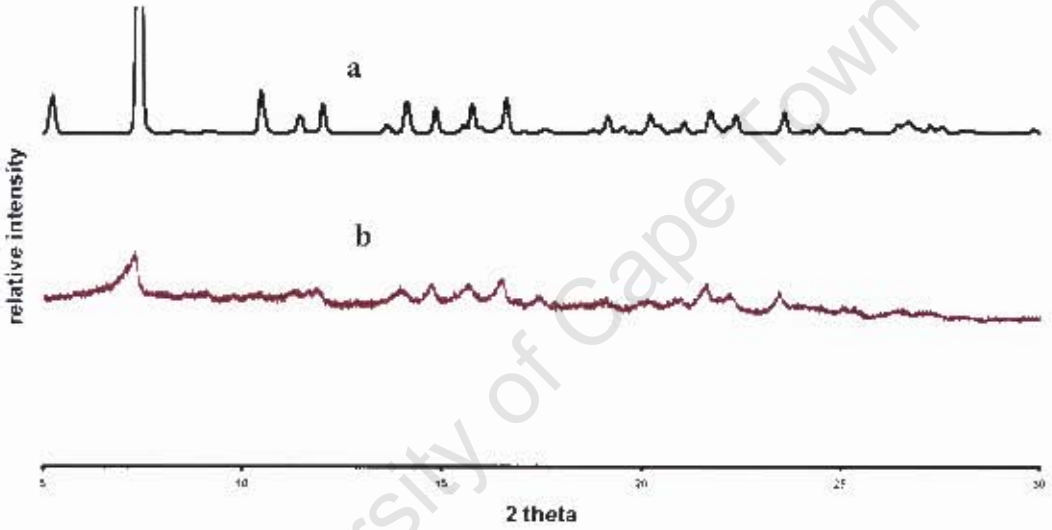

Figure 3.23: a) Computed PXRD trace for known γ-CD complex and experimental PXRD trace of (b) γ-CD-**CDM38** complex

A number of poorly soluble compounds have been dissolved in aqueous solutions of the methylated CDs DIMEB and TRIMEB.[23] It was proposed that inclusion of the target compounds, which have a strong hydrophobic nature, might be more successful in the more hydrophobic cyclodextrin TRIMEB. These experiments however also failed. Although attempts in cyclodextrin inclusion were somewhat fruitless, successful inclusion of a guest often requires unique design of a procedure 'tailor-made' to the particular guest. Exhaustive analysis of cyclodextrins and their derivatives and optimization of reaction conditions (pH, solvent and temperature) may yet lead to successful preparation of cyclodextrin inclusion complexes.

References

1. Egan, T.G. *Drug Design Reviews*, **2004**, *1*, 93 and references therein
2. Egan, T.G.; Hempelmann, E.; Mavuso, W.W. *J. Inorg. Biochem.*, **1999**, *73*, 101; Egan, T.G.; Hunter, R.; Kaschula, C.H.; Marques, H.M.; Misplon, A.; Walden, J.C. *J. Med. Chem.*, **2000**, *43*, 283.
3. Dougherty, D.A. *Science*, **1996**, *271*, 163.
4. Kawase, M.; Motohashi, N. *Current Drug Targets*, **2003**, *4*, 31.
5. Suzuki, T.; Fukazawa, N.; San-nohe, K. *J. Med. Chem.*, **1997**, *40*, 2047.
6. (a) Zamora, J.M.; Beck, W.T. *Biochem. Pharmacol.*, **1986**, *35*, 4303; (b) Zamora, J.M.; Pearce, H.L.; Beck, W.T. *Mol. Pharmacol.*, **1988**, *33*, 454.
7. Martirosyan, A.R.; Rahim-Bata, R.; Freeman, A.B.; Clarke, C.D.; Howard, R.L.; Strobl, J.S. *Biochem. Pharmacol.*, **2004**, *68*, 1729.
8. Liu, M.; Wiliarat, P.; Go, M.-L. *J. Med. Chem.*, **2001**, *44*, 4443.
9. Go, M.L.; Wu, X.; Liu, X.L. *Curr. Med. Chem.*, **2005**, *12*, 483.
10. Li, R.; Kenyon, G.; Cohen, F.E.; Chen, X.; Gong, B.; Dominguez, J.N.; Davidson, E.; Kurzban, G.; Miller, R.E.; Nuzum, E.O.; Rosenthal, P.J.; Mckerrow, J.H. *J. Med. Chem.*, **1995**, *38*, 5031.
11. Raynes, K.J.; Stocks, P.A.; O'Neill, P.M.; Park, B.K.; Ward, S.A. *J. Med. Chem.*, **1999**, *42*, 2747.
12. Gilbert, I.; Rees, D. C. *Tetrahedron*, **1995**, *51*, 6315 – 6336.
13. Anderson, M. W.; Jones, R. C. F.; Saunders, J. *J. Chem. Soc., Perkin Trans. 1*, **1986**, 205.
14. XPREP-*Data Preparation and Reciprocal Space Exploration*, Version 5.1, (Copyright Bruker Anayltical X-ray Systems, **1997**).
15. Sheldrick, G.M. *SHELXS-97, Program for Crystal Structure Solution*, Institüt für Anorganische Chemie der Universität, Tammanstrasse 4, D-3400 Göttingen, Germany, **1997**.
16. Sheldrick, G.M. *SHELXL-97, Program for the Refinement of Crystal Structures*, Institüt für Anorganische Chemie der Universität, Tammanstrasse 4, D-3400 Göttingen, Germany, **1997**.
17. Spek, A.L. PLATON, A Multipurpose Crystallographic Tool, Version 10500 © **1980-2000**.
18. Caira, M.R. *Rev. Roum. Chim.*, **2001**, *46*, 371.

19. Lubhelwana, S. *MSc Thesis*, University of Cape Town, South Africa **2005**.
20. Dimmock, J.R.; Vashishtha, S.C.; Quail, J.W.; Pugazhenthi, U.; Zimpel, Z.; Sudom, A.M.; Allen, T.M.; Kao, G.Y.; Balzarini, J.; De Clercq, E. *J. Med. Chem.*, **1998**, *41*, 4012.
21. Tramontini, M. *Synthesis*, **1973**, 703.
22. Tramontini, M.; Angiolini, L. *Tetrahedron*, **1990**, *46*, 1791 and references therein.
23. Szejtli, J.; Frömming, K.H. *Topics in Inclusion Science- Cyclodextrins in Pharmacy*, Dordrecht, The Netherlands, Kluwer Academic Publishers, **1994**.

CHAPTER 4

Biological Results and Discussion

4.1 Introduction

The following chapter discusses the results obtained from the biological evaluation of the synthesised compounds *in vitro* in appropriate cancer and malaria disease models. The synthesized target compounds were primarily generated in order to determine their abilities to inhibit both growth of malaria parasites and of tumour cells by determining the IC_{50} and ED_{50} values. The IC_{50} and ED_{50} are terms used to describe the inhibitory concentration and effective dose, respectively, of a drug necessary to produce a therapeutic effect in 50% of the test sample and are used interchangeably. The lower the IC_{50} or ED_{50} value of a compound, the greater is its efficacy. However, a property of equal importance for a good drug candidate is that it should be selectively cytotoxic towards the parasite or tumour cells and not towards normal human cells. Within the context of malaria, compounds were evaluated against both chloroquine-sensitive and chloroquine-resistant strains of the causative agent *Plasmodium falciparum*. In order to have a deeper understanding of the mechanistic basis of the observed activity, the target compounds were tested for inhibition of the cysteine protease falcipain 2 and haemozoin formation. The description of the assays and experimental details used in biological evaluation of the target compounds are given in the experimental section.

4.2 *In Vitro* Antimalarial Activity of 4-Aminoquinoline Chalcones

4.2.1 Results and Discussion

The antimalarial activity of the 4-aminoquinoline-derived chalcones **CDM04-CDM08** and **CDM13-CDM15** were evaluated in three different *in vitro* assays in the laboratories of Professor P. Rasoanaivo at Institut Malgache de recherches appliquees in Madagascar. In the first of these, the compounds were assayed against the chloroquine-sensitive strain 3D7 and then in the chloroquine-resistant W2 and

FCM29 *P. falciparum* strain and chloroquine-resistant FCM29 *P. falciparum* strains, using chloroquine as the control drug. The results for the independent test are presented in Table 10.

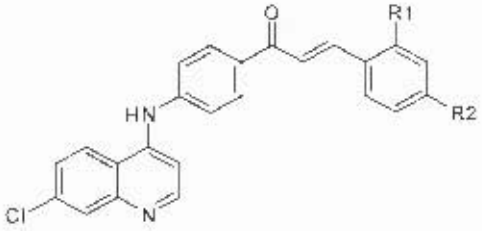

CDM04-CDM08

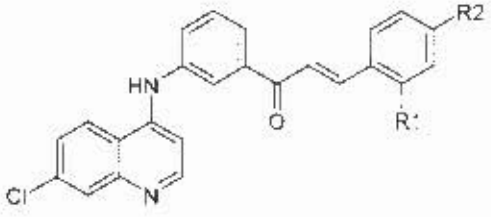

CDM06

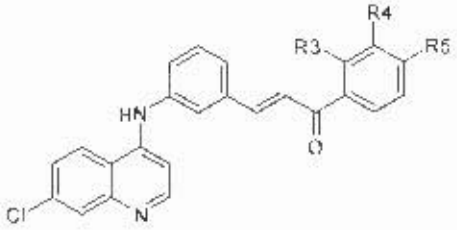

CDM13-CDM15

Table 10: *In vitro* antimalarial activity of 1-aminoquinoline chalcones

Compound code	R1	R2	R3	R4	R5	3D7 strain		FCM29 strain		W2 strain	
						IC_{50} (µg/ml)	IC_{50} (µM)	IC_{50} (µg/ml)	IC_{50} (µM)	IC_{50} (µg/ml)	IC_{50} (µM)
CDM04 (MKCl)	H	Cl				0.73	1.74	0.69	1.65	1.11	2.65
CDM05 (MKCl2)	Cl	Cl				1.25	2.75	2.03	4.47	2.33	5.13
CDM06 (mQCl)	H	Cl				0.18	0.43	0.46	1.09	0.65	1.55
CDM08 (MKDM)	OMe	OMe				0.44	0.99	0.52	1.17	0.48	1.08
CDM13 (MQMe)	-	-			OMe	0.22	0.53	0.36	0.87	0.68	1.64
CDM14 (MQ2Me)	-	-	OMe	-	OMe	0.32	0.72	0.50	1.12	0.53	1.19
CDM15 (MQ3Me)			OMe	OMe	OMe	0.39	0.82	0.55	1.16	0.79	1.66
Chloroquine							0.017 µM		0.15 µM		0.18 µM

As can be seen from the data presented in the table, relative to chloroquine none of the compounds exhibited any significant antimalarial activity in both the chloroquine-sensitive and chloroquine-resistant strains. The most active compound emerging from this study was **CDM06** against the chloroquine-sensitive strain 3D7 (IC_{50} = 0.43 μM), in which the 4-aminoquinoline moiety and the ketone linker have a *meta* relationship. On comparing the data obtained from **CDM04** (IC_{50} = 1.74 μM) and **CDM06** (IC_{50} = 0.43 μM), the *meta* position seems to be the most favourable position for substitution for target hybrid **1**. This observation may indicate a steric element is possibly involved in the interaction necessary for activity. All the other compounds were over several hundred-fold less efficacious than chloroquine. **CDM13** (IC_{50} of 0.87 μM) and **CDM08** (IC_{50} of 1.08 μM) showed the best activity against the chloroquine-resistant strains FCM29 and W2 respectively, indicating that the presence of a methoxy group is an important structural feature associated with antimalarial activity. Previous structure-activity studies on the antimalarial activity of chalcones have reported that electron-withdrawing groups on ring **A** are important for activity. [1] The results from this rather limited series suggest that this is not necessarily so and what has proven of more importance is the presence of a methoxy group. Nevertheless, more compounds need to be evaluated in this series to confirm this hypothesis. A general trend observed against all three strains is that target hybrid **2**, in which the 4-aminoquinoline moiety is attached to ring **B**, is more active than target hybrid **1**, in which the 4-aminoquinoline moiety is attached to ring **A**. A notable observation is that compounds **CDM13-CDM15** all have *meta* relationships with regard to the 4-aminoquinoline ring and the enone linker, once again implicating a steric element in the interaction necessary for activity. The observation that some of the compounds had similar activities against chloroquine-resistant and chloroquine-sensitive *P. falciparum* strains suggests that this series of 4-aminoquinoline chalcones may have a mechanism of action different to that of chloroquine and/or that the chloroquine resistance mechanism is circumvented in in this case. Despite the lower antiplasmodial activities associated with these compounds compared to chloroquine, the target compounds on average possess favourable resistance indices (Table 11). The resistance index (ratio of the IC_{50} in the resistant strain to that in the sensitive strain) is a measure of the cross resistance of a compound between two species of the parasite, with a low value being more favorable.

[1] Li, R. et al *J. Med. Chem.*, **1995**, *38*, 5031.

Table 11: Resistance indices of 4-aminoquinoline chalcones

Compound code	Resistance Index (FCM29)	Resistance Index (W2)
CDM04 (MKCl)	0.95	1.52
CDM05 (MKCl2)	1.62	1.86
CDM06 (mQCl)	2.56	3.61
CDM08 (MKDM)	1.18	1.09
CDM13 (MQMe)	1.64	3.09
CDM14 (MQ2Me)	1.56	1.66
CDM15 (MQ3Me)	1.41	2.03
Chloroquine	8.82	10.59

Target compounds have resistance index values far below those of chloroquine and thus have lower cross-resistance between the chloroquine-sensitive and chloroquine-resistant strains. Considering that the compounds bear the 4-aminoquinoline moiety, it is possible that they may in part be acting by a mechanism similar to that for chloroquine, namely, the inhibition of haemozoin formation. Investigation of the β-haematin inhibition of these compounds is thus of interest in order to access the contribution of the 4-aminoquinoline ring to the antimalarial activity. The citrate salt derivatives of the 4-aminoquinoline chalcones were screened for their ability to inhibit β-haematin formation, with only **CDM27** showing activity. The IC_{50} values are measured in equivalents, with a value of 0.449 equiv. determined for **CDM27**, which is 4 times more active than chloroquine (1.91 equiv). The lower activity observed *in vitro* against the chloroquine-sensitive and chloroquine-resistant strains compared to that of chloroquine might be due to the absence of a basic terminal nitrogen atom and/or a lipophilic side chain, which are important for accumulation in the acidic food vacuole of the parasite and crossing the parasite membrane respectively. Modifications such as introducing a basic nitrogen in the structure of the target compounds may improve activity.

4.3 *In Vitro* Anticancer Activity of 4-Aminoquinoline Chalcones

4.3.1 Results and Discussion

The anticancer activities of the 4-aminoquinoline chalcones were determined in the laboratories of Professor C. Medlen, of the Department of Pharmacology at the University of Pretoria. For evaluation of the anticancer activity, the citrate salt derivatives **CDM22-CDM29** of the synthesised 4-aminoquinoline chalcones were tested against HeLa (Human adenocarcinoma of the cervix) cells. Each experiment was done in triplicate and the biological results are summarised in Table 12.

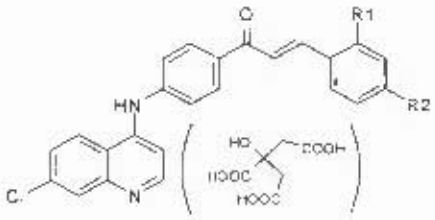

CDM22-CDM26

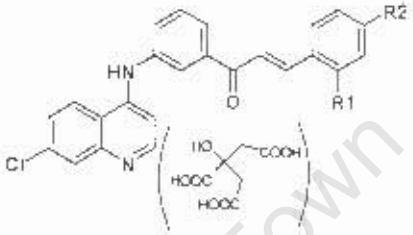

CDM24

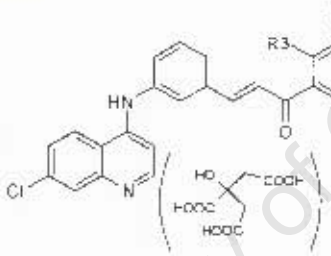

CDM27-CDM29

Table 12: *In vitro* anticancer activity of citrate salt derivatives of 4-aminoquinoline chalcones

Compound code	R1	R2	R3	R4	R5	HeLa cells IC_{50} (μM)
CDM22 (CITCl)	H	Cl	-			27.224
CDM23 (CITDC)	Cl	Cl	-	-		26.76
CDM24 (CITMQ)	H	Cl	-	-	-	1.557
CDM25 (CITF)		F	-	-	-	6.05
CDM26 (CITDM)	OMe	OMe	-	-	-	2.972
CDM27 (CITMe)				-	OMe	0.872
CDM28 (CIT2Me)			OMe	-	OMe	0.817
CDM29 (CIT3Me)	-	-	OMe	OMe	OMe	0.547
Chloroquine						75.728

The data shown in this table reveals that citrate salt derivatives of target hybrid **2**, **CDM27-CDM29**, were more active than those generated from target hybrid **1**, **CDM22-CDM26**, with IC_{50} values of the citrate salts ranging from 0.547 to 27.224 μM. These compounds are significantly more potent than chloroquine, with the most active compound **CDM29** (IC_{50} = 0.547 μM) being almost 140 times more potent. A previous study has revealed a large number of methoxylated chalcones with antimitotic activity against HeLa cells,[2] with a preference for the methoxy groups on ring **A**. Indeed, the biological results of the methoxy-substituted chalcones **CDM27** (IC_{50} = 0.872 μM), **CDM28** (IC_{50} = 0.817 μM), **CDM29** (IC_{50} = 0.547 μM) and **CDM24** (IC_{50} = 2.972 μM) confirmed this study with the more potent series **CDM27-CDM29** having the methoxy groups located on ring **A**. The methoxylated series **CDM27-CDM29** displayed good *in vitro* activity against HeLa cells with an increase in methoxy groups accompanied by an increase in activity (Figure 4.1).

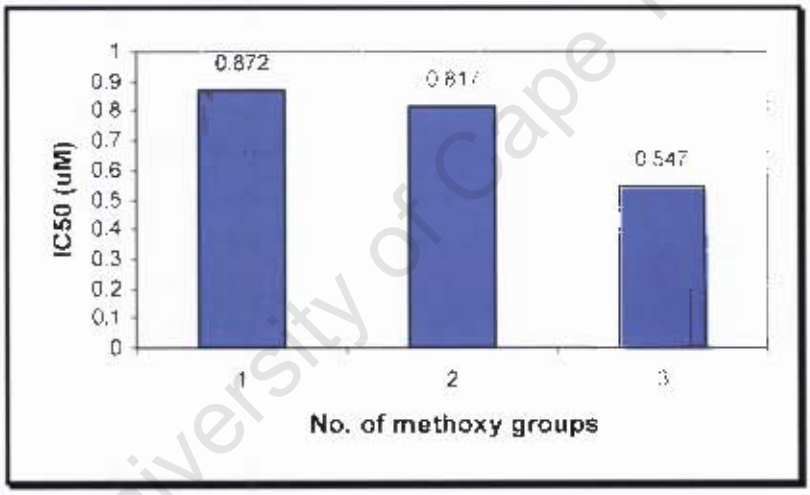

Figure 4.1: Plot depicting affect on activity with increasing number of methoxy groups

Comparisons observed within target hybrid **1**, reveals that the *meta* relationship with regard to the position of the 4-aminoquinoline moiety and the enone linker, displays superior activity to the *para* counterpart. This may be a result of more sterically favourable interactions between the drug and its site of action.

It was postulated that electron-withdrawing groups on ring **B** would render the β-carbon electron deficient by electron delocalisation along the α,β-unsaturated system, and accordingly, more inclined to nucleophilic attack by cellular thiols. Although the

[2] Edwards, M.L.; Stemerick, D.M.; Sunkara, P.S. *J. Med. Chem.*, **1990**, *33*, 1948.

more electronegative fluoro-substituted chalcone **CDM25** (IC_{50} = 6.05 μM) showed superior activity to the chloro-substituted chalcone **CDM22** (IC_{50} = 27.224 μM) and **CDM23** (IC_{50} = 26.76 μM), the presence of an electron-donating methoxy group on ring **B**, **CDM26** (IC_{50} = 2.972 μM), seemed more important for *in vitro* activity. As a consequence of the good *in vitro* activity displayed for **CDM27-CDM29**, attempts were made to form cyclodextrin inclusion complexes of these three compounds in order to potentially improve aqueous solubility and thus their efficacy.

4.4 *In Vitro* Antimalarial Activity of Phenolic Mannich Base Derivatives of 4-Aminoquinoline Chalcones

4.4.1 Results and Discussion

The phenolic Mannich base derivatives **CDM37-CDM44** were evaluated in four different *in vitro* assays. Firstly, the compounds were assayed against the chloroquine-sensitive D10 *P. falciparum* strain, using chloroquine diphosphate as the control drug, at the Department of Pharmacology (UCT). The antiplasmodial activity of the Mannich base derivatives was determined against the W2 chloroquine-resistant *P. falciparum* strain and were also evaluated for their abilities to inhibit the activity of the plasmodial cysteine protease falcipain 2. These antiplasmodial and enzyme inhibition tests were conducted at the Department of Medicine, San Francisco General Hospital, University of California at San Francisco (UCSF), in collaboration with Professor P. J. Rosenthal. Lastly, the ability of the compounds to inhibit β-haematin (haemozoin) formation was determined in the laboratories of Prof. T.J. Egan at the University of Cape Town.

The antiplasmodial activities as well as the data for inhibition of falcipain 2 and β-haematin formation of chalcones **CDM20-CDM21** and their Mannich base derivatives **CDM37-CDM44** are tabulated in Table 13.

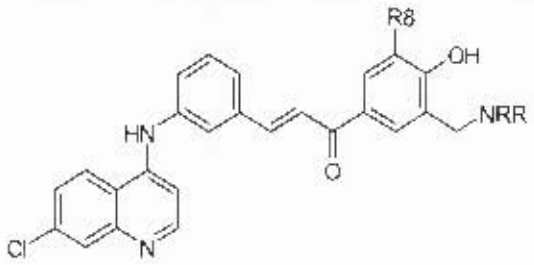

CDM20-CDM21, CDM37-CDM44

Table 13: *In vitro* antimalarial activity and inhibition of falcipain 2 and β-haematin formation of Mannich base derivatives

Compound code	R8	NRR	D10 IC_{50} (μM)	W2 IC_{50} (μM)	Rec-FP-2* IC_{50} (μM)	β-haematin (equiv.)
CDM20 (CD311)	H		0.584	0.7584	>6.000	0.190
CDM21 (CD303)	OMe		0.462	0.4843	8.465	0.279
CDM37 (CD313)	H		0.111	0.0039	11.515	0.219
CDM38 (CD314)	H		0.378	0.0428	24.130	0.235
CDM39 (CD315)	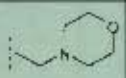		0.091	0.0503	59.415	nd[a]
CDM40 (CD316)	H		0.195	0.152	21.650	0.223
CDM41 (CD318)	H	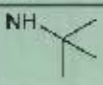	nd[a]	0.0481	27.835	nd[a]
CDM42 (CD312)	H		0.458	0.0178	24.820	nd[a]
CDM43 (CD308)	H	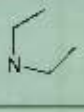	0.344	0.0830	21.675	0.232
CDM44 (CD307)	OMe		nd[a]	nd[a]	nd[a]	nd[a]
Chloroquine	–	–	0.013	0.099		1.94
E64		–	–	–	0.035	–

[a] Not determined, * Recombinant falcipain 2

The data shown in this table reveals that as antiplasmodial agents, the Mannich base derivatives are significantly more active than their corresponding chalcones against the D10 and W2 strains *in vitro*. One of the reasons for the increased potency of the Mannich base derivatives may be ascribed to the presence of an additional protonatable nitrogen atom, which is important for increased accumulation within the acidic food vacuole of the parasite. This property may also be explained by an increased interaction between these compounds and the cysteine protease at His 67 in the active site. Compared to chloroquine, all compounds showed weak to modest activity against the chloroquine-sensitive strain D10, with the most active compound being **CDM39** (IC_{50} = 0.09 μM). This observation may be due to problems experienced in solubilizing the compounds in the appropriate medium necessary for biological evaluation. On the other hand, most Mannich base derivatives showed greater antiplasmodial activities in the resistant W2 strain (IC_{50} ranging from 0.004 to 0.08 μM) than the reference drug chloroquine (IC_{50} = 0.099 μM), with exception of the chalcones **CDM20-CDM21** and the Mannich base **CDM40**. There is a fairly good correlation between antimalarial activity against D10 and inhibition of β-haematin formation. This observed correlation may be a result of similar pKa values and thus comparable vacuolar accumulation of the Mannich base derivatives. Slight deviations in the correlation between the activity and β-haematin inhibition may be a result of the small differences in pKa values. This correlation/lack of correlation between biological activity and β-haematin inhibition is only considered in chloroquine sensitive strains due to other factors in play in chloroquine resistant strains that disallow an accurate comparison. Both the chalcones and their Mannich base derivatives (0.190-0.429 equiv.) were approximately 10 times more active than chloroquine (1.91 equiv.) on the inhibition of β-haematin formation.

The phenolic Mannich base derivatives were stronger inhibitors of recombinant falcipain 2 than the corresponding chalcone **CDM20** that may be attributed to the larger number of electrophilic centers available for nucleophilic attack by cellular thiols. Interestingly, the methoxy-substituted chalcone **CDM21** (IC_{50} = 8.465 μM) showed the strongest inhibition of recombinant falcipain 2. There seems to be no correlation between the ability of a compound to inhibit falcipain 2 and antiplasmodial activity against D10 and W2 *in vitro*. This suggests that falcipain 2 is

not the primary target of these compounds and/or that the observed activity is due to multiple mechanisms including β-haematin formation. In addition it may be that the target compounds may not be reaching the target (falcipain 2) in high enough concentrations due to unfavourable physio-chemical properties. In order for the target compounds to reach its site of action, they must cross the parasite membrane and accumulate in the food vacuole. The pyrrolidine-derived Mannich base **CDM37** is a promising drug candidate as it shows superior activity in both the chloroquine-sensitive (IC_{50} = 0.111 μM) and chloroquine-resistant (IC_{50} = 0.0039 μM) *P. falciparum* strains as well as strong inhibition of falcipain 2 (IC_{50} = 11.51 μM) and β-haematin formation (0.219 equiv).

4.5 *In Vitro* Derivatives Anticancer Activity of Phenolic Mannich Base Derivatives of 4-Aminoquinoline Chalcones

4.5.1 Results and Discussion

The anticancer activities of hydroxylated chalcones **CDM20** and **CDM21** and their Mannich base derivatives **CDM37-CDM44** were assayed against HeLa cells in the laboratories of Professor C. Medlen, at the Department of Pharmacology at the University of Pretoria. This study was performed in order to determine the biological effect of conversion of these chalcones into the corresponding Mannich bases. The anticancer activities are tabulated in Table 14 and are in the IC_{50} range of 0.770 – 6.503 μM.

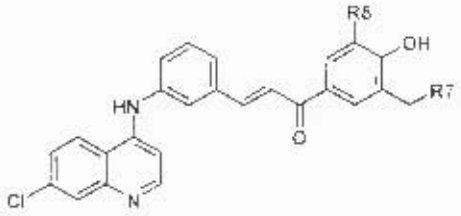

CDM20-CDM2,CDM37-CDM44

Table 14: *In vitro* anticancer activity of Mannich base derivatives of 4-aminoquinoline chalcones

Compound	R8	R7	HeLa cells IC_{50}(μM)
CDM20	H	–	6.503
CDM21	OMe	–	1.540
CDM37	H		0.770
CDM38	H	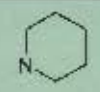	1.036
CDM39	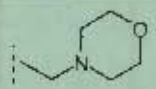	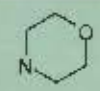	1.287
CDM40	H		0.876
CDM41	H	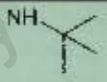	0.850
CDM43	H	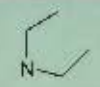	1.218
CDM44	OMe		0.921
Cisplatin	–	–	0.803

It is clear from the data presented in Table 14 that the conversion of chalcones **CDM20** and **CDM21** into the corresponding Mannich bases led to an increase in potency. The Mannich base **CDM44** (IC_{50} – 0.921 μM) was 1.7 times more cytotoxic than the corresponding chalcone **CDM21** (1.540 μM). Of interest is that the introduction of a methoxy group to the hydroxylated chalcone **CDM20**, as in **CDM21**, was accompanied by an appreciable increase in activity. This observation is consistent with previous studies in which the methoxylated chalcones were associated

with good antimitotic activity in HeLa cells.[2] The Mannich base derivatives **CDM37-CDM43** displayed significantly greater activity than the related chalcone **CDM20**. with most Mannich bases having more than six times the potency than that of **CDM20**. The most active compound emerging from this study was the pyrrolidine-derived Mannich base **CDM37** with an IC_{50} = 0.770 μM, which was comparable to the control drug Cisplatin (IC_{50} = 0.803 μM). As shown in Figure 4.2, there seems to be no trend between activity and the type of amine (cyclic or acyclic) used in the aminomethylation of the phenolic chalcones.

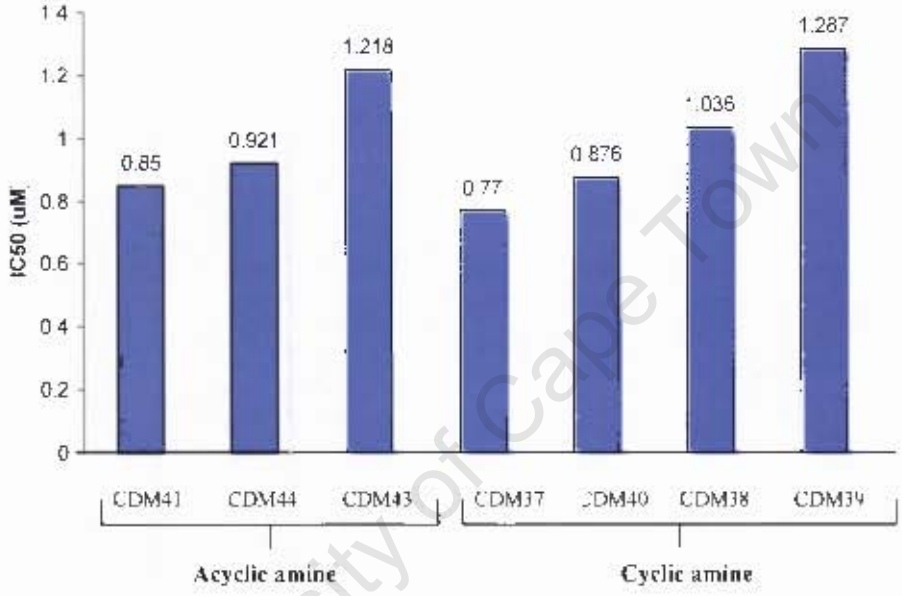

Figure 4.2: Plot depicting IC_{50} values of Mannich base derivatives

The enhanced anticancer activity of the Mannich base derivatives in comparison to their chalcone counterparts may be attributed to a number of factors. The observed activity may be a result of a greater number of nucleophilic sites in the molecule for electrophilic attack with cellular thiols but also may be due to the concept of sequential cytotoxicity[3], in which the consecutive release of two or more cytotoxic compounds is more damaging to malignant cells rather than normal cells. In order to access the viability of these compounds as prototypic anticancer molecules, an evaluation of their selective toxicity towards neoplastic rather than normal cells needs to be carried out.

[3] Dimmock, J.R., Sidhu, K.K.; Chen, M.; Reid, R.S.; Allen, T.M.; Kao, G.A. *Eur. J. Med. Chem.*, **1993**, *28*, 313.

4.6 Conclusion

In conclusion, we have successfully employed the 4-amino-7-chloroquinoline moiety to discover new potential antiplasmodial and anticancer agents. The simplicity of the chemistry employed during synthesis, coupled with the commercial availability and economic cost of reagents makes the 4-aminoquinoline chalcones attractive potential lead compounds in the search for antiplasmodial and anticancer agents. The 4-aminoquinoline chalcones showed weak to modest antiplasmodial activity against both chloroquine-resistant and chloroquine-sensitive *P. falciparum* strains. A *meta* relationship between the 4-aminoquinoline unit and the ketone linker was found to be preferential for both antimalarial and anticancer activity. Target hybrid **2** in which the 4-aminoquinoline unit is attached to the aldehyde, was more potent than target hybrid **1**, in which the 4-aminoquinoline unit is attached to the ketone. This was observed in both malaria parasites and cancer cells. Electron withdrawing groups which potentially render the β-carbon electron deficient and thus more susceptible to nucleophilic attack, were found to be of less structural importance than the presence of a methoxy substituents. The methoxy-substituted series **CDM13-CDM15** had good activity against HeLa cells and would be of interest to evaluate their selective toxicity towards neoplastic rather than normal cells. Despite the lower antiplasmodial activity of the 4-aminoquinoline chalcones than chloroquine, they possessed favourable resistance indices. This low activity may in part due to the hydrophobic nature of the molecule and introducing a terminal nitrogen atom or making different salt derivatives with a view to enhancing absorption under physiological conditions may increase activity.

The low reaction yields obtained for the phenolic Mannich bases may be attributed to factors such as the competing reaction of deprotonation of the phenolic proton as well as difficulty in purification by column chromatography as a result of fractions 'co-running'. Optimization of reaction conditions is required for use of these Mannich base derivatives as potential lead compounds. All Mannich base derivatives were found to be more potent than their corresponding chalcones against both the malaria parasite and tumour cells. These compounds showed significant activity in the W2 chloroquine-resistant strain, with most compounds being more active than chloroquine. All Mannich base derivatives and the phenolic chalcones were up to 10

times more active than chloroquine on the inhibition of β-haematin formation. The pyrrolidine-derived Mannich base **CDM37** is a promising potential drug candidate as it shows superior activity in both the chloroquine-sensitive (IC_{50} = 0.111 μM) and chloroquine-resistant (IC_{50} = 0.0039 μM) *P. falciparum* strains as well as inhibition of falcipain 2 (IC_{50} = 11.51 μM) and β-haematin formation (0.219 equiv). It would be of interest to test this compound in animal models, as the *in vitro* activity does not always translate into *in vivo* activity.

CHAPTER 5

Experimental

5.1 General

All commercial chemicals were purchased from Merck (South Africa) or Sigma-Aldrich. The host compounds β-cyclodextrin, γ-cyclodextrin and TRIMEB were obtained from Cyclolab (Budapest, Hungary). All solvents were freshly distilled and dried by appropriate techniques with the exception of analytical reagent grade absolute ethanol (EtOH) and methanol (MeOH), anhydrous dimethylsulfoxide (DMSO), dichloromethane (DCM) and acetone. Triethylamine was dried over and distilled from calcium hydride and stored over potassium hydroxide pellets. Reactions were monitored by thin layer chromatography using Merck F254 silica gel plates and were visualized by ultraviolet light or staining with iodine vapour, ninhydrin or anisaldehyde. Silica gel chromatography was performed using Merck kieselgel 60.

Melting points were determined on a Linkam THMS600 hot stage apparatus and are uncorrected. Infrared (IR) spectra were recorded on a Perkin-Elmer FT-IR spectrometer in the range from 3800 to 800 cm^{-1} as chloroform solutions on sodium chloride discs. Microanalyses were determined using a Fison's EA 1108 CHNS-O instrument. Low resolution masses were determined by the Department of Pharmacology (UCT) on an API 2000 from Applied Biosystems Mass spectra were recorded on a VG micromass 16F spectrometer operating at 70eV with an accelerating voltage of 4kV and a variable temperature source. Accurate masses were recorded using VG70-SEQ (EI, operating at 8kV) instrument at the University of the Witswatersrand.

Proton nuclear magnetic resonance (^{1}H NMR) spectra were recorded on a Varian Mercury 300 MHz or a Varian Unity 400 MHz at ambient temperature. All spectra were recorded in deuterodimethylsulfoxide (d_6-DMSO) and deuterochloroform ($CDCl_3$), using tetramethylsilane (TMS) as an internal standard. The chemical shifts (δ) are given in ppm and the coupling constant *J* is given in Hz. Carbon-13 nuclear magnetic resonance (^{13}C NMR) spectra were recorded on the same instruments at 75MHz or 100MHz using the same internal standard and deuterated solvents.

General procedure for synthesis of 4-aminoquinoline-derived methyl ketones CDM01-CDM03 and benzyl alcohols CDM09-CDM10

A solution of aldehyde or ketone (1.0 eq) and 4,7-dichloroquinoline (1.0eq) in ethanol was stirred under reflux at 85-90°C for 4 h. The resulting suspension was cooled to room temperature and basified to pH 8 by the addition of a 25% ammonium hydroxide solution. The resulting precipitate was collected by filtration, washed with distilled water and dried *in vacuo*. To remove any remaining product, the aqueous filtrate was extracted with dichloromethane, dried over anhydrous Na_2SO_4, and concentrated under reduced pressure to give a yellow solid. The combined organic products were recrystallized from ethanol to give the desired product isolated as yellow crystals.

1-[4-[(7-Chloro-4-quinolinyl)amino]phenyl]-ethan-1-one, CDM01

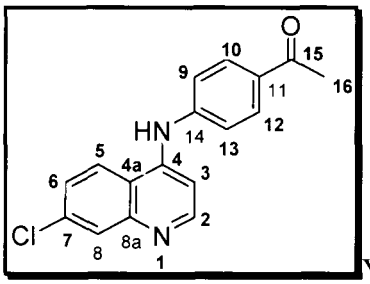

Yellow crystals (5.7445g, 79%); R_f (EtOAc:hexane, 3:2) 0.55; δ_H (300MHz, d_6-DMSO) 9.415 (1H, s, NH), 8.62 (1H, d, *J* 5.1, H-2), 8.41 (1H, d, *J* 9.3, H-5), 7.99 (3H, m, H-8, H-10 and H-11), 7.64 (1H, dd, *J* 2.1, 8.7, H-6), 7.45 (2H, d, *J* 9, H-9 and H-13), 7.25 (1H, d, *J* 5.1, H-3), 2.55 (3H, s, CH_3-16); δ_c (75MHz, d_6-DMSO) 196.2, 150.5 (2C), 147.0 (2C), 144.9, 134.9, 131.7, 129.9 (2C), 128.2, 125.8, 124.9, 120.0, 118.7, 104.2, 26.4.

1-[3-[(7-Chloro-4-quinolinyl)amino]phenyl]-ethan-1-one, CDM02

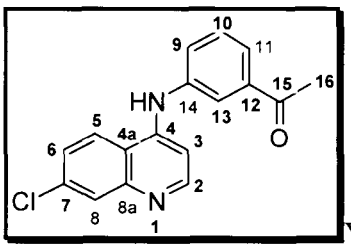

Yellow crystals (0.609g, 94%), R_f (EtOAc:hexane, 3:2) 0.306; δ_H (400MHz, d_6-DMSO) 11.32 (1H, s, NH), 8.95 (1H, d, *J* 9.2, H-5), 8.55 (1H, d, *J* 6.8, H-2), 8.21 (1H, d, *J* 2.4, H-8), 8.04 (1H, s, H-13), 7.99 (1H, d, *J* 7.6, H-11), 7.88 (1H, dd, *J* 2.4, 9.2, H-6), 7.71 (1H, d, *J* 7.8, H-9), 7.71 (1H, t, *J* 7.6, H-10), 6.87 (1H, d, *J* 6.8, H-3), 2.61 (3H, s, CH_3-16);

δ_c (100MHz, d_6-DMSO) 199.7, 151.3, 149.0 (2C) 143.0, 137.5, 134.9, 129.5 (2C), 127.2, 122.5, 120.0 (2C), 118.8, 113.1 (2C), 29.4.

1-[2-[(7-Chloro-4-quinolinyl)amino]phenyl]-ethan-1-one, CDM03

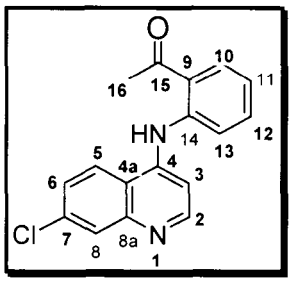

Yellow crystals (0.4298g, 60%); R_f (EtOAc:hexane, 3:2) 0.36; δ_H (400MHz, d_6-DMSO) 11.40 (1H, s, NH), 8.75 (1H, d, *J* 8.8, H-5), 8.51 (1H, d, *J* 6.4, H-2), 8.19 (1H, d, *J* 2.0, H-8), 8.03 (1H, d, *J* 7.6, H-10), 7.84 (1H, dd, *J* 2.0, 9.2, H-6), 7.74 (1H, t, *J* 8.0, H-12), 7.60 (1H, d, *J* 7.6, H-13), 7.53 (1H, t, *J*, 7.6, H-11), 6.64 (1H, d, *J* 6.8, H-3) 2.53 (3H, s, CH_3-16); δ_c (100MHz, d_6-DMSO) 198.2, 151.5 (2C), 147.5 (2C), 145.3, 134.9, 134.0, 129.6 (2C), 127.2, 122.8, 119.5, 118.7 (2C), 116.2, 27.4.

[3-(7-Chloro-quinolin-4-ylamino)-phenyl]-methanol, CDM09

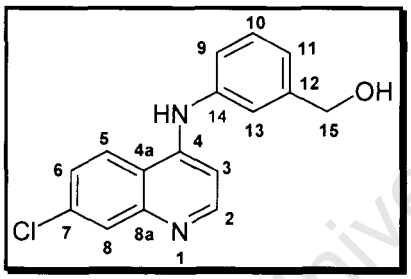

Pale yellow crystals (2.0498g, 98%); R_f (5% MeOH in DCM) 0.36; δ_H (300MHz, d_6-DMSO) 9.06 (1H, s, NH), 8.46 (1.H, d, *J* 5.7, H-2), 8.43 (1H, d, *J* 8.7, H-5), 7.88 (1H, d, *J* 2.7, H-8), 7.58 (1H, dd, *J* 2.4, 9.0, H-6), 7.38 (1H, t, *J* 7.8, H-10), 7.34 (1H, s, H-13), 7.24 (1H, d, *J* 8.1, H-11), 7.12 (1H, d, *J* 8.1, H-9), 6.93 (1H, d, *J* 5.4, H-3), 5.24 (1H, t, *J* 5.7, OH), 4.54 (2H, d, *J* 5.7, H-15); δ_C(75MHz, d_6-DMSO) 151.8, 149.5, 148.0, 143.9, 139.9, 133.8, 128.9, 127.5, 124.8, 124.4, 122.0, 120.8, 120.5, 118.2, 101.7, 62.6.

[2-(7-Chloro-quinolin-4-ylamino)-phenyl]-methanol, CDM10

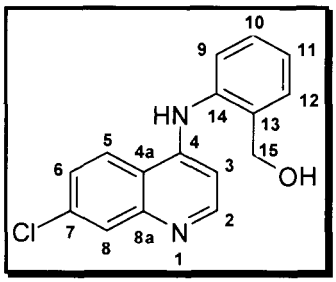

Yellow crystals (0.2274g, 33%); R_f (EtOAc-Hexane, 3:2) 0.58; δ_H (300MHz, d_6-DMSO) 8.8 (1H, s, NH), 8.38 (1.H, d, *J* 6.0, H-2), 8.35 (1H, d, *J* 9, H-5), 7.88 (1H, d, *J* 2.7, H-8), 7.61 (2H, m, H-6 and H-12), 7.35 (2H, m, H-9 and H-11), 6.28 (1H, d, *J* 5.7, H-3), 5.24 (1H, s, OH), 4.52 (2H, s, H-15); δ_C(75MHz, d_6-DMSO) 151.5, 149.3, 148.1, 140.5 (2C), 134.8, 129.5, 128.5, 127.3, 123.9, 122.0, 120.9, 119.7, 117.6, 112.0, 63.62.

General procedure for oxidation of 4-aminoquinoline-derived benzyl alcohols

The alcohol **CDM09-CDM10** (1.0 eq) was stirred with Et_3N (6.0 eq) in DMSO, followed by the addition of sulfur trioxide pyridine complex (3.0 eq), and stirred at room temperature for 72 h. The reaction mixture was extracted with ethyl acetate and the organic layers washed with distilled water and brine. The combined organic extracts were dried over anhydrous Na_2SO_4 and the solvent removed under reduced pressure to yield the corresponding aldehyde as a yellow powder.

[3-(7-Chloro-quinolin-4-ylamino)-phenyl]-benzaldehyde, CDM11

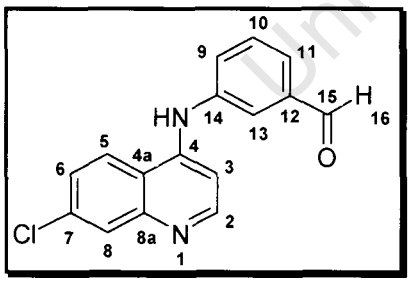

Yellow crystals (2.60g, 97%); R_f (5% MeOH:DCM) 0.56; δ_H (300MHz, d_6-DMSO) 10.01 (1H, s, (C=O)H-16), 9.4 (1H, s, NH), 8.46 (1H, d, *J* 5.4, H-2), 8.41 (1H, d, *J* 9.3, H-5), 7.89 (1H, d, *J* 2.7, H-8), 7.68 (3H, m, H-9, H-10 and H-11), 7.58 (1H, dd, *J* 2.1, 9.0, H-6), 7.02 (1H, d, *J* 5.4, H-3); δ_C(75MHz, d_6-DMSO) 192.9, 185.8, 151.8, 149.4, 147.3, 137.3, 134.1, 130.3, 127.5, 125.2, 124.7, 121.7, 118.5, 112.6, 102.5, 70.1.

[2-(7-Chloro-quinolin-4-ylamino)-phenyl]-benzaldehyde, CDM12

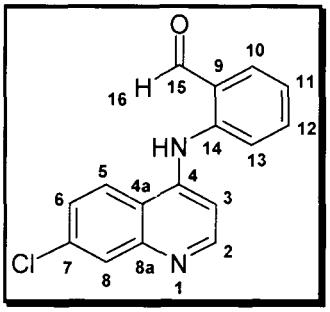

Yellow crystals (0.1475g, 81%); R_f (5% MeOH:DCM) 0.76; δ_H (300MHz, d_6-DMSO) 10.25 (1H, s, (C=O)H-16), 10.07 (1H, s, NH), 8.65 (1H, d, *J* 5.1, H-2), 8.31 (1H, d, *J* 9.0, H-5), 8.01 (1H, d, *J* 2.7, H-8), 7.73 (1H, d, *J* 7.6, H-10), 7.68 (4H, m, H-6, H-11 and H-13), 7.30 (1H, t, *J* 7.2, H-3), 7.21 (1H, d, *J* 5.4, H-3); δ_C(75MHz, d_6-DMSO) 191.8, 151.3, 149.5, 147.8, 146.4, 136.6, 134.8, 130.5 (2C), 129.1, 127.3, 123.0, 119.5 (2C), 116.4, 112.6.

General procedure for protection of hydroxyacetophenones CDM16-CDM17

A solution of 4-hydroxyacetophenone or 4-acetovanillone (1.0 eq), pyridinium *p*-toluenesulfonate (0.1eq) and 3,4-dihydro-2H-pyran (1.6 eq) in dry DCM was stirred at room temperature for 72 h. The reaction mixture was washed with 1M sodium carbonate, water and brine. The organic extracts were dried over Na_2SO_4 and then concentrated in vacuo to give the tetrahydropyranyl ether as a yellow solid.

1-[4-(Tetrahydro-pyran-2-yloxy)-phenyl]-ethanone, CDM16

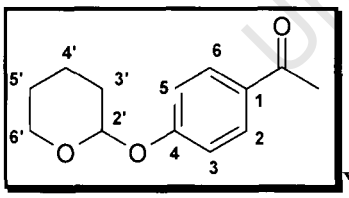

Yellow crystals (7.9747g, 98%); R_f (EtOAc:hexane, 2:3) 0.55; δ_H (300MHz;d_6-DMSO) 7.90 (2H, dd, *J* 2.1, 6.9, H-2 and H-6), 7.10 (2H, dd, *J* 2.1, 6.9, H-3 and H-5), 5.59 (1H, t, *J* 3.3, H-2'), 3.85 (1H, m, H-6'a), 3.58 (1H, m, H-6'b), 3.26 (1H, s, $COCH_3$), 1.81 (1H, m, H-3'a), 1.75 (2H, m, H-3'b and H-5'a), 1.55 (3H, m, H-4 and H-5'b); δ_c (100MHz, d_6-DMSO) 196.8, 161.0, 131.0, 130.6 (2C), 116.7 (2C), 96.2, 62.3, 30.3, 26.5, 25.2, 19.1.

1-[3-Methoxy-4-(tetrahydro-pyran-2-yloxy)-phenyl]-ethanone, CDM17

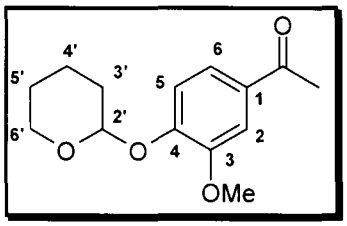

Yellow crystals (1.47g, 95%); R_f (EtOAc:hexane, 3:2) 0.56; δ_H (300MHz;$CDCl_3$) 7.53 (1H, d, *J* 8.4, H-6), 7.50 (1H, s, H-2), 7.16 (1H, d, *J* 8.4, H-5), 5.54 (1H, t, *J* 3.2 H-2'), 3.90 (3H, s, OCH_3), 3.87 (1H, m, H-6'a), 3.63 (1H, m, H-6'b), 2.54 (1H, s, $COCH_3$), 1.81 (1H, m, H-3'a), 1.75 (2H, m, H-3'b and H-5'a), 1.55 (3H, m, H-4' and H-5'b); δ_c (100MHz, d_6-DMSO) 197.8, 151.0, 149.8, 129.5, 121.4, 115.2 (2C), 96.6, 62.8, 56.2, 30.1, 28.5, 25.4, 20.2.

General procedure for synthesis of 4-aminoquinoline-derived chalcones CDM04-CDM08, CDM13-CDM15 and CDM18-CDM19

A methanolic solution of NaOH (3% w/v) and methyl ketone (1.0 eq) were stirred together at room temperature. A methanolic solution of the substituted aldehyde (1.0 eq) was added dropwise, and the mixture was refluxed with stirring for 24-48 h. The precipitate was removed by filtration and washed with cold methanol. The collected yellow solid was dried further *in vacuo*, affording the desired product.

1-[4-(7-Chloro-quinolin-4-ylamino)-phenyl]-3-(4-chloro-phenyl)-propenone, CDM04

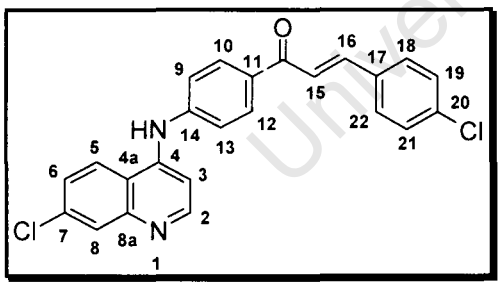

Yellow crystals (0.2765g, 66%), m.p. 230-233 °C; R_f (Hexane-EtOAc, 3:2) 0.73; ν_{max} ($CHCl_3$) / cm^{-1} 3300 (N-H), 1676 (C=O), 1609 (Ar-C=C), 1565 (C=C) and 865 (Ar-Cl); δ_H (400MHz, d_6-DMSO) 9.43 (1H, s, NH), 8.62 (1H, d, *J* 5.1, H-2), 8.41 (1H, d, *J* 8.8, H-5), 8.21 (2H, d, *J* 8.8, H-10 and H-12), 8.0 (1H, d, *J* 15.6, H-16), 7.97 (1H, d, *J* 2.4, H-8), 7.92 (2H, d, *J* 8.8, H-18 and H-22), 7.70 (1H, d, *J* 15.6, H-15), 7.64-7.61 (1H, dd, *J* 2.4 and 9.2, H-6), 7.53 (2H, d, *J* 8.4, H-9 and H-13), 7.50 (2H, d, *J* 8.8, H-19 and H-21), 7.32 (1H, d, *J* 5.2, H-3); δ_C(100MHz, d_6-DMSO) 187.0, 151.9, 149.6, 146.2, 146.1, 141.5, 134.8, 134.1,

133.8, 131.3, 130.8, 130.4, 130.4, 128.8, 128.2, 127.6, 125.4, 124.7, 122.8, 119.4, 119.1, 118.9, 105.2; Elemental analysis: (Found C, 66.23; H, 3.94; N, 6.01. $C_{24}H_{16}Cl_2N_2O.0.9H_2O$ requires C, 66.19; H, 4.16; N 6.43%).

1-[4-(7-Chloro-quinolin-4-ylamino)-phenyl]-3-(2,4-dichloro-phenyl)-propenone, CDM05

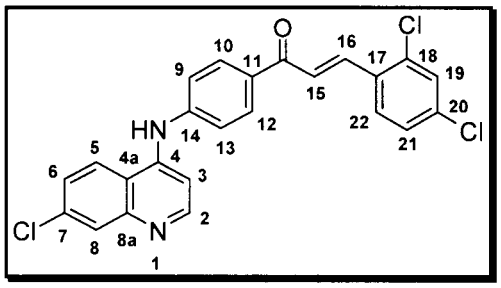

Yellow crystals (0.3380g, 74%), m.p. 229-233 °C; R_f (Hexane-EtOAc, 3:2) 0.77; δ_H (300MHz, d_6-DMSO) 9.43 (1H, s, NH), 8.62 (1H, d, *J* 5.1, H-2), 8.41 (1H, d, *J* 9.6, H-5), 8.26 (1H, d, *J* 9.0, H-22), 8.20 (2H, d, *J* 8.7, H-10 and H-12), 8.06 (1H, d, *J* 15.9, H-16), 7.97 (1H, d, *J* 15.6, H-15), 7.94 (1H, d, *J* 8.7, H-21), 7.74 (1H, d, *J* 2.1, H-8), 7.59 (1H, d, *J* 2.4, 9.0, H-6), 7.57 (2H, d, *J* 9.0, H-9 and H-13) and 7.27 (1H, d, *J* 5.1, H-3); δ_C(100MHz, d_6-DMSO) 186.4, 151.8, 149.7, 146.2, 146.1, 141.5, 136.1, 135.2, 134.9, 133.9, 131.6, 130.4, 129.7, 129.4, 128.2, 127.8, 127.5, 125.5, 125.1, 124.8, 119.4, 118.9, 118.9, 105.142; EI-MS: (found m/z = 452.0236 $C_{24}H_{15}Cl_3N_2O$ requires M 452.02; Elemental analysis: (Found C, 61.72; H, 3.42; N, 5.60 $C_{24}H_{15}Cl_3N_2O$. $0.7H_2O$ requires C, 61.81; H, 3.67; N 6.01%).

1-[3-(7-Chloro-quinolin-4-ylamino)-phenyl]-3-(4-chloro-phenyl)-propenone, CDM06

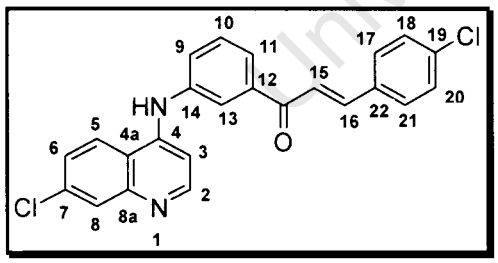

Yellow crystals (0.3135g, 75%), m.p. 218-223 °C; R_f (Hexane-EtOAc, 3:2) 0.29; δ_H (400MHz, d_6-DMSO) 9.33 (1H, s, NH), 8.53 (1H, d, *J* 5.6, H-2), 8.46 (1H, d, *J* 8.8, H-5), 8.30 (1H, s, H-13), 8.07 (1H, d, *J* 2.0, H-8), 7.94 (1H, d, *J* 16.0, H-16), 7.93 (2H, d, *J* 8.4, H-17 and H-21), 7.91 (1H, d, *J* 7.6, H-9), 7.78 (1H, d, *J* 15.6, H-15), 7.69 (1H, d, *J* 8.0, H-11), 7.64 (1H, t, *J* 7.6, H-10), 7.59 (1H, dd, *J* 2.0, 8.8, H-6), 7.53 (2H, d, J 8.4, H-18 and H-20), 7.03 (1H, d, *J* 5.6, H-3); δ_C(75MHz, d_6-DMSO)188.8, 151.9, 149.5, 147.5, 142.7,

140.9, 138.7, 135.1, 133.9, 133.5, 130.5, 129.8, 128.9, 127.7, 126.6, 125.1, 124.4, 123.9, 123.7, 122.8, 121.8, 118.5, 102.2, 48.5; EI-MS: (found m/z = 418.06397 $C_{24}H_{16}Cl_2N_2O$ requires M 418.06; Elemental analysis: (Found C, 68.57; H, 3.81; N, 6.27 $C_{24}H_{16}Cl_2N_2O$ requires C, 68.25; H, 3.85; N 6.68%).

1-[4-(7-Chloro-quinolin-4-ylamino)-phenyl]-3-(4-fluoro-phenyl)-propenone, CDM07

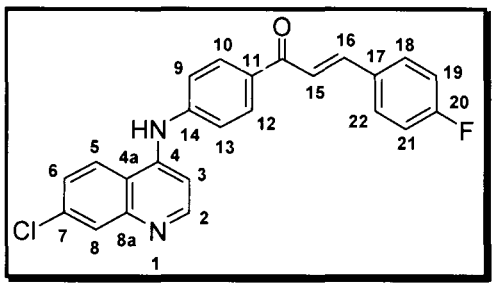

Yellow crystals (0.0393g, 30%), m.p 189-192°C; R_f (Hexane-EtOAc, 3:2) 0.74; δ_H (400MHz, d_6-DMSO) 9.43 (1H, s, NH), 8.63 (1H, d, *J* 5.2, H-2), 8.42 (1H, d, *J* 9.2, H-5), 8.21 (1H, *d*, J 8.8, H-10 and H-12), 7.98 (2H, d, *J* 9.2, H-18 and H-22), 7.96 (1H, d, *J* 2.4, H-8), 7.94 (1H, d, *J* 16.0, H-16), 7.75 (1H, d, *J* 15.6, H-15), 7.63 (1H, dd, *J* 2.4, 9.2, H-6), 7.49 (2H, d, *J* 8.8, H-9 and H-13), 7.32 (2H, d, *J* 9.2, H-19 and H-21), 7.28 (1H, d, *J* 5.2, H-3); δ_C(100MHz, d_6-DMSO) 187.0, 152.1, 151.7, 146.1, 141.8, 134.1, 131.5, 131.4, 131.1, 130.9, 130.4, 127.7, 125.4, 124.7, 121.9, 119.4, 119.1, 117.4, 115.9, 115.7,112.6, 105.1, 103.2, 63.1; EI-MS: (found m/z = 402.942 $C_{24}H_{16}ClFN_2O$ requires M 402.92; Elemental analysis: (Found C, 68.56; H, 4.55; N, 5.87 $C_{24}H_{16}ClFN_2O.0.1\ H_2O$ requires C, 68.49; H, 4.07; N 6.65%).

1-[4-(7-Chloro-quinolin-4-ylamino)-phenyl]-3-(2,4-dimethoxy-phenyl)-propenone, CDM08

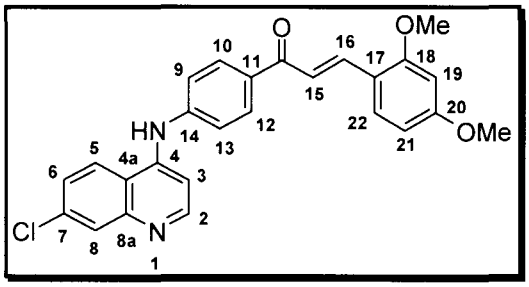

Yellow crystals (0.2415g, 54%), m.p. 239-242 °C; R_f (Hexane-EtOAc, 3:2) 0.56; δ_H (400MHz, d_6-DMSO) 9.43 (1H, s, NH), 8.62 (1H, d, *J* 5.2, H-2), 8.42 (1H, d, *J* 8.8, H-5), 8.16 (2H, d, *J* 8.4, H-10 and H-12), 8.0 (1H, d, *J* 15.6, H-16), 7.96 (1H, d, *J* 2.1, H-8), 7.92 (1H, d, J 8.4, H-22), 7.80 (1H, d, *J* 8.4, H-15), 7.64 (1H, dd, *J* 2.1, 8.8, H-6), 7.49 (2H, d, *J* 8.4, H-9 and H-13), 7.65 (1H, d, *J* 8.8, H_f), 7.29 (1H, d, *J* 5.6, H-3), 6.63(1H, dd, *J* 2.0, 8.8, H-21), 6.62 (1H, d, *J* 2.0, H-19), 3.91 (3H, s, OCH_3), 3.85 (3H, s, OCH_3); δ_C(100MHz, d_6-DMSO) 187.2, 162.9, 159.8, 151.9, 149.6, 146.1, 145.4, 137.9, 134.0, 132.1, 130.1, 130.0, 129.9, 127.7, 125.4, 124.6, 119.1, 116.1, 106.3, 104.9, 98.3, 55.8, 55.4, 30.5; EI-MS: (found m/z = 445.1 $C_{26}H_{21}ClN_2O_3$ requires M 444.91; Elemental analysis: (Found C, 69.91; H, 5.18; N, 6.27 $C_{26}H_{21}ClN_2O_3$ requires C, 70.19; H, 4.76; N 6.30%).

3-[3-(7-Chloro-quinolin-4-ylamino)-phenyl)-1-(4-methoxy-phenyl)-propenone, CDM13

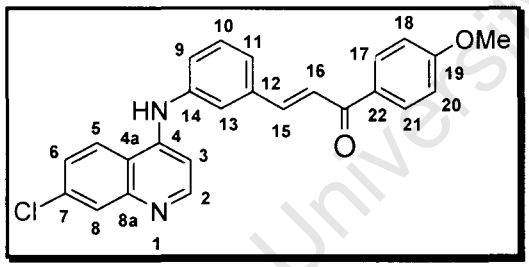

Yellow crystals (0.7830g, 75%), m.p. 254-257°C; R_f (EtOAc-Hexane, 3:2) 0.55; δ_H (300MHz, d_6-DMSO) 9.2 (1H, s, NH), 8.48 (1H, d, *J* 5.1, H-2), 8.45 (1H, d, *J* 9.0, H-5), 8.16 (2H, d, *J* 8.7, H-17 and H-21), 7.95 (1H, d, *J* 15.6, H-15), 7.89 (1H, d, *J* 2.1, H-8), 7.84 (1H, s, H-13), 7.727 (1H, d, *J* 15.6, H-16), 7.65 (1H, d, *J* 7.6, H-11), 7.59 (1H, dd, *J* 2.1, 9.0, H-6), 7.53 (1H, t, *J* 7.6, H-10), 7.43 (1H, d, *J* 8.1, H-9), 7.08 (2H, d, *J* 8.7, H-18 and H-20), 6.94 (1H, d, *J* 5.1, H-3), 3.82 (3H, s, OCH_3); δ_C(100MHz, d_6-DMSO) 187.3, 163.1, 151.9, 149, 5, 147.9, 142.6, 140.9, 136.0, 133.8, 130.8, 130.9, 130.3, 129.9, 129.3, 127.5, 124.8, 124.6, 124.4, 124.3, 122.6, 122.5, 118.3, 113.9, 101.9, 55.4. ; EI-MS: (found m/z = 414.88

$C_{25}H_{19}ClN_2O_2$ requires M 414.9; Elemental analysis: (Found C, 71.97; H, 4.66; N, 6.31 $C_{25}H_{19}ClN_2O_2$ requires C, 72.37; H, 4.62; N 6.75%).

3-[3-(7-Chloro-quinolin-4-ylamino)-phenyl)-1-(2,4-methoxyphenyl)-propenone, CDM14

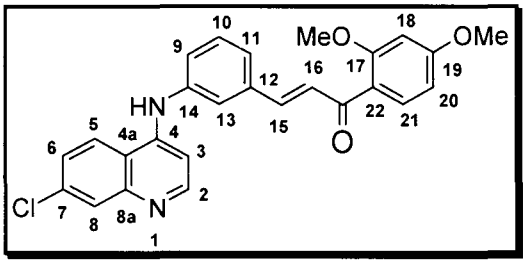

Yellow crystals (0.5428g, 70%), m.p. 175-179 °C; R_f (EtOAc-Hexane, 3:2) 0.45; ν_{max} ($CHCl_3$) / cm^{-1} 3300 (N-H), 1676 (C=O), 1609 (Ar-C=C), 1565 (C=C) and 865 (Ar-Cl); δ_H (400MHz, d_6-DMSO) 9.2 (1H, s, NH), 8.51 (1.H, d, *J* 5.2, H-2), 8.44 (1H, d, *J* 8.8, H-5), 7.92 (1H, d, *J* 2.4, H-8), 7.69 (1H, s, H-13), 7.64 (1H, d, *J* 8.8, H-21), 7.59 (1H, dd, *J* 2.0, 8.8, H-6), 7.56 (1H, d, *J* 15.6, H-15), 7.50 (1H, d, *J* 15.6, H-16), 7.47-7.43 (3H, m, H-9, H-10 and H-11), 7.01 (1H, d, *J* 5.2, H-3), 6.66 (1H, d, *J* 2.0, H-18), 6.64 (1H, dd, J 2.4, 8.8, H-20), 3.88 (3H, s, OCH_3), 3.83 (3H, s, OCH_3); δ_C(100MHz, d_6-DMSO) 189.1, 163.9, 151.7, 140.9, 140.7, 136.1, 133.9, 131.9, 129.9, 127.6, 127.5, 124.9, 124.4, 123.9 (2C), 123.8 (2C), 123.7, 121.7, 121.6, 118.4, 106.1, 102.2, 98.7, 55.9, 55.54. EI-MS: (found m/z = 445.1 $C_{26}H_{21}ClN_2O_3$ requires M 444.91; Elemental analysis: (Found C, 69.91; H, 5.18; N, 6.27 $C_{26}H_{21}ClN_2O_3$ requires C, 70.19; H, 4.76; N 6.30%).

3-[3-(7-Chloro-quinolin-4-ylamino)-phenyl)-1-(2,3,4-methoxyphenyl)- propenone, CDM15

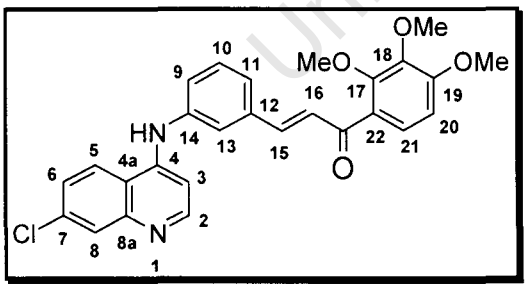

Yellow crystals (0.1782g, 70%), m.p. 179-182 °C; R_f (EtOAc-Hexane, 3:2) 0.44; δ_H (300MHz, d_6-DMSO) 9.2 (1H, s, NH), 8.51 (1.H, d, *J* 5.4, H-2), 8.44 (1H, d, *J* 9.0, H-5), 7.92 (1H, d, *J* 2.1, H-8), 7.71 (1H, s, H-13), 7.60 (1H, dd, *J* 2.1, 9.0, H-6), 7.55-7.42 (5H, m, H-9, H-10, H-11, H-15, H-16), 7.41 (1H, d, *J* 8.7, H-21), 7.01 (1H, d, *J* 5.1, H-3), 6.95 (1H, d, *J* 8.7, H-20), 3.88 (3H, s, OCH_3), 3.85 (3H, s, OCH_3), 3.79 (3H, s, OCH_3);

δ_C(100MHz, d_6-DMSO) 189.5, 156.5, 152.6, 151.7, 149.3, 147.3, 141.6, 141.3, 140.7, 135.6, 132.6, 129.6, 127.4, 126.6, 125.7, 124.9, 124.7 (2C), 123.8, 121.4, 118.1, 107.6, 102.9, 101.9, 61.4, 60.2, 55.8. EI-MS: (found m/z = 474.1346 $C_{27}H_{23}ClN_2O_4$ requires M 474.95; Elemental analysis: (Found C, 68.18; H, 4.78; N, 5.27 $C_{27}H_{23}ClN_2O_4$ requires C, 68.28; H, 4.88; N 5.90%).

3-[3-(7-Chloro-quinolin-4ylamino)-phenyl]-1-[4-(tetrahydro-2H-pyran-2-yloxy-phenyl]-propenone, CDM18

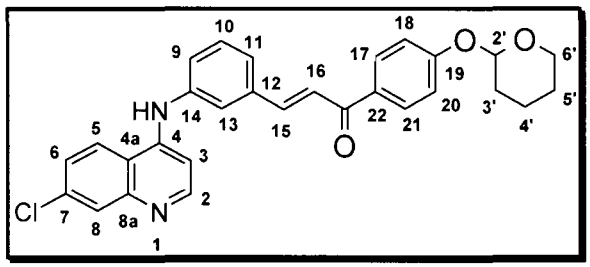

Yellow crystals (0.789g, 20%); R_f (EtOAc-Hexane, 3:2) 0.23; δ_H (400MHz, d_6-DMSO) 9.2 (1H, s, NH), 8.49 (1H, d, *J* 5.6, H-2), 8.46 (1H, d, *J* 9.2, H-5), 8.14 (2H, d, *J* 8.8, H-17 and H-21), 7.94 (1H, d, *J* 15.6, H-15), 7.90 (1H, d, *J* 2.4, H-8), 7.85 (1H, s, H-13), 7.74 (1H, d, *J* 15.6, H-16), 7.68 (1H, d, *J* 7.6, H-11), 7.59 (1H, dd, *J* 2.4, 9.2, H-6), 7.51 (1H, t, *J* 7.6, H-10), 7.44 (1H, d, *J* 8.1, H-9), 7.16 (2H, d, *J* 8.8, H-18 and H-20), 6.95 (1H, d, *J* 5.2, H-3), 5.59 (1H, t, *J* 3.3, H-2'), 3.85 (1H, m, H-6'a), 3.58 (1H, m, H-6'b), 1.81 (1H, m, H-3'a), 1.75 (2H, m, H-3'b and H-5'a), 1.55 (3H, m, H-4 and H-5'b); δ_C(100MHz, d_6-DMSO) 187.3, 163.1, 151.9, 142.6, 143.6, 136.8, 131.8, 131.6, 131.4, 130.7, 128.9, 128.4, 125.6, 125.3, 125.1, 123.4, 123.3, 120.5, 122.5, 116.9, 116.8, 111.0, 102.7, 102.4, 96.3, 62.3, 30.3, 25.3, 19.1.

3-[3-(7-Chloro-quinolin-4ylamino)-phenyl]-1-[3-methoxy-4-(tetrahydro-2H-pyran-2-yloxy-phenyl]-propenone, CDM19

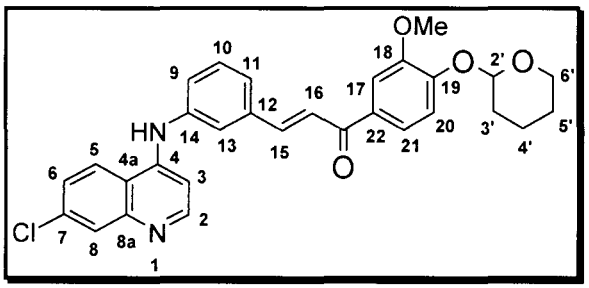

Yellow crystals (1.553g, 58%); R_f (EtOAc-Hexane, 3:2) 0.24; δ_H (400MHz, d_6-DMSO) 9.15 (1H, s, NH), 8.48 (1H, d, *J* 5.6, H-2), 8.44 (1H, d, *J* 9.2, H-5), 7.92 (1H, d, *J* 15.6, H-15), 7.89 (1H, d, *J* 2.0, H-8), 7.83 (1H, s, H-13), 7.82 (1H, dd, *J* 2.0, 8.8, H-21), 7.73 (1H, d, *J* 15.6, H-16), 7.68(1H, d, *J* 7.6, H-11), 7.63 (1H, d, *J* 2.0, H-17), 7.58 (1H, dd, *J* 2.0, 9.2, H-6), 7.50 (1H, t, *J* 7.6, H-10), 7.43 (1H, d, *J* 7.6, H-9), 7.20 (1H, d, *J* 8.8, H-20), 6.95 (1H, d, *J* 5.2, H-3), 5.59 (1H, t, *J* 3.3, H-2'), 3.86 (3H, s, OCH_3), 3.85 (1H, m, H-6'a), 3.58 (1H, m, H-6'b), 1.81 (1H, m, H-3'a), 1.75 (2H, m, H-3'b and H-5'a), 1.55 (3H, m, H-4 and H-5'b); δ_C(100MHz, d_6-DMSO) 187.5, 152.0, 151.7, 147.8, 142.8, 143.6, 136.8, 131.8, 130.7, 129.9, 127.6, 125.0, 124.9, 124.5, 123.3, 122.9, 122.7, 122.5, 116.9, 116.8,115.5, 111.7, 102.7, 102.4, 96.2, 61.5, 55.6, 29.6, 24.5, 18.3.

General procedure for synthesis of CDM20-CDM21

Hydrochloric acid was added to a stirred solution of **CDM18-CDM19** in methanol, and the mixture was stirred for 4 h at room temperature, and then diluted with water. The mixture was neutralized to pH 8 and the resulting precipitate was filtered, dried over anhydrous phosphorous pentoxide to afford the desired products.

3-[3-(7-Chloro-quinolin-4ylamino)-phenyl]-1-[4-hydroxyphenyl]-propenone, CDM20

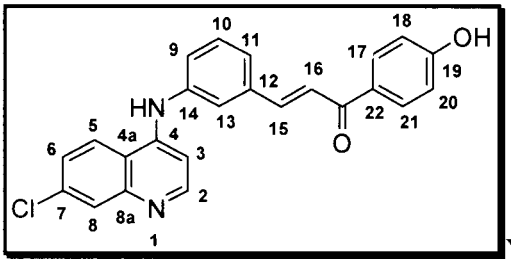

Yellow crystals (0.6281g, 98%); m.p.328-333 °C; R_f (EtOAc-Hexane, 3:2) 0.20; δ_H (400MHz, d_6-DMSO) 11.2 (1H, s, NH), 8.79 (1.H, d, *J* 9.2, H-5), 8.56 (1H, d, *J* 7.2, H-2), 8.09 (1H, d, *J* 2.1, H-8), 8.07 (2H, d, *J* 8.8, H-17 and H-21), 8.02 (1H, s, H-13), 7.99 (1H, d, *J* 15.6, H-15), 7.94 (1H, d, *J* 7.6, H-11), 7.92 (1H, dd, *J* 2.0, 9.2, H-6), 7.75 (1H, d, *J* 15.6, H-16), 7.66 (1H, t, *J* 7.6, H-10), 7.54 (1H, d, *J* 8.0, H-9), 6.90 (2H, d, *J* 8.8, H-18 and H-20), 6.87 (1H, d, *J* 7.2, H-3); δ_C(100MHz, d_6-DMSO) 187.7, 163.1, 159.6, 159.2, 158.8, 155.8, 144.4, 142.1, 139.6, 139.4, 138.2, 137.5, 131.8, 129.6, 128.9, 128.3, 125.6,125.1, 123.4, 120.5, 122.5, 116.9, 111.0, 101.34; Elemental analysis: (Found C, 65.11; H, 4.19; N, 6.31 $C_{24}H_{17}ClN_2O_2.2H_2O$ requires C, 65.98; H, 3.92; N 6.41%).

3-[3-(7-Chloro-quinolin-4ylamino)-phenyl]-1-[4-Hydroxy-3-methoxy-phenyl] propenone, CDM21

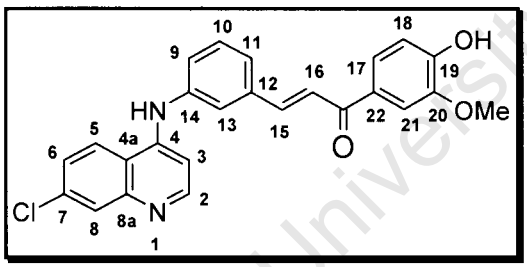

Yellow crystals (1.099g, 85%); m.p.225-227 °C; R_f (10%MeOH:DCM) 0.54; δ_H (400MHz, d_6-DMSO) 11.0 (1H, s, OH), 10.15 (1H, s, NH), 8.82 (1H, d, *J* 8.8, H-5), 8.51 (1H, d, *J* 5.6, H-2), 8.13 (1H, d, *J* 2.0, H-8), 7.99 (1H, s, H-13), 7.98 (1H, d, *J* 15.6, H-15), 7.88 (1H, d, *J* 8.0, H-11), 7.84 (1H, dd, *J* 1.6, 8.8, H-6), 7.78 (1H, dd, *J* 2.0, 8.4, H-17), 7.73 (1H, d, *J* 15.6, H-16), 7.62 (1H, t, *J* 7.6, H-10), 7.59 (1H, d, *J* 2.0, H-21), 7.52 (1H, d, *J* 8.0, H-9), 6.92 (1H, d, *J* 8.4, H-18), 6.85 (1H, d, *J* 6.8, H-3), 3.85 (3H, s, OCH_3); δ_C(100MHz, d_6-DMSO) 186.9, 153.7, 152.1, 147.8, 144.8, 141.5, 140.7, 137.1, 137.7, 136.7, 130.4, 129.3, 127.4, 127.1, 126.7, 125.7, 124.8, 123.8, 123.2, 120.6, 116.3, 114.9, 111.7, 100.8,

55.7; EI-MS: (found m/z = 430.1 $C_{25}H_{19}ClN_2O_3$ requires M 430.11; Elemental analysis: (Found C, 69.69; H, 4.44; N, 6.50 $C_{25}H_{19}ClN_2O_3.0.1H_2O$ requires C, 69.39; H, 4.43; N 6.48%).

General procedure for synthesis of citrate salt derivatives CDM22-29

A 1.5 equivalent of citric acid dissolved in a minimum amount of acetone was added dropwise to a stirring solution of free base **CDM04-CDM08**, **CDM13-CDM15.** The solution was then stirred for 1 h at 48-50°C. The product precipitated out of solution when cooled at 4°C for 24 h. The citrate salt derivatives were filtered, dried under vacuum and then over phosphorous pentoxide.

Citrate salt of 1-[4-(7-Chloro-quinolin-4-ylamino)-phenyl]-3-(4-chloro-phenyl)-propenone, CDM22

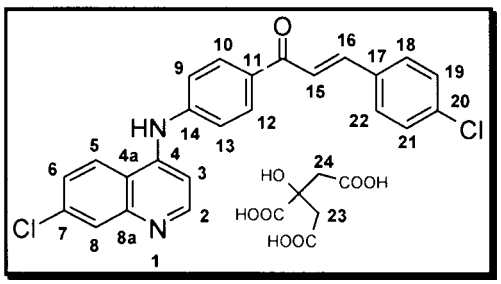

Yellow crystals (0.2703g, 93%), m.p. 197-198 °C; ν_{max} ($CHCl_3$) / cm^{-1} 3300 (N-H), 1722 (C=O), 1660 (C=C), 1591 (Ar-C=C), 1450 (CH_2 bend) and 865 (Ar-Cl); δ_H (400MHz, d_6-DMSO) 9.43 (1H, s, NH), 8.66 (1H, d, *J* 5.1, H-2), 8.50 (1H, d, *J* 8.8, H-5), 8.21 (2H, d, *J* 8.8, H-10 and H-12), 8.0 (1H, d, *J* 15.6, H-16), 8.03 (1H, d, *J* 2.4, H-8), 7.92 (2H, d, *J* 8.8, H-18 and H-22), 7.70 (1H, d, *J* 15.6, H-15), 7.67 (1H, dd, *J* 2.4 and 9.2, H-6), 7.53 (2H, d, *J* 8.4, H-9 and H-13), 7.50 (2H, d, *J* 8.8, H-19 and H-21), 7.32 (1H, d, *J* 5.2, H-3), 2.70 (2H, d, *J* 15.2, H-23), 2.65 (2H, d, *J* 15.2, H-24) ; δ_C(100MHz, d_6-DMSO) 187.0, 171.2, 158.6, 153.2, 152.0, 151.9, 149.6, 146.2, 146.1, 141.5, 134.8, 134.1, 133.8, 131.3, 130.8, 130.4, 130.4, 128.8, 128.2, 127.6, 125.4, 124.7, 122.8, 119.4, 119.1, 118.9, 105.2, 72.1, 70.1, 42.9; Elemental analysis: (Found C, 58.83; H, 4.01; N, 4.49. $C_{24}H_{16}Cl_2N_2O.C_6H_8O_7$ requires C, 58.93; H, 3.96; N 4.50%).

Citrate salt of 1-[4-(7-Chloro-quinolin-4-ylamino)-phenyl]-3-(2,4-dichloro-phenyl)-propenone, CDM23

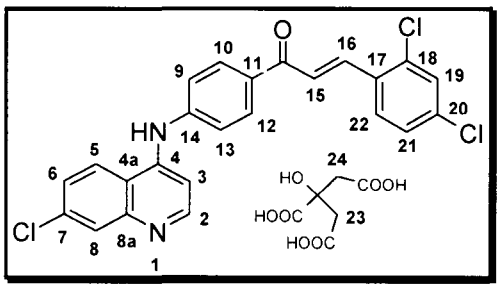

Yellow crystals (0.2788g, 62%), m.p. 208-211 °C; δ_H (300MHz, d_6-DMSO) 9.43 (1H, s, NH), 8.62 (1H, d, *J* 5.1, H-2), 8.41 (1H, d, *J* 9.6, H-5), 8.26 (1H, d, *J* 9.0, H-22), 8.20 (2H, d, *J* 8.7, H-10 and H-12), 8.06 (1H, d, *J* 15.9, H-16), 7.97 (1H, d, *J* 15.6, H-15), 7.94 (1H, d, *J* 8.7, H-21), 7.74 (1H, d, *J* 2.1, H-8), 7.59 (1H, d, *J* 2.4, 9.0, H-6), 7.57 (2H, d, *J* 9.0, H-9 and H-13), 7.27 (1H, d, *J* 5.1, H-3), 2.77 (2H, d, *J* 15.2, H-23), 2.67 (2H, d, *J* 15.2, H-24); δ_C(100, d_6-DMSO) 195.9, 186.4, 174.7, 151.8, 149.7, 146.2, 146.1, 141.5, 136.1, 135.2, 134.9, 133.9, 131.6, 130.6, 130.4, 129.8, 129.6, 128.2, 127.8, 127.5, 126.7, 125.5, 125.1, 124.8, 119.4, 118.9, 105.1, 72.2, 46.5, 42.8; Elemental analysis: (Found C, 50.52; H, 3.91; N, 3.91 $C_{24}H_{15}Cl_3N_2O$. $C_6H_8O_7.4H_2O$ requires C, 50.19; H, 3.22; N 3.90%).

Citrate salt of 1-[3-(7-Chloro-quinolin-4-ylamino)-phenyl]-3-(4-chloro-phenyl)-propenone, CDM24

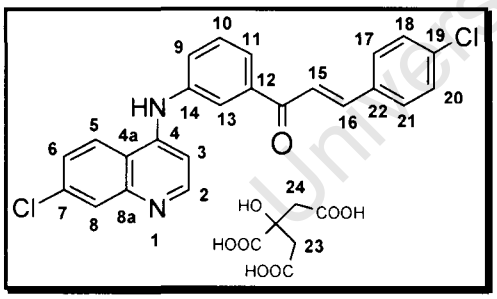

Yellow crystals (0.2182g, 60%), m.p. 219-221 °C; δ_H (400MHz, d_6-DMSO) 9.43 (1H, s, NH), 8.62 (1H, d, *J* 5.2, H-2), 8.42 (1H, d, *J* 8.8, H-5), 8.30 (1H, s, H-13), 8.07 (1H, d, *J* 2.0, H-8), 7.94 (1H, d, *J* 16.0, H-16), 7.93 (2H, d, *J* 8.4, H-17 and H-21), 7.91 (1H, d, *J* 7.6, H-9), 7.78 (1H, d, *J* 15.6, H-15), 7.69 (1H, d, *J* 8.0, H-11), 7.64 (1H, t, *J* 7.6, H-10), 7.59 (1H, dd, *J* 2.0, 8.8, H-6), 7.53 (2H, d, J 8.4, H-18 and H-20), 7.03 (1H, d, *J* 5.6, H-3) 2.74 (2H, d, *J* 15.6, H-23), 2.64 (2H, d, *J* 15.2, H-24); δ_C(75MHz, d_6-DMSO)188.8, 174.9, 171.1, 151.9, 149.5, 148.4, 147.5, 142.7, 140.9, 138.7, 134.4, 135.1, 133.9, 133.5, 130.5, 129.8, 128.9, 127.7, 126.9, 126.6, 125.1, 124.4, 123.9, 123.7, 122.8, 121.8, 118.5, 102.2, 72.091, 42.9;

Elemental analysis: (Found C, 58.93; H, 3.96; N, 4.58 $C_{24}H_{16}Cl_2N_2O.C_6H_8O_7$. $0.1H_2O$ requires C, 58.79; H, 3.94; N 4.57 %).

Citrate salt of 1-[4-(7-Chloro-quinolin-4-ylamino)-phenyl]-3-(4-fluoro-phenyl)-propenone, CDM25

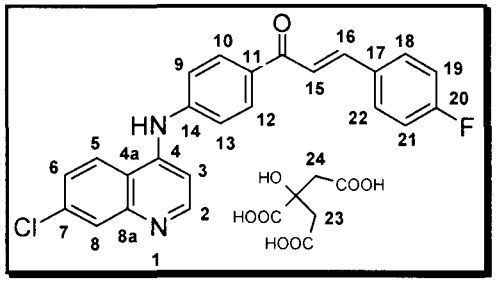

Yellow crystals (0.4986g, 92%), m.p 226-228 °C;δ_H (300MHz, d_6-DMSO) 9.43 (1H, s, NH), 8.69 (1H, d, *J* 5.2, H-2), 8.50 (1H, d, *J* 9.2, H-5), 8.21 (1H, *d*, J 8.8, H-10 and H-12), 7.98 (2H, d, *J* 9.2, H-18 and H-22), 8.04 (1H, d, *J* 2.4, H-8), 7.94 (1H, d, *J* 16.0, H-16), 7.75 (1H, d, *J* 15.6, H-15), 7.63 (1H, dd, *J* 2.4, 9.2, H-6), 7.49 (2H, d, *J* 8.8, H-9 and H-13), 7.32 (2H, d, *J* 9.2, H-19 and H-21), 7.33 (1H, d, *J* 5.2, H-3), 2.68 (2H, d, *J* 15.0, H-23), 2.59 (2H, d, *J* 15.3, H-24); δ_C(100MHz, d_6-DMSO) 187.0, 152.1, 151.7, 146.1, 141.8, 134.1, 131.5, 131.4, 131.1, 130.9, 130.4, 127.7, 125.4, 124.7, 121.9, 119.4, 119.1, 117.4, 115.9, 115.7,112.6, 105.1, 103.2, 63.1; Elemental analysis: (Found C, 60.57; H, 4.14; N, 4.04 $C_{24}H_{16}ClFN_2O$. $C_6H_8O_7$ requires C, 60.56; H, 4.09; N 4.71%).

Citrate salt of 1-[4-(7-Chloro-quinolin-4-ylamino)-phenyl]-3-(2,4-dimethoxy-phenyl)-propenone, CDM26

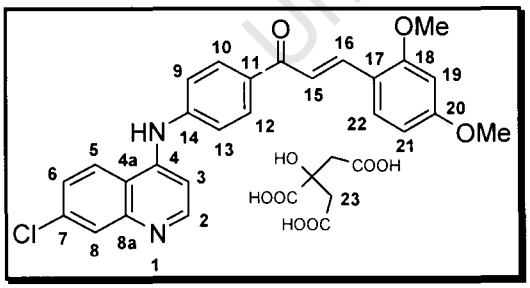

Yellow crystals (0.2182g, 60%), m.p. 219-221 °C; δ_H (400MHz, d_6-DMSO) 9.43 (1H, s, NH), 8.62 (1H, d, *J* 5.2, H-2), 8.42 (1H, d, *J* 8.8, H-5), 8.16 (2H, d, *J* 8.4, H-10 and H-12), 8.0 (1H, d, *J* 15.6, H-16), 7.96 (1H, d, *J* 2.1, H-8), 7.92 (1H, d, J 8.4, H-22), 7.80 (1H, d, *J* 8.4, H-15), 7.64 (1H, dd, *J* 2.1, 8.8, H-6), 7.49 (2H, d, *J* 8.4, H-9 and H-13), 7.65 (1H, d, *J* 8.8, H_f), 7.29 (1H, d, *J* 5.6, H-3), 6.63(1H, dd, *J* 2.0, 8.8, H-21), 6.62 (1H, d, *J*

2.0, H-19), 3.91 (3H, s, OCH_3), 3.85 (3H, s, OCH3), 2.75 (2H, d, *J* 15.6, H-23), 2.66 (2H, d, *J* 15.0, H-24); δ_C(100MHz, d_6-DMSO) 187.2, 174.7, 171.1, 162.9, 159.8, 151.9, 151.4, 149.6, 146.1, 145.4, 137.9, 134.0, 132.4, 132.1, 130.1, 130.0, 129.9, 127.7, 125.4, 124.6, 119.62, 119.5, 119.1, 116.1, 106.3, 104.9, 104.6, 98.3, 72.2, 55.8, 55.4, 42.8; Elemental analysis: (Found C, 61.66; H, 4.54; N, 4.78 $C_{26}H_{21}ClN_2O_3$. $C_6H_8O_7$. $0.1H_2O$ requires C, 59.45; H, 4.26; N 4.38%).

Citrate salt of 3-[3-(7-Chloro-quinolin-4-ylamino)-phenyl)-1-(4-methoxy-phenyl)-propenone, CDM27

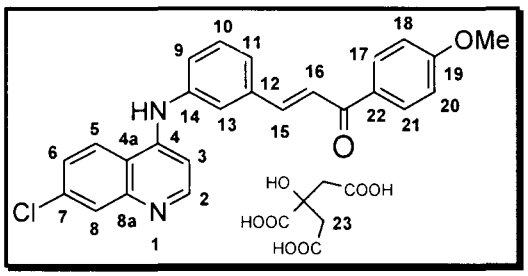

Yellow crystals (0.0727g, 47%), m.p. 250-254°C; δ_H (400MHz, d_6-DMSO) 9.2 (1H, s, NH), 8.48 (1H, d, *J* 5.1, H-2), 8.45 (1H, d, *J* 9.0, H-5), 8.16 (2H, d, *J* 8.7, H-17 and H-21), 7.95 (1H, d, *J* 15.6, H-15), 7.89 (1H, d, *J* 2.1, H-8), 7.84 (1H, s, H-13), 7.727 (1H, d, *J* 15.6, H-16), 7.65 (1H, d, *J* 7.6, H-11), 7.59 (1H, dd, *J* 2.1, 9.0, H-6), 7.53 (1H, t, *J* 7.6, H-10), 7.43 (1H, d, *J* 8.1, H-9), 7.08 (2H, d, *J* 8.7, H-18 and H-20), 6.94 (1H, d, *J* 5.1, H-3), 3.82 (3H, s, OCH_3), 2.74 (2H, d, *J* 15.2, H-23), 2.64 (2H, d, *J* 15.2, H-24); δ_C(100MHz, d_6-DMSO) 187.3, 171.1, 163.1, 151.9, 150.8, 149, 5, 147.9, 142.6, 140.36, 136.0, 134.4, 133.8, 130.8, 130.9, 130.3, 129.9, 129.3, 127.5, 126.5, 124.8, 124.6, 124.4, 124.3, 122.6, 122.5, 118.3, 113.9, 101.9, 72.1, 55.4, 42.93. Elemental analysis: (Found C, 62.84; H, 4.44; N, 4.70 $C_{25}H_{19}ClN_2O_2$. $C_6H_8O_7$ requires C, 61.34; H, 4.48; N 4.61%).

Citrate salt of 3-[3-(7-Chloro-quinolin-4-ylamino)-phenyl)-1-(2,4-methoxy-phenyl)-propenone, CDM28

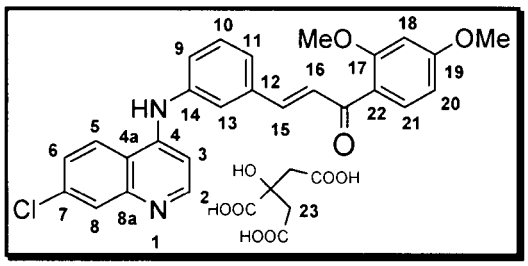

Yellow crystals (0.0745g, 42%), m.p. 89-94 °C; δ_H (400MHz, d_6-DMSO) 9.2 (1H, s, NH), 8.51 (1.H, d, *J* 5.2, H-2), 8.44 (1H, d, *J* 8.8, H-5), 7.92 (1H, d, *J* 2.4, H-8), 7.69 (1H, s, H-13), 7.64 (1H, d, *J* 8.8, H-21), 7.59 (1H, dd, *J* 2.0, 8.8, H-6), 7.56 (1H, d, *J* 15.6, H-15), 7.50 (1H, d, *J* 15.6, H-16), 7.47-7.43 (3H, m, H-9, H-10 and H-11), 7.01 (1H, d, *J* 5.2, H-3), 6.66 (1H, d, *J* 2.0, H-18), 6.64 (1H, dd, J 2.4, 8.8, H-20), 3.88 (3H, s, OCH_3), 3.83 (3H, s, OCH_3), 2.51 (2H, d, *J* 14.8, H-23), 2.43 (2H, d, *J* 15.2, H-24); δ_C(100MHz, d_6-DMSO) 189.1, 177.2, 171.2, 163.9, 160.3, 151.7, 149.5, 147.6, 140.9, 136.1, 133.9, 132.1, 131.9, 129.9, 127.6, 127.5, 127.4, 124.9, 124.4, 123.9, 123.7, 121.7, 121.6, 118.4, 106.1, 102.2, 98.7, 96.6, 70.9, 55.9, 55.54, 44.5; Elemental analysis: (Found C, 60.03; H, 4.79; N, 3.99 $C_{26}H_{21}ClN_2O_3$. $C_6H_8O_7$ requires C, 60.33; H, 4.59; N 4.40%).

Citrate salt of 3-[3-(7-Chloro-quinolin-4-ylamino)-phenyl)-1-(2,3,4-methoxy-phenyl)-propenone, CDM29

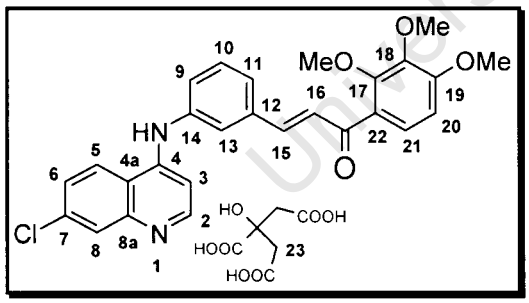

Yellow crystals (0.2053g, 97%), m.p. 158-160 °C; ν_{max} ($CHCl_3$) / cm^{-1} 3200 (N-H), 1723 (C=O), 1649 (Ar-C=C), 1592 (C=C), 1478 (CH_2 bend), and 865 (Ar-Cl); δ_H (300MHz, d_6-DMSO) 9.2 (1H, s, NH), 8.63 (1.H, d, *J* 5.4, H-2), 8.48(1H, d, *J* 9.0, H-5), 7.85 (1H, d, *J* 2.1, H-8), 7.71 (1H, s, H-13), 7.60 (1H, dd, *J* 2.1, 9.0, H-6), 7.55-7.42 (5H, m, H-9, H-10, H-11, H-15, H-16), 7.41 (1H, d, *J* 8.7, H-21), 7.01 (1H, d, *J* 5.1, H-3), 6.95 (1H, d, *J* 8.7, H-20), 3.88 (3H, s, OCH_3), 3.85 (3H, s, OCH_3), 3.79 (3H, s, OCH_3), 2.73 (2H, d, *J* 15.0, H-23), 2.63 (2H, d, *J* 15.2, H-24); δ_C(100MHz, d_6-DMSO) 189.5, 175.0, 171.1, 156.5,

152.6, 151.7, 149.3, 147.3, 141.7, 141.6, 141.3, 140.7, 135.6, 134.4, 129.6, 127.4, 126.6, 125.7, 124.9, 124.7 (2C), 122.0, 123.8, 121.4, 118.1, 107.6, 102.9, 101.9, 72.0, 61.4, 60.2, 55.8, 42.9; Elemental analysis: (Found C, 58.15; H, 4.65; N, 3.52 $C_{27}H_{23}ClN_2O_4$. $C_6H_8O_7$. 0.8 H_2O requires C, 58.16; H, 4.58; N 4.11%).

General procedure for synthesis of Mannich bases of 4-hydroxyacetophenone (CDM30-36)

Amine (2.0 eq) was treated with paraformaldehyde (2.0 eq) in methanol at 65°C for 2 h. To the reaction, a solution of 4-hydroxyacetophenone (1.0 eq) in methanol was then added. After stirring for 24 h, the reaction mixture was cooled, concentrated in vacuo and then subjected to column chromatography on silica gel.

1-(4-Hydroxy-3-(pyrrolidin-1-ylmethyl)phenyl)ethanone, CDM30

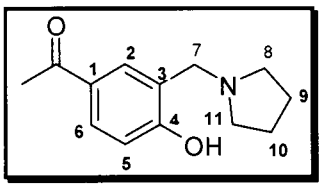

Yellow crystals (0.70718g, 15%); R_f (2% MeOH:DCM) 0.36; δ_H (300MHz, d_6-DMSO), 7.74 (1H, d, *J* 2.4, H-2), 7.72 (1H, dd, *J* 2.4, 8.4, H-6), 6.78 (1H, d, *J* 8.4, H-5), 4.18 (2H, s, H-7), 2.62 (4H, m, H-8 and H-11), 2.44 (3H, s, $COCH_3$), 1.76 (4H, m, H-9 and H-10); δ_C(100MHz, d_6-DMSO) 196.2, 162.4, 150.5 (2C), 128.5, 123.1, 115.3, 51.4 (2C), 53.6, 23.5 (2C), 23.9.

1-(4-Hydroxy-3-(piperidin-1-ylmethyl)phenyl)ethanone,CDM31

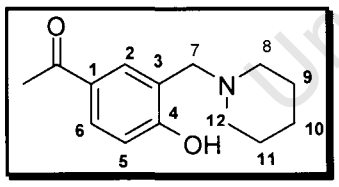

Yellow crystals (0.1147g, 22%); R_f (Hexane: EtOAc, 3:2) 0.13; δ_H (300MHz, d_6-DMSO), 7.80 (1H, dd, *J* 2.4, 8.4, H-6), 7.67 (1H, d, *J* 2.0, H-2), 6.86 (1H, d, *J* 8.4, H-5), 3.76 (2H, s, H-7), 2.52 (3H, s, $COCH_3$), 2.74 (4H, m, H-8 and H-12), 1.75 (6H, m, H-9, H-10 and H-11); δ_C(100MHz, d_6-DMSO) 196.5, 162.2, 130.5, 129.6, 128.7, 123.4, 115.3, 61.7 (2C), 53.7, 26.2, 25.5 (2C), 22.9.

1-(4-Hydroxy-3,5-bis(morpholinomethyl)phenyl)ethanone,CDM32

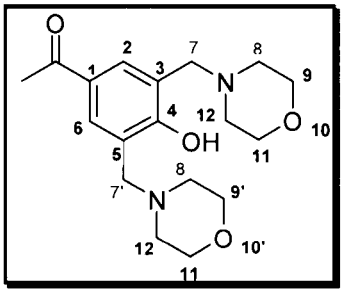

Yellow oil (0.3669g, 15%); R_f (Hexane: EtOAc, 3:2) 0.21; δ_H (400MHz, d_6-DMSO), 7.78 (2H, s, H-2 and H-6), 3.76 (4H, s, H-7 and H-7'), 3.67 (8H, t, *J* 4.4, H-9/9' and H-11/11'), 2.61 (8H, t, *J* 4.0, H-8/8' and H-12/12'), 2.53 (3H, s, $COCH_3$); δ_C(100MHz, d_6-DMSO) 196.5, 161.3, 128.7 (2C), 128.5, 122.4 (2C), 66.7, 58.8, 53.2, 30.4.

1-(3-((4-Ethylpiperazin-1-yl)methyl)-4-hydroxyphenyl)ethanone,CDM33

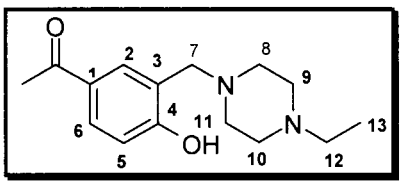

Pale yellow crystals (0.4271g, 44%); R_f (5% MeOH:DCM) 0.24; δ_H (400MHz, d_6-DMSO), 7.78 (1H, d, *J* 2.0, H-2), 7.75 (1H, dd, *J* 2.4, 8.0, H-6), 6.87 (1H, d, *J* 8.0, H-5), 4.15 (1H, s, OH), 3.77 (2H, s, H-7), 2.45 (3H, s, $COCH_3$), 2.43 (8H, m, H-8, H-9, H-10 and H-11), 2.23 (2H, q, *J* 7.6, H-12), 1.01 (3H, t, *J* 7.6, H-13); δ_C(75MHz, d_6-DMSO) 195.9, 161.7, 129.7, 129.3, 128.4, 122.1, 115.2, 58.3, 52.1, 52.0, 51.3, 26.1, 11.9.

1-(3- ((*tert*-Butylamino)methyl)-4-hydroxyphenyl)ethanone, CDM34

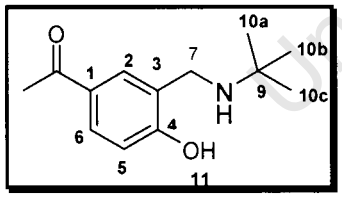

Yellow crystals (0.33g, 41%); R_f (2% MeOH:DCM) 0.13; δ_H (400MHz, $CDCl_3$), 7.77 (1H, d, *J* 2.0, H-2), 7.75 (1H, dd, *J* 2.4, 8.4, H-6), 6.83 (1H, d, *J* 8.4, H-5), 4.04 (2H, s, H-7), 2.50 (3H, s, $COCH_3$), 1.26 (9H, s, H-10a,b,c); δ_C(100MHz, $CDCl_3$) 195.9, 163.7, 131.3, 130.0(2C), 123.5, 115.2, 52.3, 46.4, 28.1, 26.2.

1-(3- ((Dimethylamino)methyl)-4-hydroxyphenyl)ethanone, CDM35

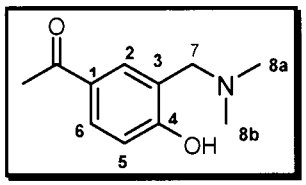

Brown oil (0.554g, 78%); R_f (2% MeOH:DCM) 0.16; δ_H (400MHz, $CDCl_3$), 7.82 (1H, dd, *J* 2.0, 8.4, H-6), 7.74 (1H, s, OH), 7.64(1H, d, *J* 2.4, H-2), 6.82 (1H, d, *J* 8.8, H-5), 3.65 (2H, s, H-7), 2.50 (3H, s, $COCH_3$), 2.48 (6H, s, H-8a,b); δ_C(100MHz, $CDCl_3$) 199.8, 163.7, 130.0(2C), 129.6, 122.4, 115.2, 59.8, 26.8, 17.4.

1-(3-((Diethylamino)methyl)-4-hydroxy-phenyl)-ethanone, CDM36

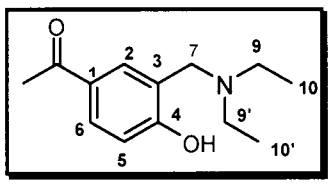

Yellow oil (0.3215g, 40%); R_f(hexane:EtOAc, 3:2) 0.18; δ_H (400MHz, d_6-DMSO), 7.79 (1H, dd, *J* 2.4, 8.4, H-6), 7.75(1H, d, *J* 2.0, H-2), 6.79 (1H, d, *J* 8.4, H-5), 3.80 (2H, s, H-7), 2.61 (4H, q, *J* 7.2, H-9/9'), 2.44 (3H, s, $COCH_3$), 1.02 (6H, t, *J* 7.2, H-10/10'); δ_C(100MHz, d_6-DMSO) 199.8, 160.2, 130.4, 129.0, 128.8, 122.6, 58.6, 49.1, 29.4, 13.8.

General procedure of synthesis of 4-aminoquinoline-based Mannich bases CDM37-CDM44

A methanolic solution of NaOH (3% w/v) and the phenolic Mannich base (1.0 eq) were stirred together at room temperature. A methanolic solution of the 4-aminoquinoline-based aldehyde (1.0 eq) was added dropwise, and the mixture was refluxed with stirring for 72 h. The precipitate was removed by filtration and washed with cold methanol. The collected yellow solid was dried further *in vacuo*, affording the desired product. When little or no precipitate was obtained, the solution was diluted with water, neutralized with 1M hydrochloric acid, and extracted with ethyl acetate. The organic layer was dried with anhydrous Na_2SO_4 and removed by evaporation under reduced pressure to give the desired product.

(*E*)-3-(3-(7-Chloroquinolin-4-ylamino)phenyl)-1-(4-hydroxy-3-(pyrrolidin-1-ylmethyl)phenyl)prop-2-en-1-one, CDM37

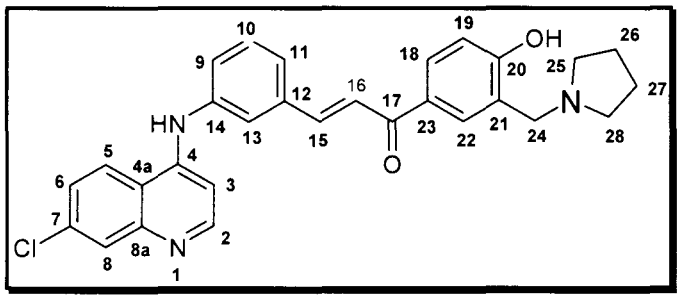

Yellow crystals (0.0621g, 17%); m.p.328-333 °C; m.p. 209-211 °C; R_f (5% MeOH:DCM) 0.33; δ_H (300MHz, d_6-DMSO) 9.20 (1H, s, NH), 8.50 (1H, d, *J* 5.1, H-2), 8.47 (1.H, d, *J* 9.0, H-5), 8.04 (2H, m, H-18 and H-22), 7.92 (1H, d, *J* 2.4, H-8), 7.91 (1H, d, *J* 15.6, H-15), 7.83 (1H, s, H-13), 7.72 (1H, d, *J* 15.6, H-16), 7.68 (1H, d, *J* 7.5, H-11), 7.60 (1H, dd, *J* 2.1, 9.0, H-6), 7.54 (1H, t, *J* 7.8, H-10), 7.48 (1H, d, *J* 8.1, H-9), 6.95 (1H, d, *J* 5.1, H-3), 6.90 (1H, d, *J* 9.3, H-19), 3.99 (2H, s, H-24), 2.76 (4H, m, H-25 and H-28), 1.82 (4H, m, H-26 and H-27); δ_C(75MHz, d_6-DMSO)186.9, 162.2, 151.9, 147.8, 142.2, 140.8, 136.1, 133.9, 130.7, 130.3, 129.8, 128.6, 127.5, 124.9, 124.6, 124.4, 124.3, 122.6, 115.4, 101.9, 59.6, 55.1, 52.9, 22.9, 13.9; EI-MS: (found m/z = 483.4 $C_{29}H_{26}ClN_3O_2$ requires M 483.17; Elemental analysis: (Found C, 70.00; H, 5.11; N, 8.56 $C_{29}H_{26}ClN_3O_2.1H_2O$ requires C, 69.95; H, 5.23; N 8.39%).

(*E*)-3-(3-(7-Chloroquinolin-4-ylamino)phenyl)-1-(4-hydroxy-3-(piperidin-1-ylmethyl)phenyl)prop-2-en-1-one, CDM38

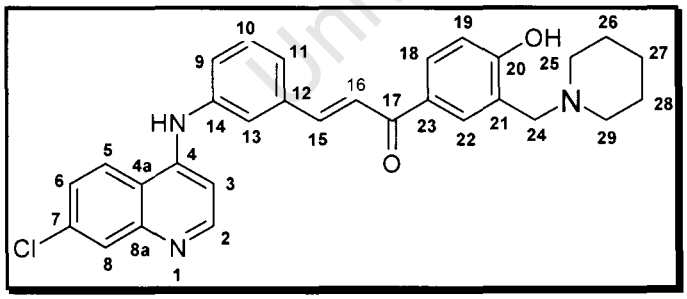

Yellow crystals (0.2949g, 38%); m.p. 223-225 °C; R_f (5% MeOH:DCM) 0.29; ν_{max} ($CHCl_3$) / cm^{-1} 3354 (C-N stretch), 2939-2855 (C-H stretch), 1719 (C=O), 1648 (C=C),1604 (Ar-C=C), 1578-1534 (C-N bend), 1441 (CH_2 bend), and 865 (Ar-Cl); δ_H (300MHz, $CDCl_3$) 8.53 (1H, d, *J* 5.4, H-2), 8.05 (1.H, d, *J* 9.3, H-5), 8.04 (1H, d, *J* 1.8, H-8), 7.89 (1H, dd, *J* 2.4, 8.7, H-6), 7.75 (1H, d, *J* 15.6, H-15), 7.75 (1H, d, *J* 1.8, H-13),

7.55 (1H, d, *J* 15.6, H-16), 7.54 (1H, d, *J* 2.4, H-22), 7.46 (3H, m, H-9, H-11, H-18), 7.36 (1H, m, H-10), 6.96 (1H, d, *J* 5.4, H-3), 6.86 (1H, d, *J* 8.4, H-19), 3.76 (2H, s, H-24), 2.55 (4H, m, H-25 and H-29), 1.67 (4H, m, H-26 and H-28), 1.52 (2H, m, H-27); δ_C(75MHz, $CDCl_3$) 188.2, 163.7, 151.1 (2C), 148.9, 148.9, 148.1, 142.4, 140.1, 137.0, 135.9, 130.1, 129.7, 129.2, 128.3, 136.4, 124.9, 124.3, 122.8, 122.3, 121.8, 121.6, 118.1, 116.0, 102.7, 61.7 (2C), 53.8, 25.6, 23.7 (2C). EI-MS: (found m/z = 497.2 $C_{30}H_{28}ClN_3O_2$ requires M 497.19; Elemental analysis: (Found C, 70.26; H, 5.37; N, 8.12 $C_{30}H_{28}ClN_3O_2.1H_2O$requires C, 69.83; H, 5.46; N 8.14%).

(*E*)-3-(3-(7-Chloroquinolin-4-ylamino)phenyl)-1-(4-hydroxy-3,5-bis (morpholinomethyl)phenyl)prop-2-en-1-one,CDM39

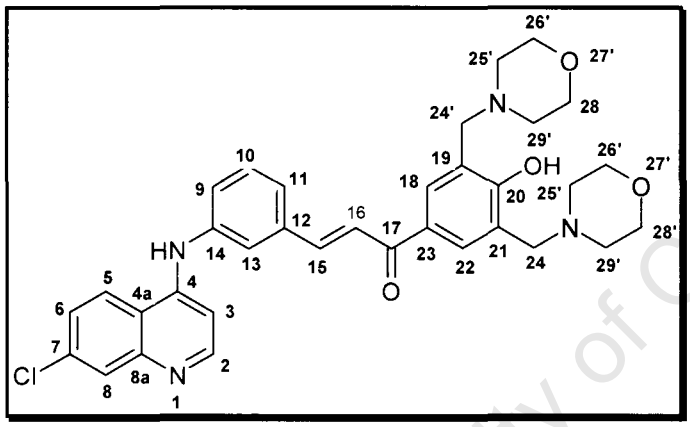

Yellow crystals (0.0969g, 15%); m.p. 233-235 °C; R_f(5% MeOH:DCM) 0.23; δ_H (300MHz, $CDCl_3$) 8.53 (1H, d, *J* 5.4, H-2), 8.05 (1.H, d, *J* 9.3, H-5), 8.04 (1H, d, *J* 1.8, H-8), 7.89 (1H, dd, *J* 2.4, 8.7, H-6), 7.75 (1H, d, *J* 15.6, H-15), 7.75 (1H, d, *J* 1.8, H-13), 7.55 (1H, d, *J* 15.6, H-16), 7.54 (1H, d, *J* 2.4, H-22), 7.46 (3H, m, H-9, H-11, H-18), 7.36 (1H, m, H-10), 6.96 (1H, d, *J* 5.4, H-3), 6.86 (1H, d, *J* 8.4, H-19), 3.76 (2H, s, H-24), 2.55 (4H, m, H-25 and H-29), 1.67 (4H, m, H-26 and H-28), 1.52 (2H, m, H-27); δ_C(75MHz, $CDCl_3$) 188.2, 163.7, 151.1 (2C), 148.9, 148.9, 148.1, 142.4, 140.1, 137.0, 135.9, 130.1, 129.7, 129.2, 128.3, 136.4, 124.9, 124.3, 122.8, 122.3, 121.8, 121.6, 118.1, 116.0, 102.7, 61.7 (2C), 53.8, 25.6, 23.7 (2C). EI-MS: (found m/z = 598.3 $C_{30}H_{28}ClN_3O_2$ requires M 598.23; Elemental analysis: (Found C, 64.84; H, 5.78; N, 9.26 $C_{30}H_{28}ClN_3O_2.2H_2O$ requires C, 64.30; H, 5.55; N 8.82%).

(*E*)-3-(3-(7-Chloroquinolin-4-ylamino)phenyl)-1-(3-((4-ethylpiperazin-1-yl)methyl)-4-hydroxyphenyl)prop-2-en-1-one, CDM40

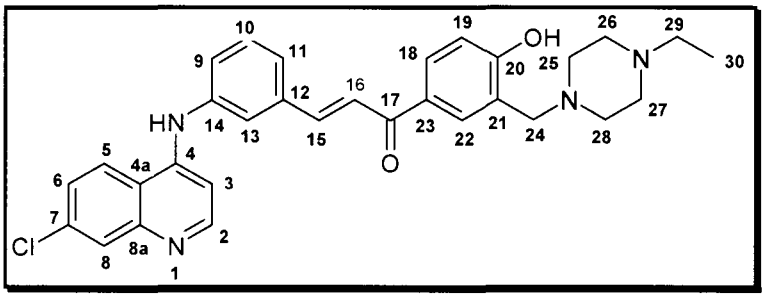

Yellow crystals (0.0931g, 17%); m.p. 214-216 °C; R_f (5% MeOH:DCM) 0.22; δ_H (300MHz, d_6-DMSO)9.24 (1H, s, NH), 8.49 (1H, d, *J* 5.4, H-2), 8.05 (1.H, d, *J* 8.8, H-5), 8.02 (2H, m, H-18 and H-22), 7.91 (1H, d , *J* 2.4, H-8), 7.89 (1H, d, *J* 15.6, H-15), 7.82 (1H, s, H-13), 7.71 (1H, d, *J* 15.6, H-15), 7.65 (1H, d, *J* 7.6, H-11), 7.57 (1H, dd, *J* 2.4, 9.0, H-6), 7.51 (1H, t, *J* 8.0, H-10), 7.44 (1H, d, *J* 8.1, H-9), 6.96 (1H, d, *J* 5.4, H-3), 6.86 (1H, d, *J* 8.4, H-19), 3.74 (2H, s, H-24), 2.43 (8H, m, H-25, H-26, H-27 and H-28), 2.23 (2H, m, H-29, H-12), 1.07 (3H, t, *J* 7.2, H-30); δ_C(75MHz, d_6-DMSO) 186.9, 161.5, 151.6, 149.2, 147.9, 142.2, 140.7, 136.1, 133.9, 130.9, 129.9, 129.7, 128.8, 127.4, 124.9, 124.5, 124.4, 124.3, 122.5, 122.1, 118.2, 115.3, 101.9, 79.24, 78.8(2C), 78.4, 57.0, 51.2, 50.9, 50.7; EI-MS: (found m/z = 526.4 $C_{31}H_{31}ClN_4O_2$ requires M 526.21 Elemental analysis: (Found C, 68.52; H, 5.73; N, 10.33 $C_{31}H_{31}ClN_4O_2.1H_2O$ requires C, 68.31; H, 5.73; N 10.28%).

(*E*)-1-(3-((*tert*-Butylamino)methyl)-4-hydroxyphenyl)-3-(3-(7-chloroquinolin-4-ylamino)phenyl)prop-2-en-1-one, CDM41

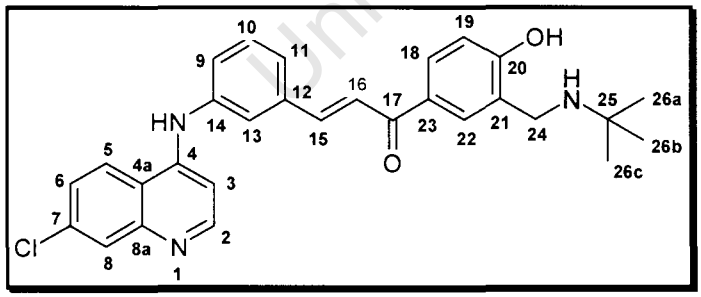

Yellow crystals (0.025g, 11%); m.p. 232-234 °C; R_f (5% MeOH:DCM) 0.10; δ_H (400MHz, d_6-DMSO) 9.22 (1H, s, NH), 8.48 (1H, d, *J* 5.2, H-2), 8.46 (1.H, d, *J* 9.2, H-5), 8.08 (1H, s, H-13), 8.01 (1H, d , *J* 8.4, H-18), 7.92 (1H, d, *J* 15.6, H-15), 7.90 (1H, d, *J* 2.0, H-8), 7.81 (1H, s, H-13), 7.69 (1H, d, *J* 15.6, H-15), 7.67 (1H, d, *J* 8.0, H-11), 7.59 (1H, dd, *J* 2.0, 8.8, H-6), 7.52 (1H, t, *J* 8.0, H-10), 7.43 (1H, d, *J* 8.0, H-9),

6.94 (1H, d, *J* 5.6, H-3), 6.82 (1H, d, *J* 8.8, H-19), 4.02 (2H, s, H-24), 1.45 (1H, s, CH_2-NH), 1.24 (9H, s, H-26a,b,c); δ_C(75MHz, d_6-DMSO) 186.9, 162.9, 152.8, 142.8, 136.9, 134.7, 132.9, 131.8, 130.8, 130.7, 128.4, 125.7, 125.1, 123.9, 123.7, 123.4, 120.8, 116.7, 111.0, 106.6, 106.5, 102.6, 95.9, 93.2, 66.6, 27.1(3C); EI-MS: (found m/z = 485.2 $C_{29}H_{28}ClN_3O_2$ requires M 485.19 Elemental analysis: (Found C, 67.52; H, 5.69; N, 7.51 $C_{29}H_{28}ClN_3O_2.2H_2O$ requires C, 67.24; H, 5.44; N 7.25%).

(*E*)-3-(3-(7-Chloroquinolin-4-ylamino)phenyl)-1-(3-((dimethylamino)methyl)-4-hydroxyphenyl)prop-2-en-1-one, CDM42

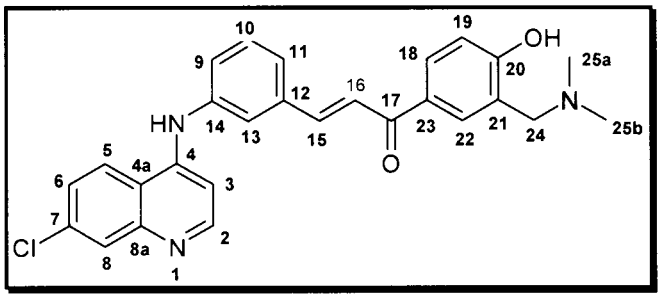

Yellow crystals (0.121g, 34%); m.p. 216-218 °C; R_f (5% MeOH:DCM) 0.14; δ_H (300MHz, d_6-DMSO) 9.19 (1H, s, NH), 8.50 (1H, d, *J* 5.4, H-2), 8.48 (1.H, d, *J* 9.0, H-5), 8.09 (1H, s, H-22), 8.06 (1H, d , *J* 8.4, H-18), 7.92 (1H, d, *J* 2.4, H-8), 7.91 (1H, d, *J* 15.6, H-15), 7.84 (1H, s, H-13), 7.74 (1H, d, *J* 15.6, H-15), 7.69 (1H, d, *J* 7.5, H-11), 7.61 (1H, dd, *J* 2.4, 9.0, H-6), 7.52 (1H, t, *J* 8.1, H-10), 7.45 (1H, d, *J* 8.1, H-9), 6.97 (1H, d, *J* 8.4, H-19), 6.94 (1H, d, *J* 5.1, H-3), 3.98 (2H, s, H-24), 2.29(overlap with DMSO, H-25a,b); δ_C(75MHz, d_6-DMSO) 187.2, 161.7, 151.3, 149.0, 148.6, 145.2, 142.9, 136.0, 134.9, 131.6, 130.2, 129.8, 129.5 (2C), 127.4, 123.8, 122.5, 121.0, 119.8, 116.4, 116.1, 115.5, 113.6, 110.7, 58.9, 45.5 (2C); EI-MS: (found m/z = 487.2 $C_{27}H_{24}ClN_3O_2$ requires M 457.16 Elemental analysis: (Found C, 67.41; H, 4.65; N, 8.02 $C_{27}H_{24}ClN_3O_2.2.5H_2O$ requires C, 66.87; H, 4.98; N 8.66%).

(*E*)-3-(3-(7-Chloroquinolin-4-ylamino)phenyl)-1-(3-((diethylamino)methyl)-4-hydroxyphenyl)prop-2-en-1-one, CDM43

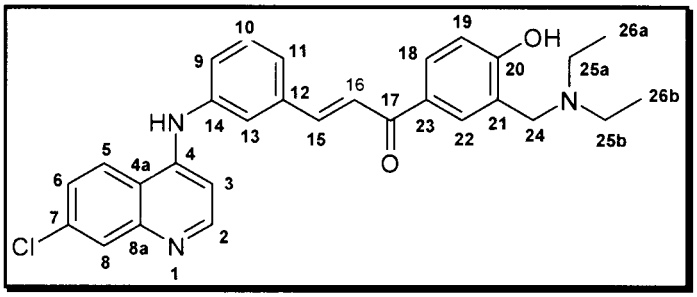

Yellow crystals (0.1198g, 20%); m.p. 207-210 °C; R_f (5% MeOH:DCM) 0.16; ν_{max} ($CHCl_3$) / cm^{-1} 3365 (C-N stretch), 2924-2851, (C-H stretch), 1647 (C=O), 1604 (C=C),1604 (Ar-C=C), 1582-1542 (C-N bend), 1439 (CH_2 bend), and 815 (Ar-Cl); δ_H (400MHz, d_6-DMSO) 9.15 (1H, s, NH), 8.48 (1H, d, *J* 5.2, H-2), 8.45 (1.H, d, *J* 9.2, H-5), 7.99 (1H, dd, *J* 2.4, 8.4, H-18), 7.93 (1H, d, *J* 2.0, H-8), 7.90 (1H, d , *J* 2.4, H-22), 7.89 (1H, d, *J* 15.6, H-15), 7.82 (1H, s, H-13), 7.69 (1H, d, *J* 15.6, H-15), 7.66 (1H, d, *J* 7.6, H-11), 7.58 (1H, dd, *J* 2.4, 9.2, H-6), 7.51 (1H, t, *J* 8.0, H-10), 7.42 (1H, d, *J* 8.0, H-9), 6.94 (1H, d, *J* 5.6, H-3), 6.78 (1H, d, *J* 8.4, H-9), 3.85 (2H, s, H-24), 2.61 (4H, q, *J* 7.2, H-25a,b), 1.03 (6H, t, *J* 7.2, H-26a,b); δ_C(75MHz, d_6-DMSO) 186.9, 163.4, 151.9, 149.5, 148.3, 147.8, 142.0 (2C), 140.7, 136.2, 134.2, 129.9, 129.8, 129.7, 128.4, 127.6, 124.9, 124.5, 124.4, 124.3, 122.6 (2C), 115.5, 102.0, 55.0, 45.7 (2C), 10.8 (2C); EI-MS: (found m/z = 485.3 $C_{29}H_{28}ClN_3O_2$ requires M 485.19 Elemental analysis: (Found C, 70.73; H, 5.68; N, 8.74 $C_{29}H_{28}ClN_3O_2.0.5H_2O$ requires C, 70.38; H, 5.70; N 8.49%).

(*E*)-3-(3-(7-Chloroquinolin-4-ylamino)phenyl)-1-(3-((dimethylamino)methyl)-4-hydroxy-5-methoxyphenyl)prop-2-en-1-one, CDM44

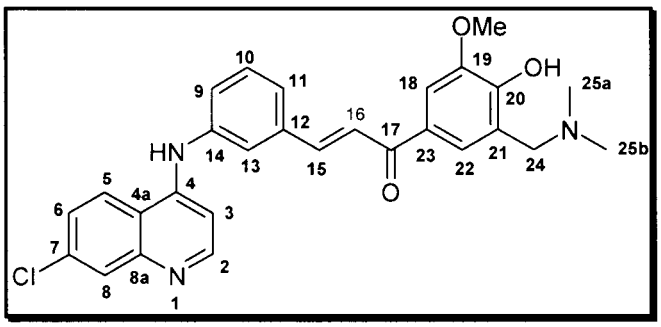

Yellow crystals (0.0226g, 20%); m.p. 280-282 °C; R_f (10% MeOH:DCM) 0.36; δ_H (400MHz, d_6-DMSO) 11.25 (1H, s, OH), 10.65 (1H, s, NH), 8.90 (1H, d, *J* 8.8, H-5), 8.54 (1.H, d, *J* 6.8, H-2), 8.25 (1H, s, H-8), 8.17 (1H, s, H-22),

8.12 (1H, d , *J* 15.2, H-15), 8.05 (1H, s, H-13), 8.00 (1H, d, *J* 8.1, H-11), 7.89 (1H, d, *J* 9.2, H-6), 7.78 (1H, d, *J* 15.2, H-16), 7.66 (1H, s, H-18), 7.65 (1H, t, *J* 8.0, H-10), 7.55 (1H, d, *J* 7.6, H-9), 6.86 (1H, d, *J* 7.2, H-3), 4.39 (2H, s, H-24), 3.98 (3H, s, $C_{19}OCH_3$), 2.71 (6H, s, H-25a,b); δ_C(75MHz, d_6-DMSO) 187.7, 155.4, 151.6, 148.7, 144.6, 142.6, 140.1, 139.5, 138.5, 137.4, 131.4, 129.6, 128.7, 128.6, 127.9, 127.5, 126.2, 124.0, 117.5, 116.7, 112.3, 108.6, 101.4, 56.9, 54.6, 44.9; EI-MS: (found m/z = 487.2 $C_{28}H_{26}ClN_3O_3$ requires M 487.17 Elemental analysis: (Found C, 65.91; H, 5.24; N, 8.64 $C_{28}H_{26}ClN_3O_3.1H_2O$ requires C, 66.47; H, 5.18; N 8.31%).

5.2 Single Crystal X-ray Diffraction

Single crystals of **CDM06** and **CDM14** were prepared by dissolving the compounds in a minimum amount of heated ethyl acetate and methanol, respectively. Each solution was filtered while hot through a 0.45 μM nylon microfilter and allowed to slowly evaporate at room temperature. A single crystal which extinguished plane polarized light was selected and cut to an appropriate size to minimize X-ray absorption. The crystal was coated with Paratone oil and mounted on a glass fibre on a goniometer head. Reflection intensity data were measured on a Nonius Kappa CCD single crystal diffractometer using graphite-monochromated MoKα radiation (λ = 0.71069 Å) generated by a Nonius FR590 generator operating at 53 kW and 23mA. Data collections were performed at low temperatures (113K and 173K), which were maintained by a constant N_2 gas flow of 20 cm^3/min. Cell refinement and data reduction were performed by Denzo Scalepack and SADABS was used for absorption corrections.[1] XPREP[2] was used to determine the crystal space group by examining systematic absences and intensity statistics. The structures were solved by direct methods using SHELXS-97[3] and refined by the method of least-squares against F^2 using SHELXL-97,[4] incorporated in the X-Seed[5] interface.

5.3 Cyclodextrin Inclusion Complexes

5.3.1 Materials

The cyclodextrin host compounds β-cyclodextrin, γ-cyclodextrin and TRIMEB were obtained from Cyclolab (Budapest, Hungary).

5.3.2 Preparation Methods

Kneading, co-precipitation and co-solvent methods were employed in attempts to include target compounds **CDM13-15** and **CDM38** in cyclodextrin hosts. Co-precipitation or co-solvent methods involve dissolving β-CD or γ-CD in a minimum amount of water at an elevated temperature. A stoichiometric amount of guest compound (1:1 or 2:1 host:guest) was slowly added to the stirring solution, either directly as for co-precipitation or as a methanol solution for the co-solvent method. The resulting suspension was stirred for 24 h and then filtered through a 0.45 μM nylon microfilter and allowed to evaporate slowly. A similar procedure was employed for attempted formation of TRIMEB inclusion complexes, the difference being due to TRIMEBs inverse solubility relationship with temperature and it was thus necessary to prepare saturated solutions of host compound at low temperatures (0°C- room temperature). After addition of the guest, the cold solution was stirred for 5 h, filtered through a 0.45 μM nylon microfilter and heated at 60°C in order to encourage crystallization. The method of kneading involved making a paste of the cyclodextrin with water using a mortar and pestle. An equimolar amount of drug was slowly added with continual grinding for an hour. The consistency of the paste was maintained by dropwise addition of water during this period.

5.3.3 Powder X-ray Diffraction (PXRD)

PXRD was used to ascertain whether a CD complex had been formed by comparing the PXRD pattern of the kneaded material to that of the native CD and that of the guest. PXRD patterns that are different from those of the host and guest indicate that a potential complex has formed and are then used to determine if the complex is isostructural to any known isostructural series of complexes.[5] PXRD patterns of kneaded samples were recorded on a HUBER Imaging Plate Guinier Camera 670 with Ni-filtered CuKα-radiation (λ = 1.5406Å) generated by a Philips X-ray generator operated at 40kV and 25mA. The kneaded paste was spread on Mylar® film and exposed to radiation for 10-20 min with 10 multiscans to collect the data.

5.4 Thermogravimetric Analysis

The three thermal analytical methods used in this study were Hot Stage Microscopy (HSM), Thermogravimetric Analysis (TGA) and Differential Scanning Calorimetry (DSC).

5.4.1 Hot stage Microscopy (HSM)

HSM was used to observe crystal morphologies and visual physical changes (melting, desolvation) as crystals were heated. Crystals were submerged in silicone oil and placed between cover-slides and viewed with a Nikon SMZ-10 stereoscopic microscope with the images captured by a real-time Sony Digital Hyper HAD colour video camera. These images were viewed with the Soft Imaging System program, analySIS.[6] Heat was provided by a Linkam THMS600 hot stage apparatus and controlled with a Linkam TP92 temperature control unit.

5.4.2 Thermogravimetric Analysis (TGA)

TGA gives quantitative data for loss of mass with increasing temperature and was used to determine the solvent content of **CDM14**. TGA experiments were performed on a Mettler Toledo Star TGA/SDTA 851 instrument. Samples of mass 2-4 mg were placed in an open crucible and heated at a constant rate of 10K min^{-1} under nitrogen with a flow rate of 30 cm^{-3} min^{-1}.

5.4.3 Differential Scanning Calorimetry (DSC)

DSC measures the heat flow required to increase the temperature of a sample at a constant rate relative to an empty reference pan. This analytical method was used to measure endothermic and exothermic changes in the inclusion complexes and guest compounds, and was used to accurately determine melting points and onset temperatures of thermal events. DSC experiments were performed on a Perkin- Elmer PC7-series Differential Scanning Calorimeter. Samples of mass 2-5mg were sealed in a crimped, vented aluminum pan with a sealed, empty pan used as reference. The sample was heated at a rate of 10 $Kmin^{-1}$ under nitrogen with a flow rate of 30 cm^{-3} min^{-1}.

5.5 Procedures for Biological Assays

In Vitro Activities of compounds against 3D7

All samples were tested in triplicate against the *P. falciparum* 3D7 strain, a clone of NF54, which is known to be sensitive to all anti-malarials. The cultures are naturally asynchronous (65 – 75% ring stage) and are maintained in continuous log phase growth in RPMI1640 medium supplemented with 5% washed human A+erythrocytes, 25 mM Hepes, 32 nM $NaHCO_3$, and AlbuMAXII (lipid-rich bovine serum lbumin) (GIBCO, Grand Island, NY). All cultures and assays are conducted at 37°C under an atmosphere of 5% CO_2 and 5% O_2, with a balance of N_2.

Primary screen

The preliminary screen uses the 3D7 strain. The compounds are tested at four concentrations (30, 10, 3, 1, 0.3, and 0.1 μg/ml) and their potency classified according to the observed activity at these concentrations. The test compound is classified as inactive if it does not affect parasite growth at 10 μg/ml, is designated as partially active between 10 and 1 μg/ml, and if it affects parasite growth <1 μg/ml, the compound is classified as active and is further evaluated by three-fold serial dilutions in a repeat test.

Secondary screen

The compound is diluted three-fold over at twelve different concentrations with an appropriate starting concentration based on the preliminary screen. For each assay, the IC_{50} and IC_{90} values for each parasite line are determined against chloroquine.

In Vitro Activities of compounds against W2 *P. falciparum*,

W2-strain *P. falciparum* parasites (1% parasitaemia, 2% hematocrit) were cultured in 0.5 ml of medium in 48-well culture dishes.[7] The test inhibitors from 10 mM stocks in DMSO were added to cultured parasites to a final concentration of 20 μM. From 48-well plates, 125 μM of culture was transferred to two 96 well plates (duplicates). Serial dilutions (1%) of inhibitors were made to final concentrations of 10 μM, 2 μM, 0.4 μM, 80 nM, 16 nM and 3.2 nM. Cultures were maintained at 37 °C for 2 days after which the parasites were washed and fixed with 1% formaldehyde in PBS. After two days, parasitaemia was measured by flow cytometry using the DNA stain YOYO-1 as a marker for cell survival.[8]

In Vitro* Activities of compounds against D10 *P. falciparum

All experiments were performed in duplicate on a single occasion against the chloroquine-sensitive strain of *P. falciparum* D10. Continuous *in vitro* cultures of asexual erythrocyte stages of *P. falciparum* were maintained using a modified method of Trager and Jensen.[7] Quantitative assessment of antiplasmodial activity *in vitro* was determined via the parasite lactate dehydrogenase (pLDH) assay using a modified method described by Makler.[9] The average percentage parasite viability was determined at three different concentrations and compounds showing significant activity (reduction of parasite viability below 50%) were tested further to determine their 50% inhibitory concentration (IC_{50}) values. These values were obtained from dose-response curves, using nonlinear dose-response curve fitting analyses with GraphPad Prism® v3.0 software. All compounds were dissolved in 100% DMSO and were then diluted with water to a concentration of 20 µg/ml. Samples were stored at –20°C until use. All samples were further diluted to 2 µg/ml in complete medium on the day of the experiment. The highest concentration of DMSO to which the parasites were exposed had no measurable effect on the parasite viability. Chloroquine diphosphate was used as the positive control in all experiments.

\

***In Vitro* Activities of compounds against Falcipain-2**

IC_{50} values against the recombinant enzyme (falcipain-2) were determined as described by Rosenthal and coworkers.[8] Briefly, an equal amount of recombinant protein (~1 nM) was incubated with different concentrations of test compounds (added from 100x stock solutions in DMSO) in 100 mM sodium acetate (pH 5.5)-10 mM dithiothreitol for 30 min at room temperature before addition of the substrate benzoxycarbonyl-Leu-Arg-7-amino-4-methyl-coumarin. Fluorescence was continuously monitored for 30 min at room temperature in a Labsystems Fluoroskan® II spectrofluorometer. IC_{50} values were determined from plots of activity over inhibitor concentration with GraphPad Prism® software.

Assay of β-Haematin inhibition

All samples were screened for their ability to inhibit synthetic haemozoin (β-haematin) as describe by Egan and co-workers.[10] β-Haematin was prepared in 4.5 M acetate at 60 °C from hemin dissolved in 0.1 M NaOH as described previously.[11] High-throughput screening was performed using 1 and 5 equivalents of test compounds relative to haematin. A 20 µl stock solution of haematin was mixed with a 1M HCl or methanol solution of test compound. Prewarmed acetate solution was then added (11.4 µl, 12.9 M, pH 5.0) and after 1 h incubation, 250 µl of 12% (v/v) pyridine solution (pH 7.5, 20 mM Hepes, ambient temperature) was added. Supernatants were transferred to a 96-well plate and detection of β-haematin inhibition was carried out by visual inspection and by absorbance measurement at 405 nm.

***In Vitro* Activities of compounds against HeLa (human adenocarcinoma of the cervix) cells**

An adapted MTT method as desribed by Van Rensburg *et al*[11] was performed to establish the sensitivity of the HeLa cancer cell line to the test compounds. [3-(4,5-dimethylthiazol-2-yl)-2-5-diphenyl tetrazolium bromide] (MTT) is a pale yellow substance that is metabolized to dark blue formazan crystals by metabolically active cells. An 80 µl medium was dispensed into each well of a 96 well tissue culture plate and 100 µl of cell suspension was then added to each well. Cultures were incubated at 37 °C in an atmosphere of 5% CO_2 for an hour and then 20 µl dilutions of the test compound was added at different concentrations. Cultures were incubated for 7 days, after which 20 µl MTT (5mg/ ml) was added to each well, incubated for a further 4 h and then centrifuged for 10 min at 800g. Supernatant was carefully removed, washed with 150 µl PBS and allowed to dry. DMSO was then added to solubilize the formazan crystals and then detected by absorbance measurement at 570 nm. Percentage survival was calculated and used in IC_{50} determination.

References

1. Sheldrick, G.M.; *SADABS-Bruker/ Siemans area detector absorption and other corrections*, V2.03.
2. Sheldrick, G.M. *SHELXS-97, Program for Crystal Structure Solution*, Institüt für Anorganische Chemie der Universität, Tammanstrasse 4, D-3400 Göttingen, Germany, **1997**.
3. Sheldrick, G.M. *SHELXL-97, Program for the Refinement of Crystal Structures*, Institüt für Anorganische Chemie der Universität, Tammanstrasse 4, D-3400 Göttingen, Germany, **1997**.
4. Barbour, L.J. *X-Seed-A graphical interface to SHELX*, University of Missouri, Columbia, U.S.A., **1999**.
5. Caira, M.R. *Rev. Roum. Chim.*, **2001**, *46*, 371.
6. Soft Imaging System GmbH, *Digital Solutions for Imaging and Microscopy*, Version 3.1 for Windows (Copyright 1987-2000).
7. Trager, W.; Jensen, J.B. *Science*, **1976**, *193*, 673.
8. Greenbaum, D. C.; Mackey, Z.; Hansell, E.; Doyle, P.; Gut, J.; Caffrey, C. R.; Lehman, J.; Rosenthal, P. J.; McKerrow, J. H.; Chibale, K. C. *J. Med. Chem.*, **2004**, *47*, 3212.
9. Makler, M.Y.; Ries, J.M.; Williams, J.A.; Bancroft, J.E.; Piper, R.C.; Gibbins, B.L.; Hinrichs, D.J. *Am. Soc. Trop. Med. Hyg.*, **1993**, *48*, 739.
10. Ncokazi, K.K.; Egan, T.J. *Anal. Biochem.*, **2005**, *338*, 306.
11. Van Rensburg, C.E.J.; Anderson, R.; Joone, G.K.; Myer, M.S.; O' Sullivan, J.F. *Anti-Cancer Drugs*, **1997**, *8*, 708.